Frontispiece. *View of Suminandig hill, Mt. Rangas and Matacla Dome (from left to right) along the road going to Sorsogon (looking north).*

PETROLOGY AND GEOCHEMISTRY OF VOLCANIC ROCKS FROM THE POCDOL MOUNTAINS, BICOL ARC (PHILIPPINES)

A thesis
submitted in partial fulfilment
of the requirements for the Degree
of
Master of Science (with Honours) in Geology
in the
University of Canterbury
by

Henry J. Tebar

University of Canterbury
May 1988

"...How odd it is that anyone should not see that all observation must be for or against some view, if it is to be of any service".

Charles R. Darwin

ABSTRACT

The Pocdol Mountains are part of the Bicol arc-- a SE-trending calcalkaline volcanic belt adjacent to the Philippine Trench. Recent volcano-stratigraphic studies and five new K-Ar ages have delineated seven lithostratigraphic units in the Pocdol Mountains. The rocks are grouped into : **(i) a Western Pocdol Mountains (WPM) series**, and **(ii) an Eastern Pocdol Mountains (EPM) series.**

WPM eruptives comprise Early Pliocene basaltic tuff breccias and lavas (Malobago volcanics) and Middle to Late Pleistocene (0.478-0.065 Ma) andesitic lavas and tuff breccias (Lison and Kayabon volcanics). EPM volcanism produced (i) Middle Pliocene dacitic tuff breccias and minor lavas and the Matacla Dome (Suminandig volcanics). The stratified unit is intercalated with lenses of siltstones and sandstones (Rangas conglomerate), and was later (0.065 Ma) intruded by the Rangas microdiorite; (ii) Middle Pliocene to Early Pleistocene andesitic tuff breccias, laharic breccias and lavas (Pangas volcanics), which were erupted mostly from four flank vents, with associated igneous intrusives (Pangas intrusives), and (iii) Late Pleistocene to Recent andesitic lavas, tuff breccias and lahars of the Cawayan volcanics (<0.04 Ma) and basaltic tephras and minor lavas of the Pulog volcanics (<0.03 Ma).

The rocks are plagioclase-phyric, with minor clino- and orthopyroxene, titanomagnetite and hornblende. Olivine is only found in the Malobago volcanics. Glomerophyric and pilotaxitic textures are common, and most phenocrysts show normal or oscillatory zonation. Disequilibrium features are rare. The inferred crystallisation sequence of WPM lavas is titanomagnetite-olivine-pyroxene-amphibole, accompanied by plagioclase. EPM rocks have the same order of crystallisation as WPM lavas, except that olivine was not involved. Overall mineralogy of the lavas suggests a low pressure (<9 kb) crystallisation and estimated equilibration temperatures from coexisting two pyroxenes range from 1006°C to 1135°C. The absence of ilmenite phases precludes an estimate of oxygen fugacity. WPM lavas comprise medium-K high-Al basalt to medium-K and high-K andesite, whereas the EPM rocks consist of low-K basaltic andesite to medium-K andesite and dacite. Major oxide and trace element variations indicate two possible parental liquids, each generating the WPM and EPM series; the EPM lavas also show two fractionation trends : a dacite and an andesite crystallisation paths. WPM lavas generally contain greater abundances in large-ion lithophile (LIL) and high field strength (HFS) ions, but they have lower concentrations of ferromagnesian elements. Low $Mg/(Mg+Fe^2)$, Ni and Cr values in both series suggest that the liquids are not in equilibrium with mantle peridotite.

Both WPM and EPM lavas are considered to have been derived by closed-system low pressure POAM fractionation (Gill, 1981) of a basaltic source, that may have been generated by higher degrees of partial melting within the mantle wedge and/or the subducted slab, together with some degree of enrichment from the downgoing slab. Stratigraphic criteria and least-squares mixing models indicate that by precipitating plagioclase, orthopyroxene, titanomagnetite and clinopyroxene, both Lison and Kayabon andesites (WPM series) were probably derived from a high-alumina basaltic source (Malobago volcanics), whereas the Suminandig, Pangas and Cawayan volcanics (EPM series) originate from a low-K basaltic andesite liquid (Pulog volcanics). However, if it is assumed that a dacitic melt was sitting on top of the EPM reservoir, then it is necessary to invoke liquid fractionation (McBirney *et al.*, 1985), whereby the more fractionated liquids move upward and are collected at the roof of the chamber, due to density stratification in the magma reservoir.

TABLE OF CONTENTS

Table of Contents (Con't)

LIST OF FIGURES

LIST OF TABLES

CHAPTER I

GENERAL INTRODUCTION

CHAPTER I

GENERAL INTRODUCTION

1.1 NATURE AND SCOPE OF THIS STUDY

1.1.1 Objectives

The primary aim of this study is to establish the petrology, geochemistry and petrogenesis of the volcanic rocks of Pocdol Mountains. This information, combined with general field observations, will provide important constraints in understanding the volcanism and associated hydrothermal activity in the area.

1.1.2 Scope and Limitations

Thirty lava flow sections were selected in the field area and fresh rock samples were collected for detailed petrographic and chemical studies. Borehole specimens were excluded from the sample population because most minerals show hydrothermal alteration. Five of the "freshest" samples from different stratigraphic levels were potassium-argon dated at the Institute of Nuclear Sciences (DSIR), Lower Hutt in order to assist in determining an absolute chronology. These data, together with the results of additional aerial photo and ground traverses, were used to construct a new geologic map of the area.

Since the volcanic products were formed by major cone-building episodes, the use of aerial photographs in mapping individual volcanic flow units is invaluable, particularly in a heavily-forested area like the Pocdol Mountains. However, internal differentiation of the extrusives is difficult because of poor outcrop sections, compounded by the intensity of weathering and in some cases, hydrothermal alteration. For this reason, a sampling bias was introduced by collecting rock samples only from relatively fresh lava flows and clasts of tuff breccias.

The thesis comprises six major sections. The first section (chapter I) outlines the general background of the study. This is followed by a major section on field relations; chapter II documents

the volcanic stratigraphy of Pocdol Mountains based on petrologic and volcanological considerations. As part of this exercise, a review of fault structures is necessary. Detailed petrography and mineral chemistry are then used to document the petrology of the volcanic rocks in chapter III, and in chapter IV bulk rock compositions are described. Particular attention is given to various aspects that indicate petrogenetic processes. In chapter V these data, in conjunction with stratigraphic interpretations and plate tectonic concepts, are used to examine several hypotheses on petrogenesis. Finally, the major findings of this study are summarised in chapter VI.

Borehole geology, hydrothermal alteration, water chemistry, reservoir and geophysical data are beyond the scope of this study except to assist in geologic interpretation. No additional field data on fault structures are given, but new interpretations are proposed which are constrained mainly by the modified volcanic stratigraphy and existing surface and subsurface fault data.

1.2 REGIONAL SETTING

The study area (Fig. 1) is characterised by clusters of small eruptive centres, collectively known as the **"Pocdol Mountains"** (PBM, 1963), which belong to the Bicol arc (see chapter V for discussion on tectonics of the region).

Volcanic rocks at Pocdol Mountains (Fig. 2) overlie Oligocene-Pleistocene sedimentary sequences, which are well-exposed near Prieto Diaz, but in general exposures are very limited within the study area (see Fig. 8). This rock sequence is probably underlain by pre-Tertiary schists and ultramafic rocks, outcropping as steeply-dipping units at Rapu-rapu Island, Balete and San Ramon, which are interpreted as a part of an accreted terrane that originated from the south (Defant *et al.*, 1988).

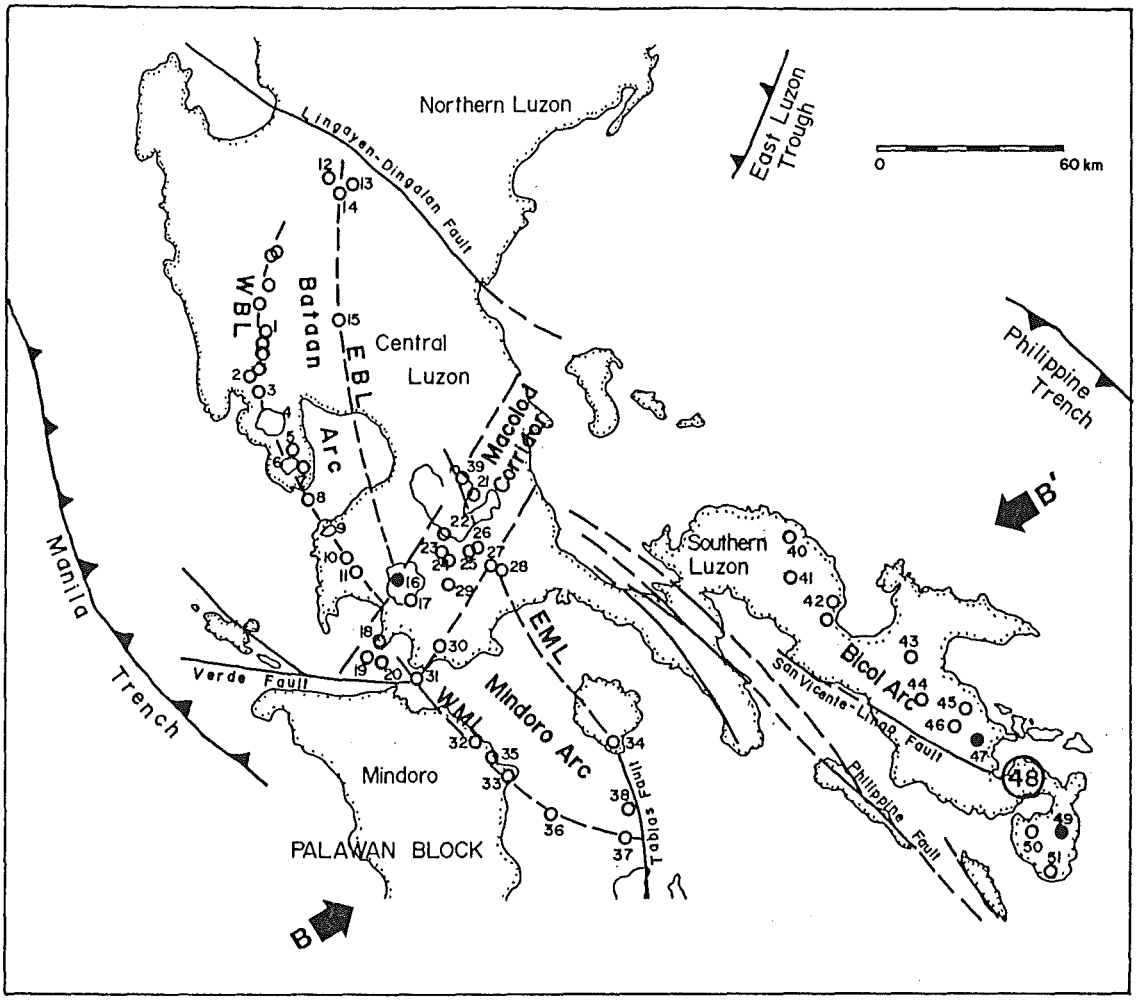

FIG. 1 Major tectonic features and Pliocene-Quaternary volcanism in the central Philippines (modified from Newhall, 1979; Defant et al., 1988; Knittel and Defant, 1988). Filled circle denotes active volcano; open circle, inactive volcano. EBL (Eastern Bataan Lineament); WBL (Western Bataan Lineament); EML (Eastern Mindoro Lineament); WML (Western Mindoro Lineament). Numbers correspond to the following volcanoes : (1) Pinatubo; (2) Balakibok; (3) Santa Rita; (4) Natib; (5) Samat; (6) Mariveles; (7) Limay; (8) Corregidor Complex; (9) Palay-palay or Mataas na Gulod; (10) Carilao; (11) Batulao; (12) Balungao; (13) Amorong; (14) Bangcay; (15) Arayat; (16) Taal; (17) Macolod; (18) Panay; (19) Maricaban West Complex; (20) Casapao; (21) Sembrano; (22) Makiling; (23) Mapinggon; (24) Bulalo; (25) Nagcarlang; (26) Atimbia; (27) San Cristobal; (28) Banahaw; (29) Malepunyo; (30) Lingayen; (31) Verde Island Complex; (32) Macapili; (33) Dumali; (34) Marlanga; (35) Pola; (36) Maestro de Campo; (37) Simara; (38) Bantoi; (39) Laguna de Bay Complex; (40) Bagacay; (41) Labo; (42) Colasi; (43) Isarog; (44) Iriga; (45) Malinao; (46) Masaraga; (47) Mayon; (48) POCDOL MOUNTAINS; (49) Bulusan; (50) Juban, and (51) Gate Mountains. Line BB' is a section line of earthquake hypocentres shown in Fig. 35.

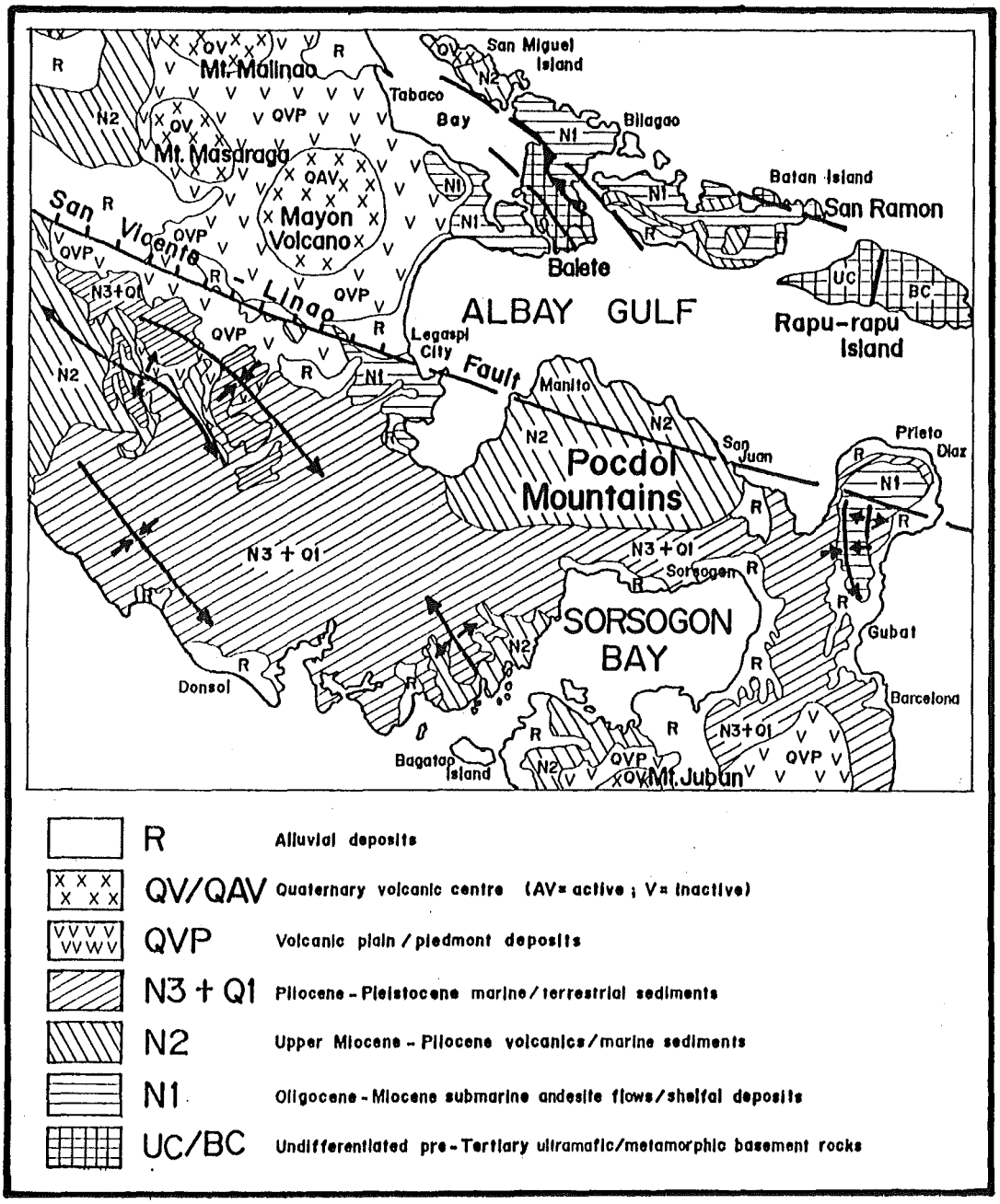

FIG. 2 Generalised geology of Pocdol Mountains and vicinity (after PBM, 1963). Lines with arrows represent fold axes; shorter coupled arrows are synclines (converging) and anticlines (diverging). Bold lines are faults; dashed where inferred. The QVP east of Mt. Juban includes distal products of Bulusan volcano, which is located several kilometres south.

Initiation of volcanism in the Pocdol Mountains probably started in Late Miocene, as indicated by volcanic flows unconformably underlain by Upper Miocene sedimentary units (Travaglia and Baes, 1979; Balce *et al.*, 1979). The volcanic activity may have continued until Pleistocene or Recent times (De Leon *et al.*, 1983).

The San Vicente-Linao Fault (SVLF) is a major fault structure bisecting the Pocdol Mountains (Fig. 2), and appears to be related to movements along the Philippine Fault. The SVLF trace in the study area is characterised by a 5 km-wide east-trending sheared zone in pre-Pulog volcanic rocks (see chapter II). Other major faults in the region trend north-northwest, northwest, north-northeast and northeast whereas local faults usually have north-south or east-west strikes (Ferrer *et al.*, 1986). The north-south faults are inferred to be the youngest, as well as the dominant trend in the Pocdol Mountains (Panem and Alincastre, 1985). Seismic activity has been recorded along these faults (e.g., Acharya, 1980), and slickensides are found where the SVLF cuts Pleistocene limestones (Travaglia and Baes, 1976).

1.2.1 Physiography and Drainage

Major geomorphic features of the Pocdol Mountains are presented in Fig. 3. The morphology of the study area is typical of an eroded volcanic region. Here, closely-spaced eruptive vents still display their distinctive crater-like structures or in cases where they are heavily-eroded, hydrothermal activity is sometimes present. A radial-trellis drainage system commonly separates volcanic flows, and several rivers follow geologic contacts (i.e., Manitohan and Menito rivers).

For the purposes of this study, the Pocdol Mountains will be subdivided into two broad sectors (Fig. 3). These are :

(i) Western Pocdol Mountains (or WPM). This sector is defined by intensely-eroded volcanic flow units, particularly within the region of the SVLF zone (i.e., from Calpi to Lison). Several collapse features are present in the vicinity of Lison Dome, but hydrothermal manifestations are absent. To the north of the WPM are the Manito Lowlands, a low undulating and hummocky terrain, typical of lahar fields (Neall, 1976).

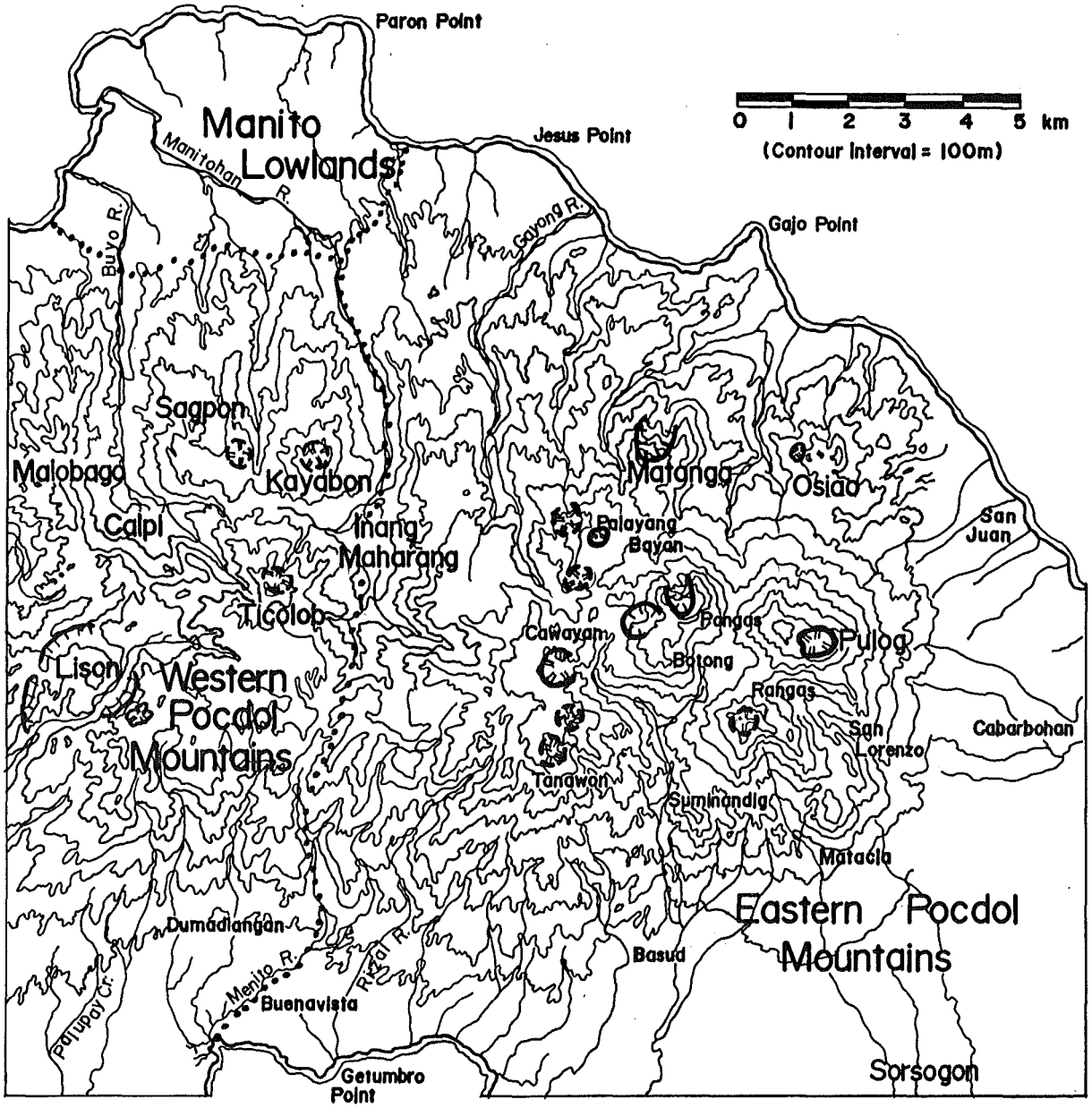

FIG. 3 Major geomorphic features of Pocdol Mountains. Former eruption sites are drawn as circular features (with double hachures); dashed where inferred; depressions/slumps, single hachures. Contour line starts at 100 m (interval is 100 m). Locality and rivers mentioned in the text are shown. Dotted line represents the approximate boundary between Western- (WPM) and Eastern Pocdol Mountains (EPM).

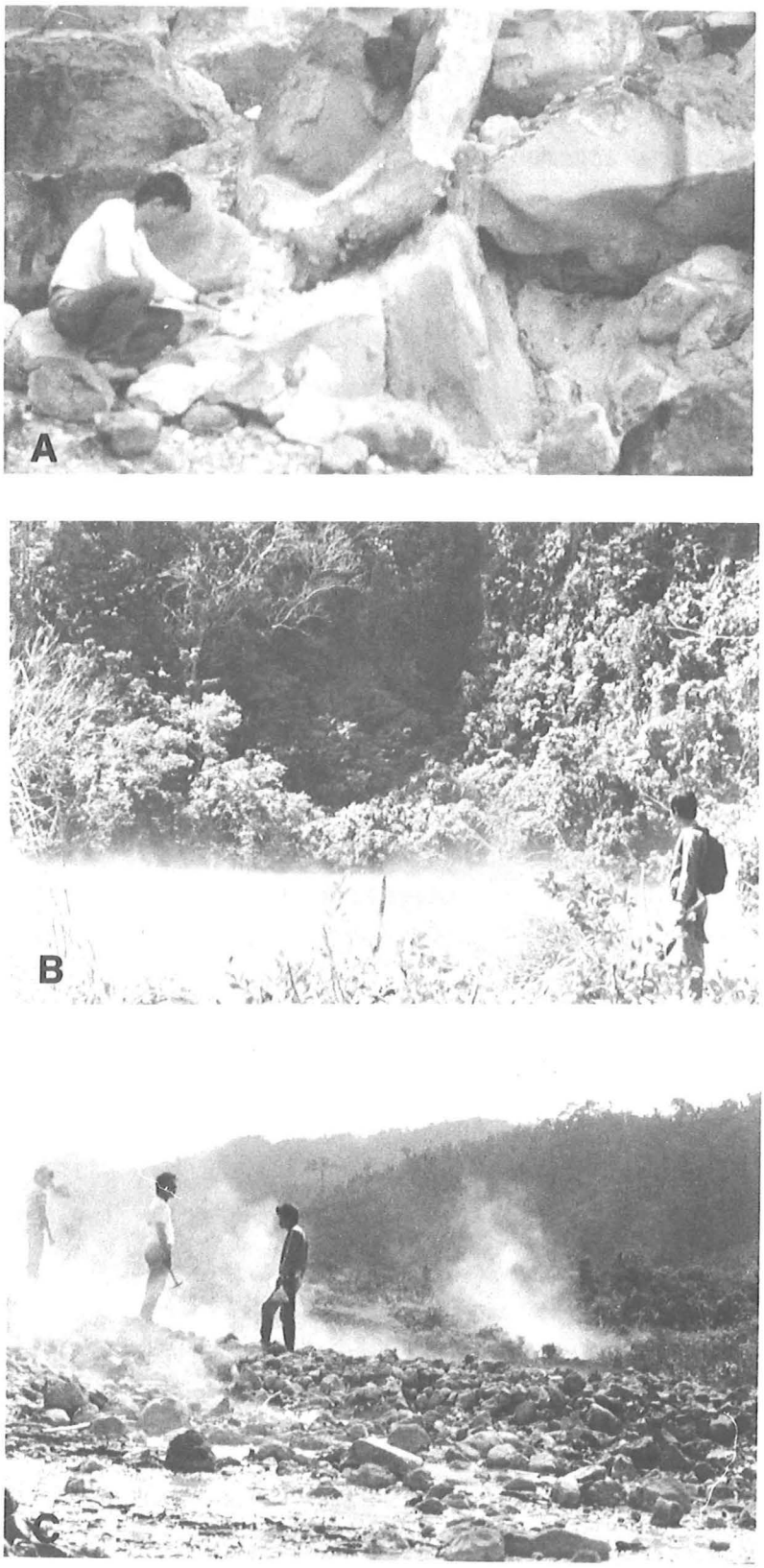

Fig. 4 Hydrothermal features of Pocdol Mountains : (A) Sulfur deposits in the northern slopes of Pangas Dome; (B) Boiling pool near Nagotgot, and (C) Inang Maharang hot springs.

(ii) Eastern Pocdol Mountains (or EPM). This area is formed by clusters of heavily-dissected multiple-vent composite cones and domes. Of these, the highest is Mt. Pangas (1082m). The majority of the thermal features (Fig. 4) and geothermal developments are confined to this sector.

Vegetation cover in both EPM and WPM consists of thick tropical forest. These areas are uncultivated primarily due to the precipitous terrain; however, crops are abundant in the Manito Lowlands.

1.2.2 Hydrothermal Activity

The Pocdol Mountains host an active hydrothermal system (Fig. 5), which is currently developed for geothermal power generation. The hydrothermal activity in the area is characterised by numerous thermal discharges, i.e., hot and warm springs, cold sulfur springs, fumaroles, solfataras, steaming ground (Fig. 4), cold altered ground, and discrete zones of hydrothermally-altered fault scarps.

Subsurface delineation of hot water bodies, using the Schlumberger resistivity method, has been successful in New Zealand geothermal fields (e.g., Risk, 1986), and this method is now being used in the Pocdol Mountains. Schlumberger resistivity traversing and sounding exercises have traced areas showing anomalous resistivity, and these are contained within a northwest-trending 100 ohm-metre apparent resistivity contour line (Layugan, 1986); the 100 ohm-metre contour line encloses most of the thermal features in the area. A minor resistivity anomaly is also present near Osiao (Fig. 5).

Moreover, the resistivity "lows" are bounded in the north, south and east by high (>50 ohm-metre) "true" bottom resistivity values that indicate unaltered rock bodies to depths of 800 to 1000 metres.

Overall, data such as borehole measurements (i.e., bottomhole temperatures), iso-resistivity and spring chemistry data (e.g., PNOC-EDC, 1985; 1986) therefore suggest that the upflow of hydrothermal fluids in the Pocdol Mountains is probably centered in the highly-faulted Cawayan-Pangas-Botong sector (Fig. 6); hydrothermal waters then flow downslope along permeable horizons, such as fault zones

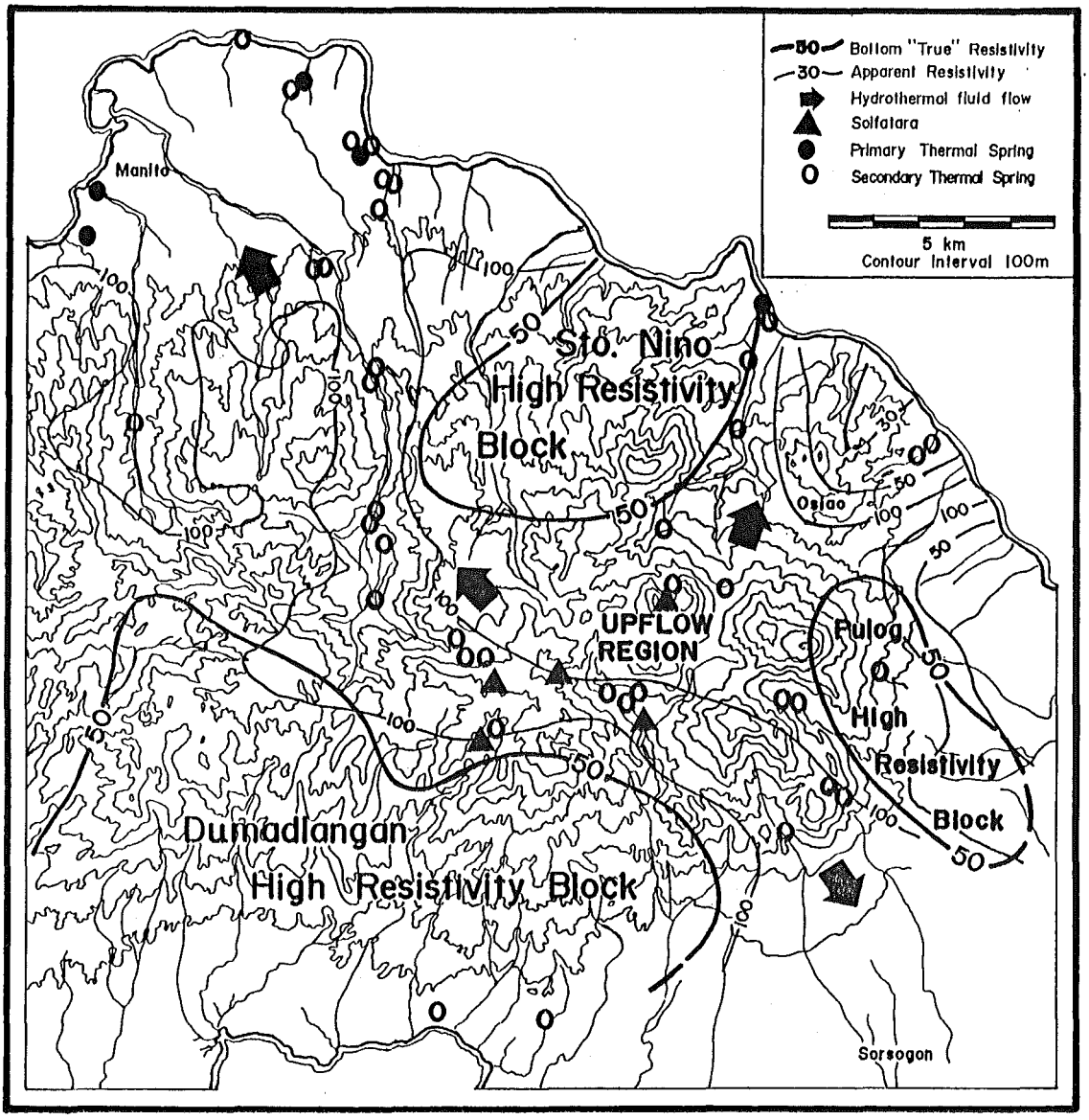

FIG. 5 Simplified hydrological model of geothermal fluid flow in the Pocdol Mountains. Field resistivity are taken from Layugan (1986) and thermal spring locations, from Zapanta (1985) and Baltazar (1987). "Primary" and "secondary" thermal springs contain >100 and <100 ppm Cl^- concentrations, respectively.

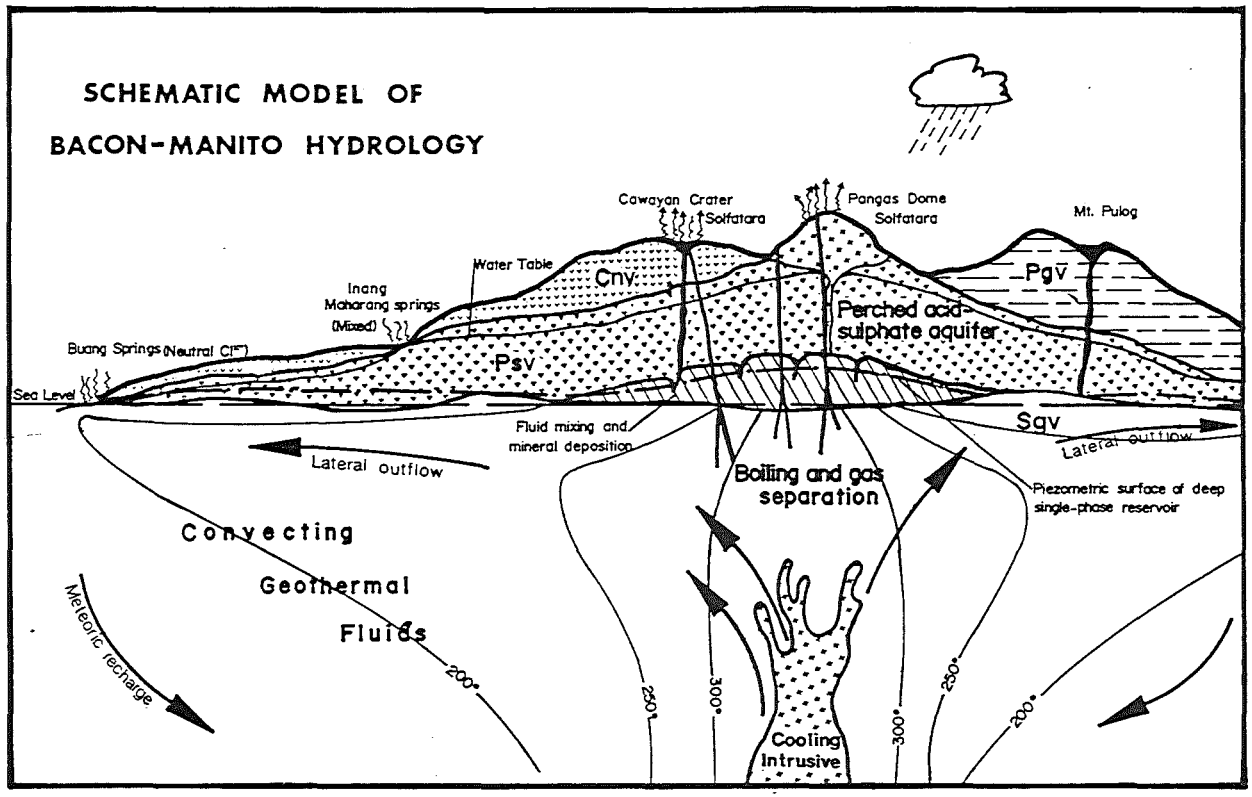

FIG. 6 Schematic section across Manito and Sorsogon showing some aspects of Pocdol Mountains' geothermal system (lithologic symbols as in FIG. 8). Upflow of hydrothermal fluids is centered in the highly-faulted Cawayan-Pangas area, with borehole temperatures of >320°C. Fluid flow is controlled by faults and/or permeable stratigraphic horizons (i.e., Rangas conglomerate, Suminandig-Pangas volcanics).

and/or stratigraphic contacts, towards Manito Lowlands (northwest) and Sorsogon (southeast). There is also a significant northeast flow towards Osiao.

1.3 PREVIOUS WORK

Initial geological investigation of southeastern Luzon and documentation of the major thermal areas in the region have been undertaken by Abella (1885), Centeno (1889), Abella and Vera (1893), and Adams and Pratt (1910). Feliciano (1928) investigated in detail the major thermal springs in the country, and grouped them into physiographic provinces. Those found in southeastern Luzon he regarded as belonging to the "*...southern volcanic region of Luzon*", and he further subdivided the thermal springs based on mineral substances present. Thus, a volcanic origin is implied for these springs. Pelaez (1953) grouped the Philippine volcanoes according to their eruptive phases, and classified the Pocdol Mountains as clusters of volcanic centres in their "*...solfataric and fumarolic stage without known activity*". The developments of Philippine geology from 1920 to 1960 are outlined by Alcaraz (1963).

Allen (1962) presented surface and bathymetric evidence suggesting a large sinistral fault (Philippine Fault) bisected the archipelago, comparable in displacement to the San Andreas Fault in western United States and the Alpine Fault in New Zealand. This structure is clearly present off the southern coast of Pocdol Mountains (Allen, 1962) striking southeast across the island of Leyte (e.g., Delfin and Tebar, 1986). Its control on the tectonics of the region, particularly the Pocdol Mountains, is discussed by Ferrer *et al.* (1986).

During the next 15 years, there was rapid evaluation of the 42 identified thermal fields (Fig. 7) for potential power generation. In 1966 the geothermal possibilities of the Tiwi thermal area were the first thermal springs to be investigated in Luzon (Alcaraz, 1976) while the Bacon-Manito hot springs located in the Pocdol Mountains are more recent.

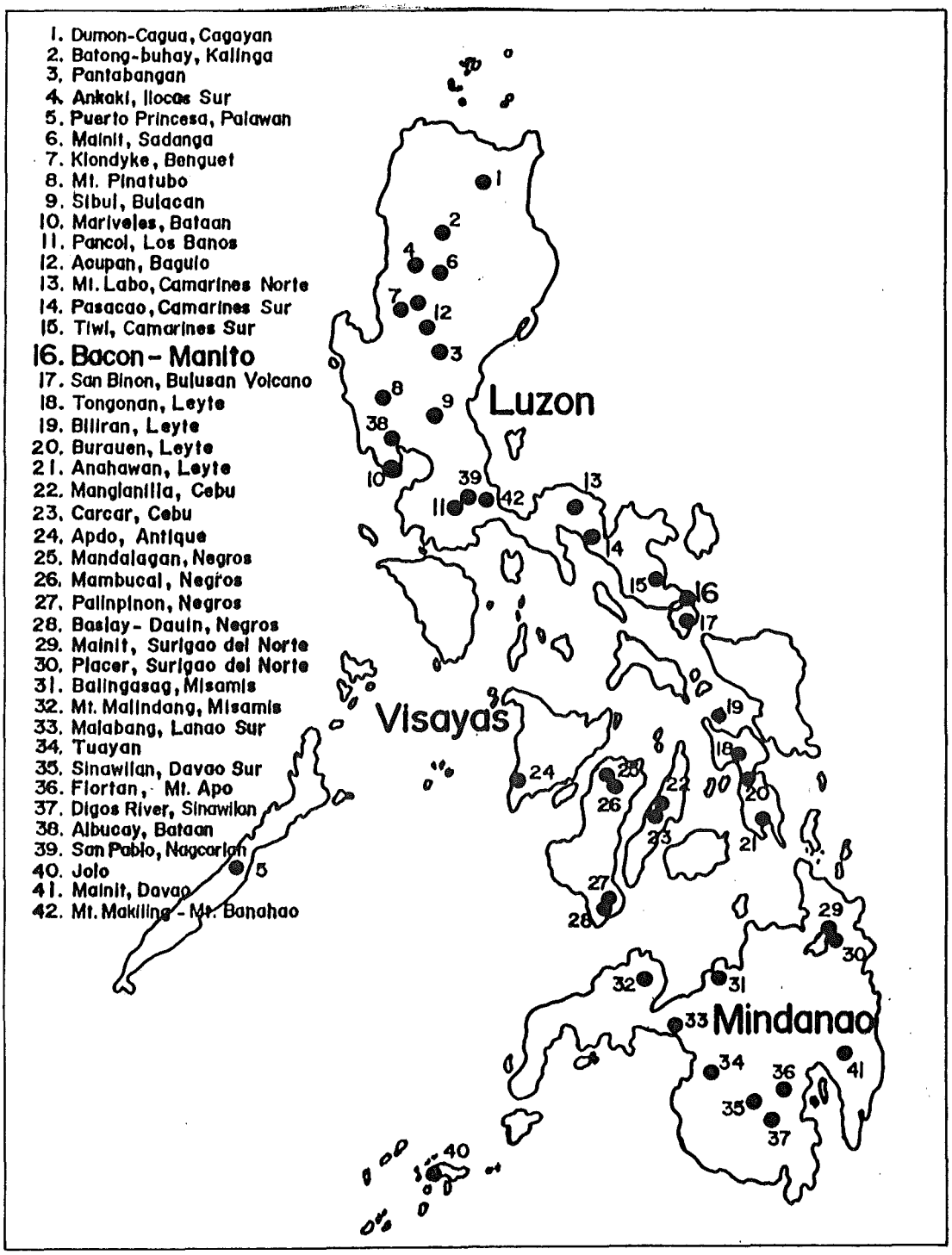

FIG. 7 Location of thermal fields in the Philippines (modified from Alcaraz, 1976).

In 1977, the Philippine National Oil Company's Energy Development Corporation (PNOC-EDC) commenced the initial phases of geothermal exploration of the area, which was later named **"Bacon-Manito (BacMan) Geothermal Field (or BMGF)"**. After two years of geoscientific investigations, the PNOC-EDC drilled two exploration wells.

From 1977 onwards, most of the work conducted in the field area relates to geothermal development, and this is summarised in the succeeding paragraphs.

The first detailed account on the geology of Pocdol Mountains was done by Obusan (1977; 1979) and Espiritu (1979). These results, together with Schlumberger resistivity traverse data, were used to constrain the initial drilling strategy. As more information was available, it became apparent that the hydrology of the field was far more complex than was initially conceived. Additional resistivity sounding exercises and detailed geological reviews were conducted. Because of the inaccessibility and the need of immediate data for the on-going drilling programme, aerial photographs were used with little field verification (De Leon *et al.*, 1983).

Alincastre (1984) undertook additional fieldwork in the EPM, earlier defined as a priority area for geothermal development. At the same time, drilling continued in the Palayang Bayan-Cawayan sector. Two major problems were encountered : **(i)** lack of permeability, and **(ii)** difficult drilling conditions (i.e., stuck pipes, sloughing, etc.). These were attributed to major fault intersections and formation characteristics. It became clear that the quality of existing geologic data was insufficient to construct consistent subsurface geological prognoses. A re-investigation of the surface geologic data was conducted in order to define : **(i)** permeable structures; **(ii)** detailed volcanic stratigraphy, and **(iii)** thermal manifestations (Panem and Alincastre, 1984a; 1984b; 1985). These reports contain the most definitive field data prior to this study.

Surface hydrothermal features were documented by Zapanta (1985) and Baltazar (1987). Borehole geology and hydrothermal alteration studies were undertaken by Reyes (1979-1984), Aniceto (1982), Zaide

(1983), Reid (1983-1984), Leach (1984-1986) and Bueza (1985-1987). In 1985, Reyes completed a MSc thesis comparing the "acid" and "neutral" pH alteration mineralogy from borehole samples.

Potassium-argon dates of one borehole and three surface samples, collected from the EPM (Bruinsma, 1983), suggested an average age of 1.7 Ma. However, these ages were suspect because of the effects of hydrothermal alteration. In addition, fossil-bearing specimens (Dizon, 1983) provided only broad age control (i.e., Late Miocene to Pleistocene), and hence, were of little use.

Parallel reviews were conducted by Kingston, Reynolds, Thom and Allardice (KRTA), Ltd., a consulting firm based in New Zealand, whose findings are outlined in KRTA (1986) Part I and Part II reports.

In summarising previous geologic work, it is clear that although there has been much work done in the Pocdol Mountains, the volcanic geology of the area is little understood. For example, no detailed stratigraphy has been established, and the different rock units have been described only as a '*...thick pile of volcanic materials and intrusives collectively named as "Pocdol volcanics"*' (Alincastre, 1983; Panem and Alincastre, 1985; Reyes, 1985; KRTA, 1986). This, however, is clearly an over-simplification of a complex volcanic terrane.

Likewise, the absence of petrochemical data and absolute chronology, combined with poor outcrop sections and inaccessibility, resulted in conflicting interpretations by previous workers.

CHAPTER II

GEOLOGY OF POCDOL MOUNTAINS

CHAPTER II

GEOLOGY OF POCDOL MOUNTAINS

Seven distinct lithostratigraphic units (Table 1) comprise the Pocdol Mountains, and their subaerial distributions are shown in Fig. 8. These rocks, together with two sedimentary units (Gayong Formation and Rangas conglomerate) and two intrusive units (Rangas microdiorite and Pangas intrusives), form the **Pocdol Volcanic Field (or PVF).**

A detailed 1:50,000 scale geologic map is contained in the back pocket of this thesis.

2.1 NOMENCLATURE

The PVF comprises several closely spaced strato-cone complexes, which are covered with thick vegetation. In such terrane, terminology based on superposition and lateral continuity has only limited application (Williams and McBirney, 1979, p.311; Fisher and Schmincke, 1984, p.350-351). For this reason, formal names are not proposed in this study, and units are referred to as **"volcanics"** (e.g., Pulog volcanics), in the manner originally suggested by Ashley *et al.* (1933, p.443-444). Informal nomenclature used here follows Van Eysinga (1970).

Furthermore, it is also not possible to designate a truly representative stratotype for each unit. Instead, a reference area (or areas) is designated, where the fullest variety of rocks are exposed.

2.1.1 Pyroclastic Terminology

Wright *et al.* (1980; 1981) invoked that no unique classification for pyroclastic deposits can be made, and they proposed a dual classification, namely :

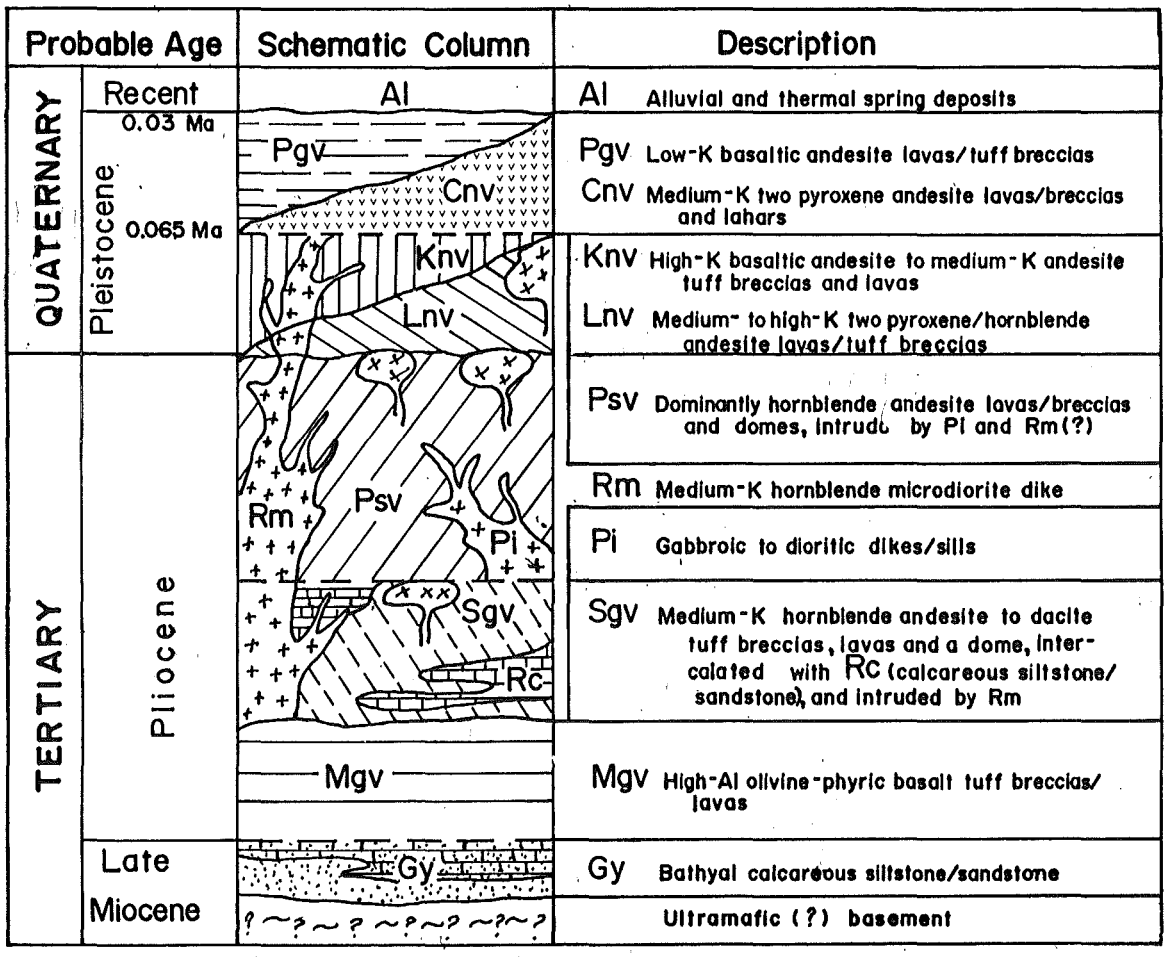

TABLE 1 Proposed volcanic stratigraphy of Pocdol Mountains (lithologic symbols as in FIG. 8).

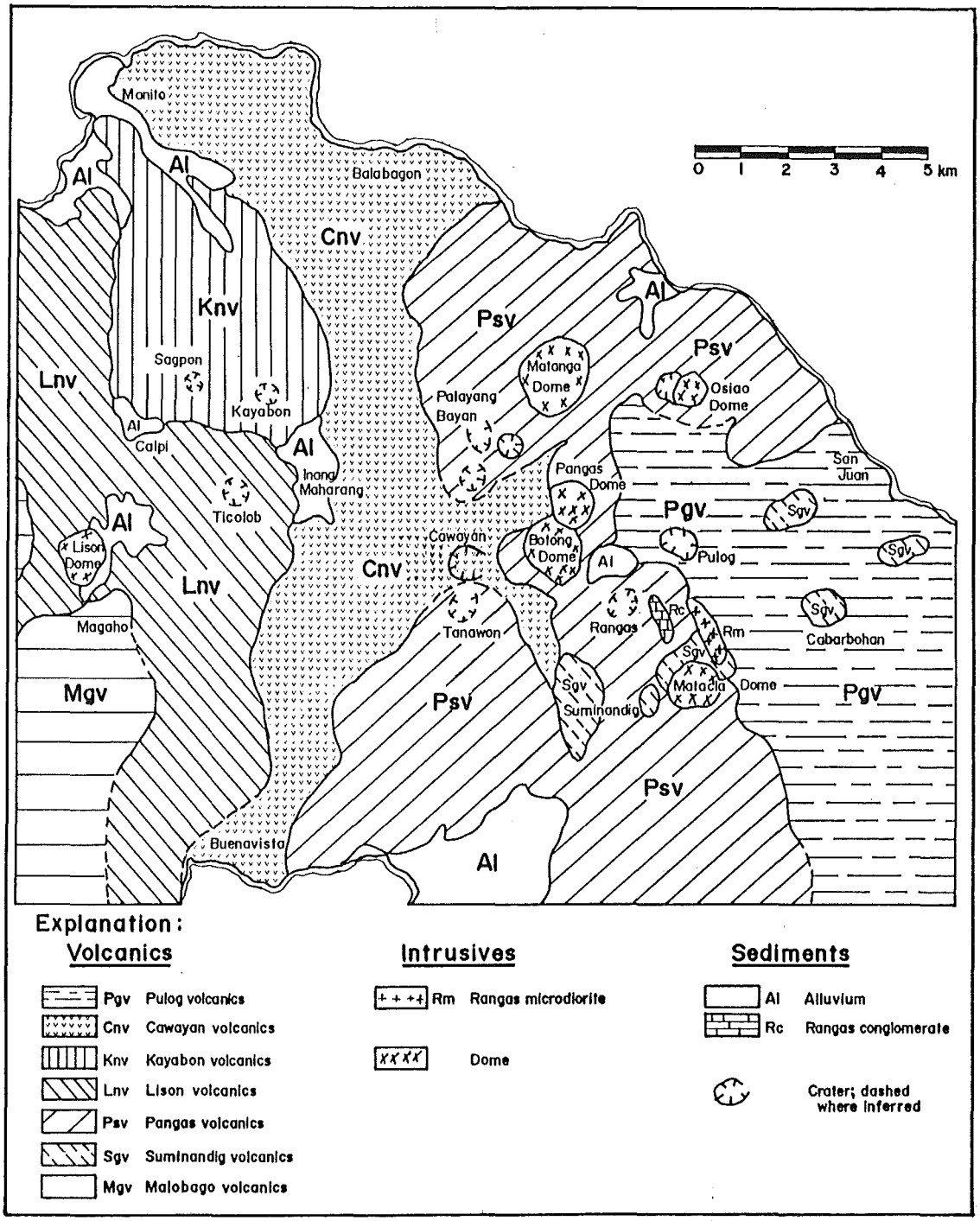

FIG. 8 Proposed geologic map of Pocdol Mountains (modified from Panem and Alincastre, 1985). Former eruption centres are indicated as bold circle (with single hachure); dashed where inferred.

(i) a **lithological classification** which may be solely descriptive, but which may also be used to discriminate on a lithological basis the mechanisms which produce a particular pyroclastic deposit, and

(ii) a **genetic classification** to interpret the genesis of a deposit.

For the purposes of this study, lithologic types are based on grain size (Fig. 9A) and distribution of pyroclastic fragments (Fig. 9B).

The general term **volcaniclastic** (Fisher, 1961) includes all clastic volcanic materials formed by any process of fragmentation, dispersed by any kind of transporting agent, deposited in any environment or mixed in any significant portion with nonvolcanic fragments. Rocks composed predominantly of angular fragments of any rock greater than 2 mm in size, the brecciation or emplacement, or both, of which was the result of volcanic action are termed **volcanic breccias** (Wright and Bowes, 1963); but the use of the word "volcanic" is only intended to mean the fragment origin and not the origin of the breccia, as suggested by Fisher (1963).

The term **pyroclastic breccia** refers to pyroclastic rocks whose average pyroclast size exceeds 64 mm, and in which angular pyroclasts predominate; if rounded pyroclasts are dominant, the term **agglomerate** is used (Schmid, 1981). **Tephra** (Thorarinsson, 1954) is applied to all unconsolidated pyroclastic accumulations irrespective of size and is synonymous with "pyroclastic materials" (Fisher and Schmincke, 1984) or "pyroclasts" (Schmid, 1981).

Tuff deposits are described using the scheme of Cook (1965) and is shown in Fig. 9C.

For the genetic classification of fragmental volcanic deposits, Fisher (1966) emphasises the process of fragmentation, and secondly, the size of the fragments. He notes that :

A

Grain size (mm)	Epiclastic	Pyroclastic	
256	Boulders / blocks	Coarse	Blocks and bombs
64	Cobble	Fine	
2	Pebble	Lapilli	
1/16	Sand	Coarse	Ash
1/256	Silt	Fine	
	Clay		

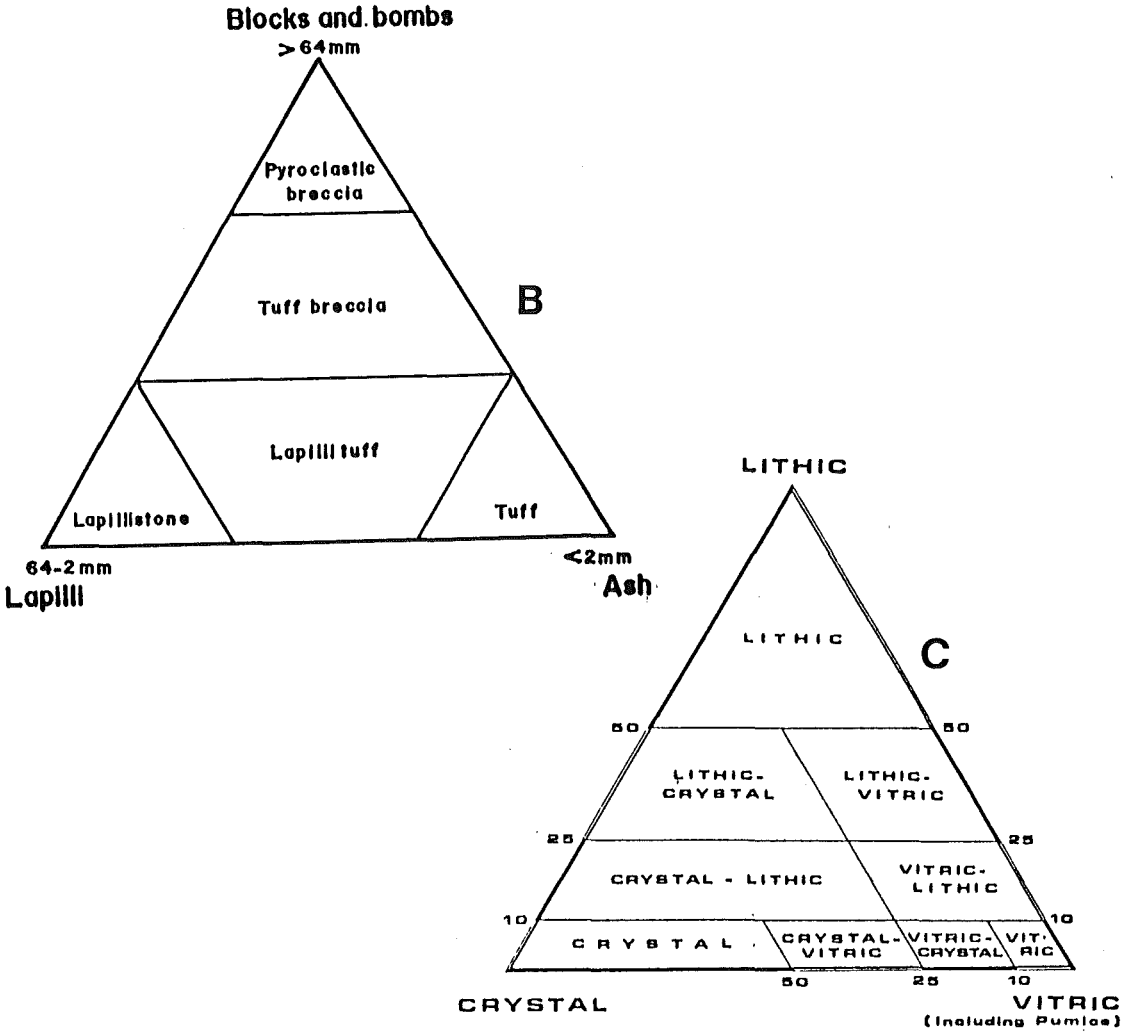

FIG. 9 (A) Lithologic classification of volcanic fragments (after Fisher, 1961); (B) Lithologic types of fragmental volcanic rocks (after Fisher, 1966); note that precise percentage boundaries for the mixtures are omitted in order to allow usage without quantitative grain size data, and (C) Tuff nomenclature (after Cook, 1965).

> *"Genetic categories are autoclastic, pyroclastic, and epiclastic (to which hydroclastic should be added), thereby placing emphasis on the manner of fragmentation. It is important to distinguished between fragments that are produced instantly such as the pyroclasts, and those that are produced over a long period of time by the weathering of volcanic rocks... .Pyroclastic deposits may be dispersed and deposited by streams, but such dispersal does not alter the fact that the fragments are pyroclastic in origin. Thus, there may be 'primary' (unreworked) as well as 'secondary' (reworked) pyroclastic* deposits" *(Fisher, 1966, p.226)*

In addition, "alloclastic" (Wright and Bowes, 1963) should also be included; these are fragments disrupted from pre-existing volcanic rocks due to igneous activity, with or without intrusion of fresh magma.

Lithological classification will be applied in this study, and when genetic interpretations are possible, these will be discussed separately from lithologic descriptions.

2.1.2 Volcanic Facies

The recognition of volcanic facies has proved valuable during the volcano-stratigraphic investigation of strato-cone complexes at PVF, and follows the treatment of Parsons (1969). Two major facies can usually be recognised. These are :

(i) vent or cone-complex facies; piles of volcanic materials, both flows and pyroclastic rocks, produced directly by volcanism and deposited haphazardly with little or no modification by geomorphic agencies, and

(ii) epiclastic or alluvial facies; clastic rocks formed by erosion or reworking, or both, of the volcanic debris, but having the same overall composition as vent-facies materials.

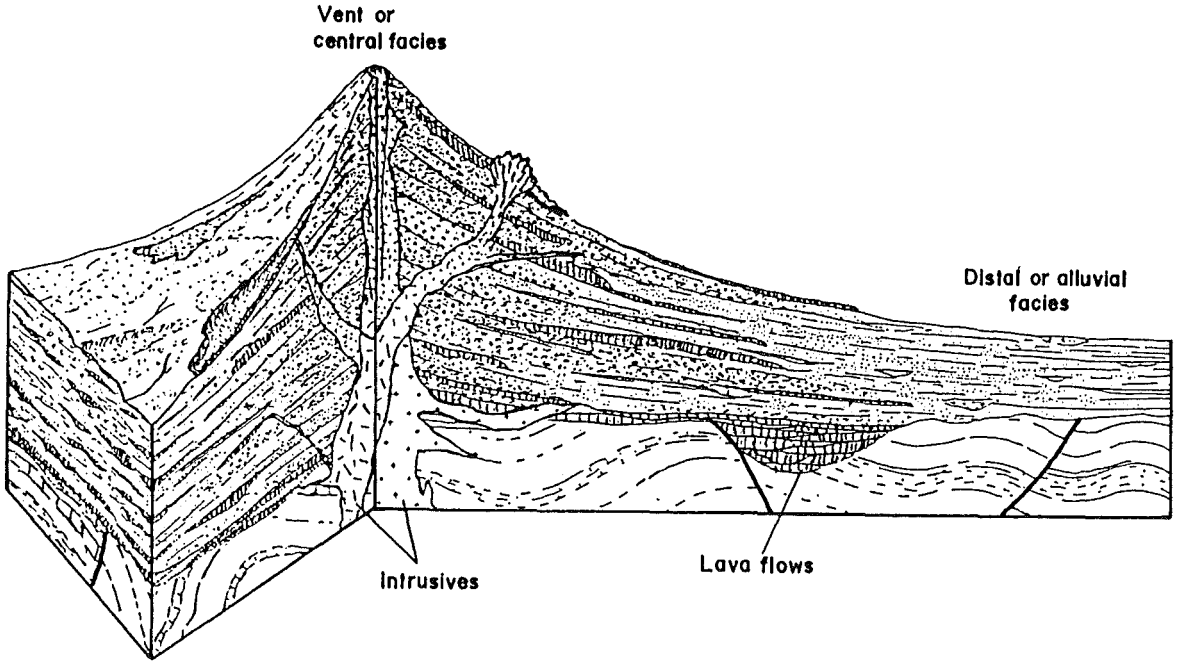

FIG. 10 Hypothetical section of a strato-volcano, showing the spatial relationship of vent facies and alluvial facies rocks (after Parsons, 1969).

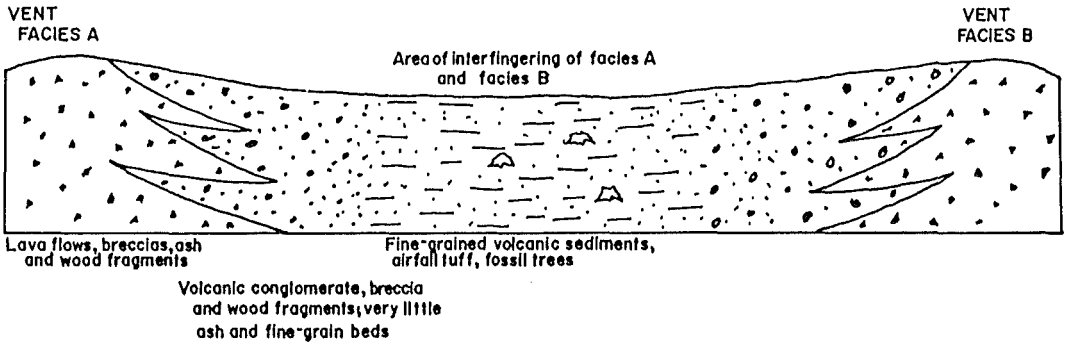

FIG. 11 Hypothetical section of two adjacent strato-cones, showing facies relationships (after Smedes and Prostka, 1972).

A generalised scheme of these volcanic facies, and facies relationship between two vent complexes are presented as Figs. 10 and 11, respectively.

In the Pocdol Mountains, the cone-complex facies occurs within 5-10 kms of the source regions. This association is characterised by features such as : **(i)** lava flows with associated autoclastic breccias which are often volumetrically subordinate to fragmental deposits; **(ii)** coarse, poorly sorted volcanic breccias with angular to subrounded clasts up to several metres in size; **(iii)** steep primary dips ($>20^{o}$) which are radial to the central vent; **(iv)** small, irregular intrusive bodies which have deformed the deposits of the host cone, and **(v)** pervasive hydrothermal alteration with steep lateral gradients.

Away from the source regions, the cone-complex facies interfingers with, and grades into, aprons of well-bedded to poorly sorted reworked volcaniclastic materials, having primary dips of less than 5^{o} which are referred to as epiclastic or alluvial facies. This facies has not been extensively studied at PVF. The facies encompasses deposits which are generally referred to as "ring plain" deposits, and includes : **(i)** lahars with subrounded clasts and abundant sand- to mud-size matrix; **(ii)** interlayered soils and organic matter, and **(iii)** lava flows largely restricted to isolated vents and to local valley-filling flows.

2.2 VOLCANIC STRATIGRAPHY

Seven lithostratigraphic units are described below, from oldest to youngest, based on field relations and five new potassium-argon ages (Table 2). A brief note on the nature and distribution of the basement rocks at PVF is given first.

Localities and rivers mentioned in the text are given in Figs. 3 and 8.

INS TR No.	SAMPLE NO. (Location)	ROCK TYPE (Lithologic Unit)	K wt%	Ar(40)* nl/g	Ar(40) %total	Age2 (Ma)
12832TR	13(25)	Two pyroxene hornblende-phyric andesite/Lison Dome (Lnv)	1.676	.031 .038	13 6	.478 (+ .12) .580 (+ .15)
12833TR	3(10)	Two pyroxene andesite/Buyo river (Knv)	1.128	<.001 <.002	2 .3	<.08 <.05
12834TR	22(12)	Hypersthene augite-phyric andesite/Cawayan crater (Cnv)	.767	<.0004	.2	<.04
12835TR	17(29)	Two pyroxene hornblende micro-diorite/San Lorenzo river (Rm)	.733	<.001 <.002	2 .5	<.08 <.05
12836TR	40(6)	Hypersthene augite-phyric basic andesite/Sta. Cruz river (Pgv)	.318	<.0004	.2	<.04

TABLE 2 List of five new K-Ar ages of five surface rocks. Samples are indicated in the attached geologic map, and descriptions are given in the appendix.

TR = total rock, 200-400 μ size

Decay constants ^{40}K : $\lambda_\beta = 0.4962 \times 10^{-9}yr^{-1}$; $\lambda_e = 0.581 \times 20^{-10}yr^{-1}$
Isotopic abundance $^{40}K/K = 0.01167\%$
Errors are two standard deviations

Fig. 12 Panoramic view of Malobago volcanics (Mgv), looking NE. Foreground is Magaho area and the mid-section of Pili river. The skyline (centre) is Li-son Dome.

2.2.1 Basement Rocks

Subvolcanic basement rocks at PVF comprise lenses of Late Miocene-Early Pliocene calcareous to carbonaceous siltstones and sandstones of the Gayong Formation (Gy), which are encountered at about -1500m (reduced level) in boreholes Pal-8D and 6D in the EPM (Reyes, 1985). The contact between the overlying highly altered volcanic rocks, which are inferred here to be Malobago volcanics, and the Gayong Formation is marked by sedimentary breccias. The contact horizon shows angular to subrounded clasts which are cemented by diagenetic calcite (Reyes, 1985).

The rock unit unconformably rests on ultramafic rocks, and some of these have been disrupted and have been included in younger lavas as xenoliths (i.e., in the lavas of Pulog volcanics).

2.2.2 Malobago Volcanics (Mgv)

The name Malobago volcanics (Mgv) is here proposed for dominantly basaltic rocks, exposed mainly along river valleys and beds at Magaho area (Fig. 12). The rocks only occur in the southwestern part of the study area and are named after the Malobago ridge, a prominent amphitheatre-like feature to the west of the mapped area. The best exposures occur at the headwater section of Pili river, where the greatest thickness exceeds 50 metres. However, total volume cannot be estimated, as only the eastern part of the deposit has been studied.

The unit is believed to be the oldest volcanic deposit in the field area although no potassium-argon age is available. This inference is substantiated by a greater degree of erosion relative to the volcanic rocks at PVF. An age of Early Pliocene is proposed.

Malobago volcanics show a great lithologic but little petrographic variation. Most of the rocks are vent facies assemblage, consisting of lava flows, monolithologic and heterolithologic tuff breccias. However, at lower elevations (i.e., near Buenavista), rounded fragmental deposits such as unconsolidated sand and gravel deposits are common. Lava flows occur both in the upper and lower portions of the cone complex (i.e., Magaho area; Palupay creek), and in most outcrops the flow interiors are cut by blocky jointing, and platy joint-

ing is always developed near the base. Flow banding is largely absent. Monolithologic tuff breccias are almost invariably associated with the lavas. They are poorly sorted, unwelded and clast-supported subangular to subrounded clasts, <0.5 m in diameter. The tops of the flows, however, are not exposed.

Massive weakly-bedded heterolithologic tuff breccias dominate the lower portion of the cone complex (i.e., at lower sections of Palupay river) and consist of angular to subrounded dense blocks (<2 m) and subordinate rounded vesicular highly oxidised bombs. Clasts are matrix-supported consisting of subrounded to subangular lapilli and coarse- to medium-sized crystal lithic tuff. The tuffaceous matrix is indurated but not welded.

The base of the Malobago volcanics is not exposed, but at depth the rocks rest unconformably on Tertiary marine sediments of the subvolcanic basement. The unit is unconformably overlain by the Lison volcanics in the headwaters of Pili river (Fig. 12).

2.2.3 Suminandig Volcanics (Sgv)

The name Suminandig volcanics (Sgv) is proposed for the sequence of andesitic to dacitic rocks in the EPM, which are interbedded with sedimentary lenses and are intruded by dikes. The unit is named after Suminandig hill (Fig. 13), a volcanic remnant adjacent the Cawayan river. No absolute age exists for the Suminandig volcanics, but they were erupted perhaps concurrently or following the volcanic activity at Malobago volcano. Hence, an age of Early to Middle Pliocene is proposed; the unit is the oldest in the EPM.

Outcrops of the Suminandig volcanics are sparse, and several of the rocks form knobs east of Mt. Pulog, i.e., Cabarbohan hill (Fig. 14). Good exposures are found in the lower sections of Cawayan and Makabug river valleys and the headwater section of San Lorenzo river; the greatest thickness is <30 m exposed at Makabug river adjacent the Matacla Dome. However, the original volume of this unit cannot be estimated due to limited outcrop sections, but the disposition of the paleo-Suminandig cone can be inferred.

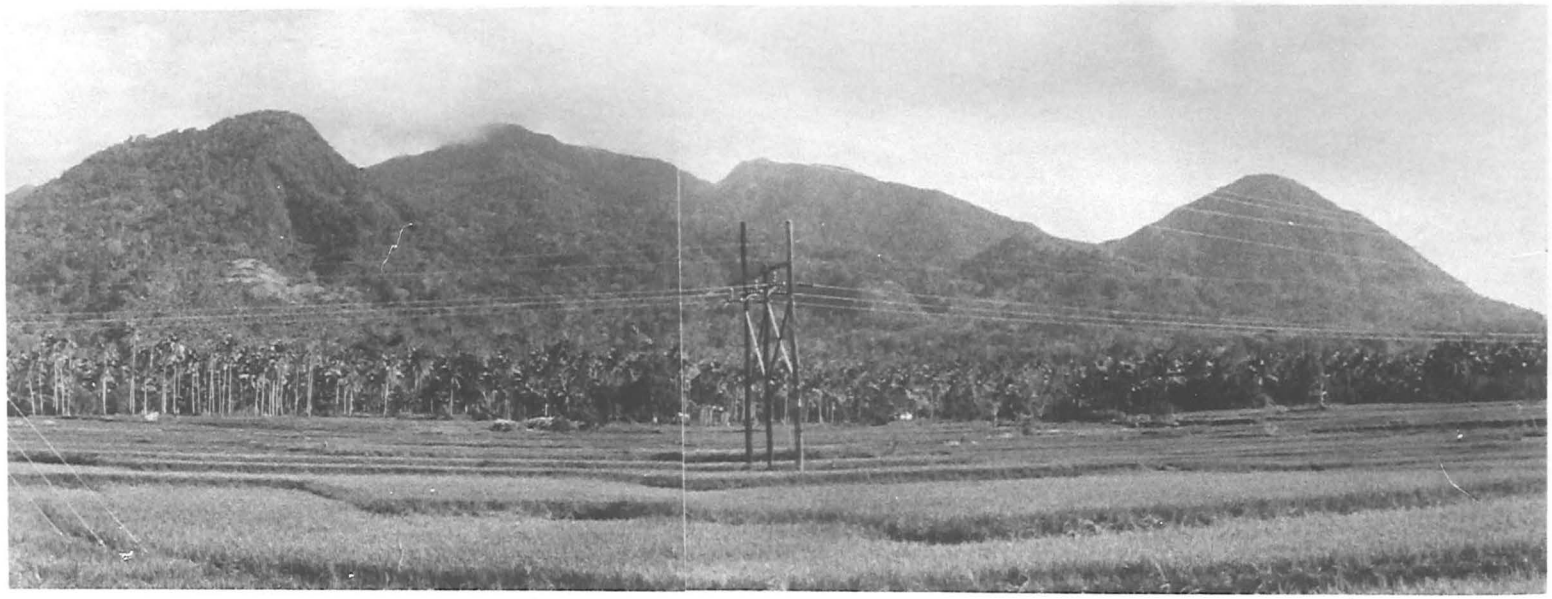

Fig. 13 Panoramic view of Suminandig volcanics (SGV) , looking N. The Suminandig hill is the leftmost volcanic pile, and to the far right is the Matacla Dome. The highest peak (centre) is Mt. Rangas, and the adjacent rocks are those of the Rangas conglomerate unit (Rc).

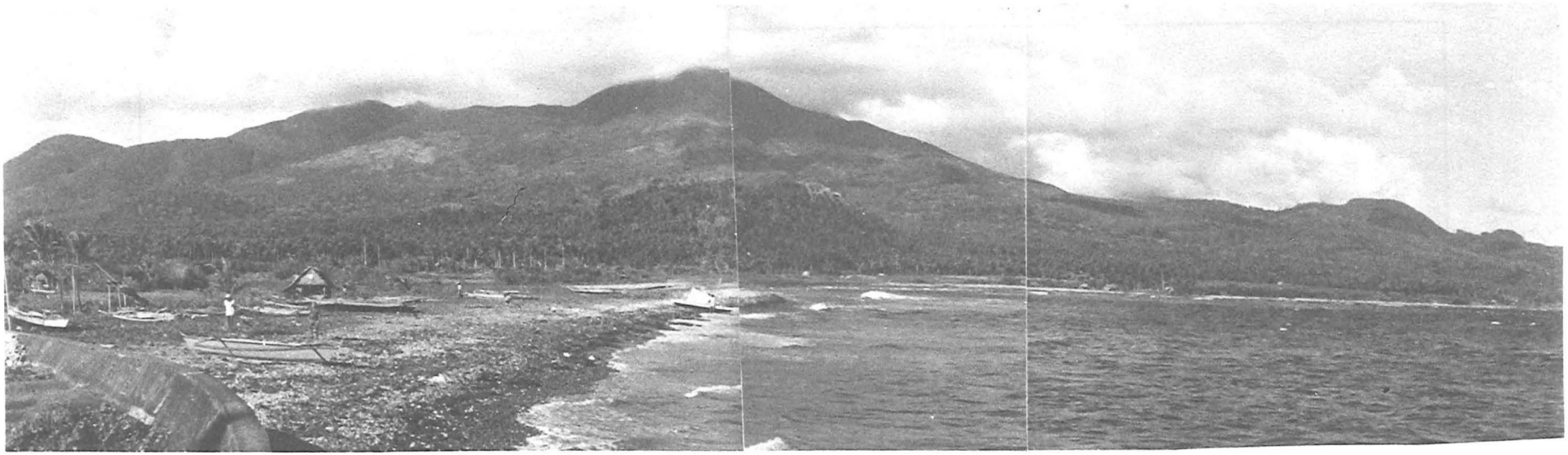

Fig. 14 Panoramic view of Mt. Pulog (centre), looking W. Low-lying hills in the foreground are outcrops of Suminandig volcanics, i.e., Cabarbohan hill, which is a small conical hill to the left of the photo. The skyline to the far left is the Matacla Dome, and the Rangas conglomerate unit (touching the clouds) is in-between Matacla and Pulog peaks. The cloud-covered peak (farthest) to the right of Rangas conglomerate is Mt. Rangas. The humped-back feature near Matacla Dome is the Rangas microdiorite. On the other side of the photo (far right) is Osiao Dome.

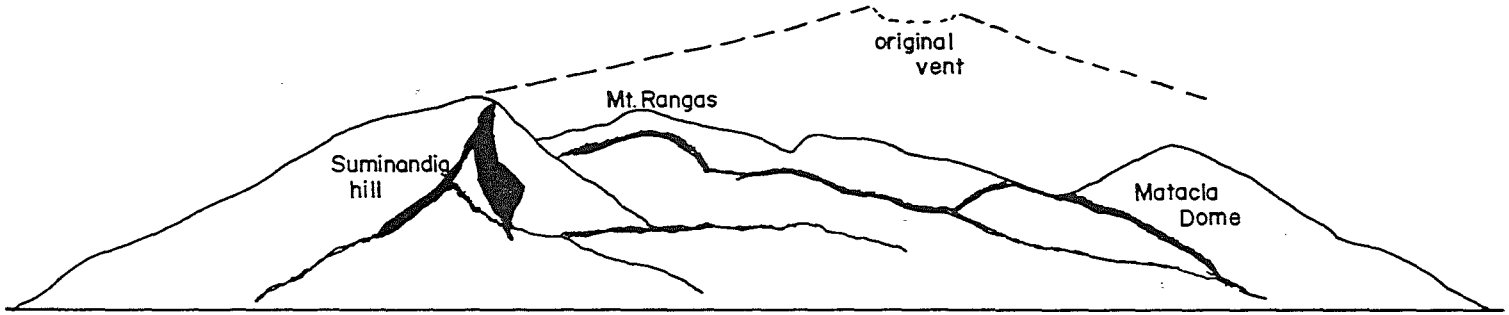

FIG. 15 Schematic reconstruction of Suminandig volcano, looking north.
N.B. The foreground view is drawn from FIG. 13; NOT DRAWN TO SCALE.

A possible reconstruction of Suminandig volcano (Fig. 15), based on the distribution of outcrops, shows the central vent regions to be near Matacla Dome and Rangas microdiorite.

The rocks show great lithologic and moderate petrographic variation. The vent facies consists of a highly-eroded assemblage of volcanic breccias, agglomerates and minor lavas. Interbedded with these rocks are abundant moderately graded and sorted conglomeratic breccias and pyroclastic breccias, showing heterolithologic clasts. The clasts are usually dense, subrounded to subangular, and range in size from pebbles to boulders. The clasts are supported by a tuffaceous to sandy matrix materials.

Near the contact between the "ring plain" deposits and cone-complex rocks (i.e., lower sections of Makabug river and San Lorenzo river), a low-lying lava dome (Matacla Dome) is exposed. The Matacla Dome (Fig. 13) is inferred to be a parasitic vent erupted on the southern slopes of the Suminandig cone.

In the vicinity of Matacla Dome, a fault-bounded microdiorite dike, named here as the **Rangas microdiorite (Rm)**, has metamorphosed the adjacent Suminandig volcanics (Reyes, 1985). Hence, the unit is considered in this study as a part of the Suminandig volcanics. A potassium-argon age of 1.79 Ma has been reported (Bruinsma, 1983), but a recent potassium-argon date yielded an age of <0.065 Ma (CJ Adams, pers. comm., 1987). The younger age could be due to argon loss resulting from hydrothermal alteration.

In addition, the Rangas microdiorite appears to be intruding the Kayabon and Lison volcanics as shown in Table 1; however, this is not so. There is no field evidence for its presence in the WPM and in fact, Table 1 only portrays the similarity in age between the Rangas microdiorite and the Kayabon-Lison volcanics.

Fluviatile materials, mixed with pyroclastic rocks, travertine, calcareous siltstone and sandstone clasts, are found in the vicinity of Osiao and Matacla Dome. The rocks are named here as **Rangas conglomerate (Rc)**, which were eroded from the "saddle" of Mt. Rangas (Panem and Alincastre, 1985; JB Pornuevo, pers. comm., 1985). These rocks are perhaps the debris that were deposited during periods of volcanic quiescence.

The Rangas conglomerate is a poor marker horizon because of its discontinuous outcrops; however, the unit provides some control on the flow of hydrothermal solutions (i.e., stratigraphic permeability), based on a recently completed borehole in the Pangas-Pulog area (CM Recio, pers. comm., 1988).

The base of the Suminandig volcanics is not exposed, and at depth it is not known if the deposit overlies pre-Tertiary sediments or the alluvial facies of the Malobago volcanics. This part of the field area has never been drilled.

2.2.4 Pangas Volcanics (Psv)

The name Pangas volcanics (Psv) is here proposed for a thick series of dominantly andesitic rocks in the EPM. The unit is named after Mt. Pangas, a faulted dome which together with Botong Dome, is interpreted to constitute the core of a large strato-volcano referred to in this study as the Pangas volcano. The Pangas Dome currently shows active hydrothermal activity.

Flank eruptions occurred from four distinct groups of vents, which are listed below in terms of increasing degree of erosion, namely :

(i) the Rangas crater (Figs. 13 and 14) in the southeast;
(ii) the Tanawon crater in the southwest;
(iii) the Matanga Dome (Figs. 13 and 14) and Palayang Bayan craters in the north, and
(iv) the Osiao crater (Fig. 14) in the northeast, which is partly covered by the Osiao Dome.

A potassium-argon date of the Osiao Dome (Fig. 14) yielded a minimum age of 1.5 Ma (Bruinsma, 1983), and hence, the Pangas volcanics are considered here to be Middle Pliocene to Early Pleistocene in age.

In the Cawayan area, gabbroic to dioritic dikes or sills occur below +500 m (reduced level). The intrusives are spatially and mineralogically related to the Pangas volcano; thus, are named here as the **Pangas intrusives (Pi)**. The timing of hypabyssal intrusions is poorly-known, but it is believed to be a separate event from the one that produced the Rangas microdiorite.

The upper boundary of the Pangas volcanics is defined at the headwater section of Osiao river, where laharic breccias, tuff breccias and minor lavas are unconformably underlain by basaltic tuff breccias of the Pulog volcanics. This boundary also appears to be a geomorphic contact between contemporaneous deposits of adjacent Mts. Pangas and Pulog (KRTA, 1986); however, the youthful morphology of Mt. Pulog suggests the contrary.

The contact between the Pangas volcanics and the underlying Suminandig volcanics is observed in the lower section of Cawayan river valley, near Matacla Dome, but thick vegetation cover precluded a detailed description.

2.2.5 Lison Volcanics (Lnv)

The Lison volcanics (Lnv) are named after the low-lying Lison Dome (Fig. 16), which was emplaced 0.478 Ma ago (CJ Adams, pers. comm., 1987). Several collapse or circular depressions occur nearby, which could have formed as a result of magma withdrawal. Hence, this area is probably once a major eruption site.

The extrusives consist of voluminous tuff breccias, laharic breccias, and minor lavas and pyroclastic breccias and agglomerates. Most of these are exposed along river valleys, and lavas are usually found as vertical cliffs along ridges. A good section is observed near the highly-eroded peak of Mt. Ticolob (Fig. 16), where 60 m of columnar-jointed and sheeted lavas grade vertically into monolitho-

Fig. 16 Panoramic view of Lison volcanics (Lnv), looking SW. Foreground is the Inang Maharang valley, and to the left is an unconformable contact relationship between the overlying Cawayan volcanics and the underlying Lison volcanics exposed in the headwaters of Menito river. Mt. Ticolob is the nearest peak to the right of the photo.

logic tuff breccias. This unit is the most widespread volcanic deposit in the WPM, covering an area of about 25 km^2; a minimum volume is estimated at 20 km^3.

The base of this unit is not exposed, however, an unconformable relationship is apparent with respect to the nearby Malobago volcanics, as indicated by an abrupt lithologic change near Magaho area, i.e., light grey outcrops are found in higher elevations (Lison-Ticolob area) whereas dark massive rocks are common downstream (i.e., Magaho area; Palupay creek).

The upper portions of the Lison volcanics are dominated by volcanic breccias and tephras, and these rocks are juxtaposed against laharic breccias and tuff breccias of the Cawayan volcanics; sections along the headwaters of Menito river (Fig. 16) suggest that the Cawayan volcanics are unconformably overlying the Lison volcanics.

2.2.6 Kayabon Volcanics (Knv)

The name Kayabon volcanics (Knv) is given for dominantly basaltic andesites exposed in the WPM. The unit is named after Mt. Kayabon (708 m), which is one of the two inferred source regions; the other suspected vent, Sagpon peak (487 m), is more eroded and is separated by the Balasbas creek.

A recent potassium-argon date of a lava erupted from Mt. Sagpon yielded a minimum age of <0.065 Ma (CJ Adams, pers. comm.,1987). Since the degree of erosion and the disposition of both Kayabon and Ticolob volcanics are similar, it is inferred that the two deposits were contemporaneous and were extruded probably during Middle to Late Pleistocene.

The rocks are mostly tuff breccias and minor lavas, and are bounded by Buyo and Manitohan rivers, where most of the good sections (<20 m) are found. Slumping of upper slope materials formed intermontane debris piles, such as the Inang Maharang (Fig. 16) and Calpi valley deposits. Assuming a simple cone-like geometry and allowing for material removed by erosion, the original volume was probably on the order of 15 km^3.

Fig. 17 Deposits of the Cawayan volcano: (A) Weathered lahars near the vent regions; (B) Jointed blocky lavas about 4 kms NW of the crater, and (C) Lahar section near Manito, about 10 kms NW of the crater.

The upper boundary rocks, i.e., tuff breccias and minor lavas outcropping along the Manitohan river, are unconformably underlain by lahars, volcanic breccias, laharic breccias and volcaniclastic materials of the Cawayan volcanics; the basal portion of the Kayabon volcanics is not exposed.

2.2.7 Cawayan Volcanics (Cnv)

The Cawayan volcanics (Cnv) are named after the Cawayan crater in the EPM, and form two major flow units towards Manito and Buenavista and two minor northeast- and southeast-trending flows. The unit is heavily cut by faults, commonly marked by thermal seepages and hydrothermally-altered outcrops. The rocks cap variably altered eruptives of the Pangas volcanics, which attain a maximum thickness of <300 m from borehole data (e.g., Reyes, 1985). A minimum volume of 25 km^3 is estimated.

A recent potassium-argon date of a lava from the Cawayan crater yielded a maximum age of <40,000 years B.P. (CJ Adams, pers. comm., 1987), and a similar potassium-argon age was also obtained for a crystal lithic tuff of Mt. Pulog. Since no contact relationship between these rocks has been observed, their relative stratigraphic position is inferred on the degree of erosion. It appears that Cawayan volcanism pre-dated Mt. Pulog eruptions by perhaps 10^4-10^5 years.

In the near-vent region (Figs. 17A and 17B), voluminous lavas, tuff breccias and minor lahars occur, and these rocks grade into moderately- to gently-dipping unwelded and poorly sorted tuff breccias and laharic breccias some 6-10 kms north-northwest of the crater at Balabagon area. No basal or fall-out pyroclastic units however were mapped. From here, the deposit imperceptibly grades into unconsolidated and poorly sorted mudflows consisting of volcanic detritus near Manito (Fig. 17C).

The Manito lahars cover an area of nearly 15 km^2, and are characterised by undulating and hummocky topography. This is typical of lahar fields along the distal margins of pyroclastic flows (Neall, 1976). Since no evidence for "hot" emplacement was found, the lahar deposit was probably initiated by heavy rains on loose materials from

the Cawayan crater or perhaps, by admixing of a pyroclastic flow with running or ponded water, as happened at Mt. Hibok-hibok (MacDonald and Alcaraz, 1956). Furthermore, the type of matrix materials (i.e., muddy to soily) precluded the possibility that these deposits were formed by "dry" rock avalanches (Ui, 1986).

2.2.8 Pulog Volcanics (Pgv)

Pulog volcanics (Pgv) are named after Mt. Pulog (Fig. 14), the least-eroded volcanic cone in the Pocdol Mountains; the summit region is occupied by a well-preserved crater (800 m) adjacent to a dome-shaped protrusion (1032 m), which has steep margins down to the western flanks of the volcano whereas the eastern slopes show moderately-dipping tuff breccias and lavas.

Abundant oxidised basaltic bombs are found in the summit area, and several of these occur as subangular to subrounded clasts mostly in the heterolithologic tuff breccias exposed downstream. The pyroclastic flows are valley-filling deposits, showing even top surfaces consisting mostly of poorly- to moderately sorted and unwelded lithic crystal-rich tuffs. Juvenile lapilli clasts are usually subangular to subrounded and several of these are vesicular. The rocks grade imperceptibly downslope into indurated volcanic breccias, usually enclosing large (>1 m) subangular to subrounded blocks.

2.3 FAULTING

No active faulting is recognised in the Pocdol Mountains (Fig. 18). Fault scarps do not show "free faces", and advanced rounding and gullying of the bases and crests of these scarps indicate movement occurred at least 10^3 years ago (Wallace, 1977). The lack of historic seismicity and geologic evidence of displacement in the recent geologic past further indicates a period of at least 10^4 years since the last faulting event occurred.

Detailed fault data in the study area are given by Panem and Alincastre (1985).

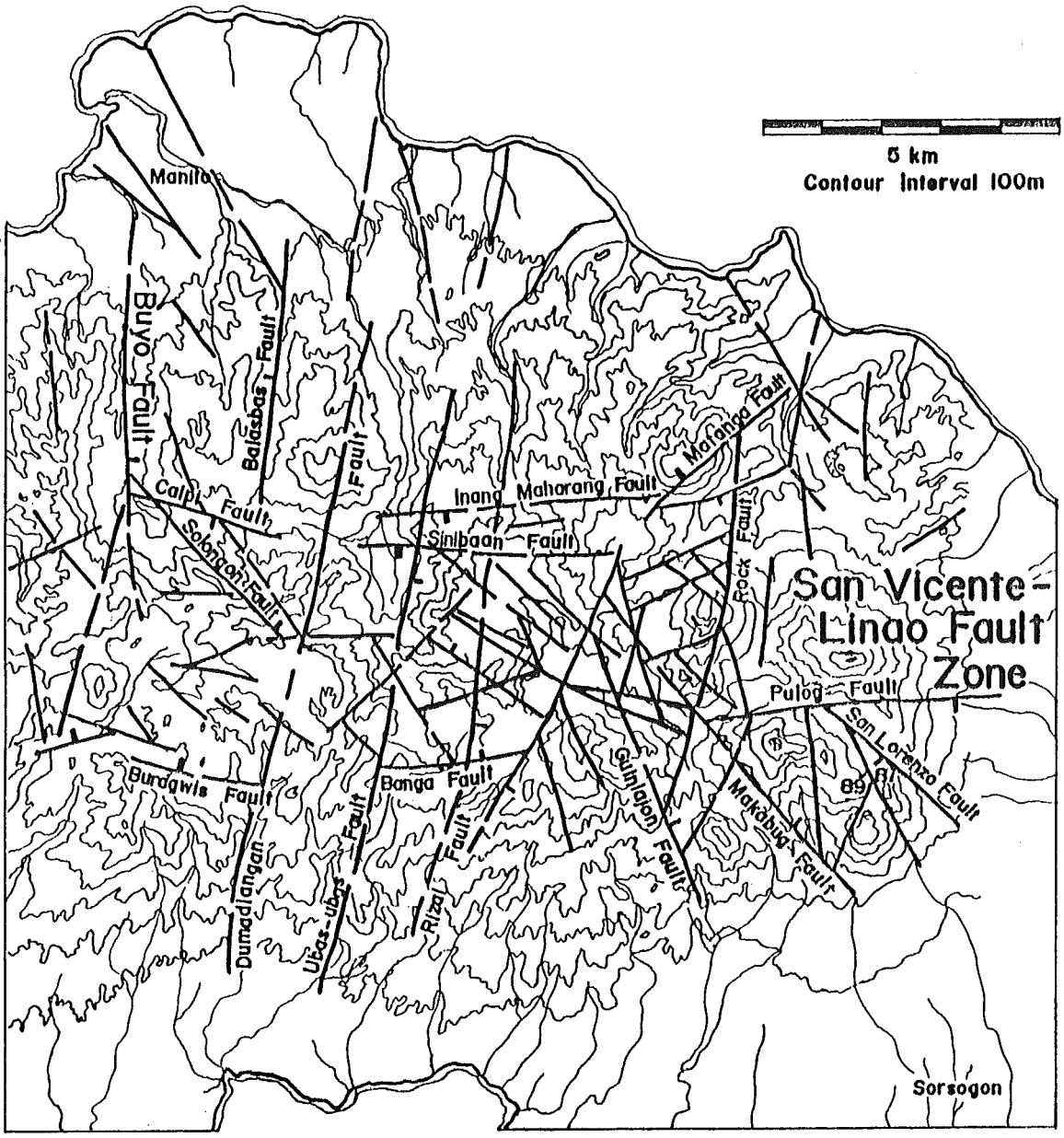

FIG. 18 Proposed fault map of Pocdol Mountains (modified from Panem and Alincastre, 1985). The San Vicente-Linao Fault zone is defined in the field area by the Calpi-Inang Maharang Faults in the north, and the Buragwis-Banga-Pulog Faults in the south (see text).

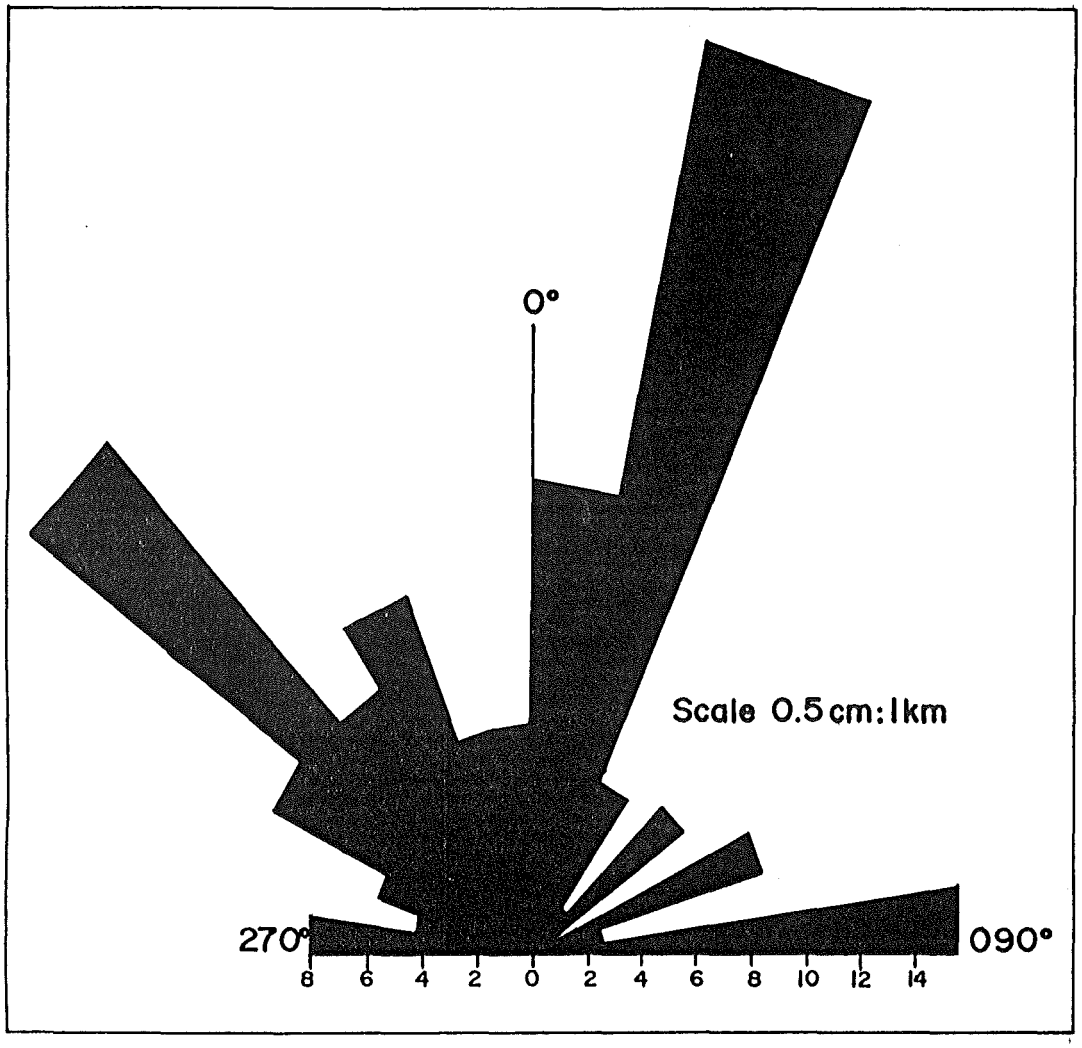

FIG. 19 Overall rose diagram of faults, showing preferred fault orientations in the field area.

In the Pocdol Mountains, three major fault sets--- east-west, northwest and northeast, and north-north northeast fault sets, are recognised (Fig. 19). The north-north northeast fault set is the most dominant, and fault traces in this group generally exceeds 5 kms in length. In contrast, both the northwest- and northeast sets, and the east-west sets have short (<5 kms) fault traces.

Generally no horizontal component of faulting has been noted and most of the faults are normal faults, involving tens of metres of vertical displacements (Panem and Alincastre, 1985). Each of these fault sets, from the oldest to the youngest, is discussed briefly in the succeeding paragraphs.

2.3.1 East-West Fault Set

East-west trending faults form a 5-km zone of imbricate faulting across the Pocdol Mountains (Fig. 18). The fault zone is bounded by the Calpi-Inang Maharang Faults in the north, and the Buragwis-Banga-Pulog Faults in the south, and is interpreted here as the extension of the San Vicente-Linao Fault (see Fig. 2).

The San Vicente-Linao Fault (SVLF) zone was the site of Late Pleistocene to Recent volcanism in the study area (i.e., Lison Dome, Cawayan, Pangas and Pulog vents), and is now characterised by a block-faulted topography. It is also apparent that the SVLF provides the vertical discontinuity for the subsurface flow of hydrothermal fluids, as indicated by resistivity data (see Fig. 5).

Alternatively, the SVLF can be interpreted as a dextral wrench fault, following the treatment of Moody and Hill (1956), and its inception is probably associated with the Malobago volcanism in Early Pliocene; the most recent movements perhaps occurred prior to Mt. Pulog eruptions (<30,000 years B.P.).

2.3.2 Northwest and Northeast Fault Set

The northwest fault set is generally oriented between 310^{o}-320^{o}, and minor 330^{o}-340^{o} fault trends; these faults (i.e., Makabug and San Lorenzo Faults) bisect the San Vicente-Linao Fault at acute angles. No horizontal displacements have been observed; slickensides suggest

dominantly vertical movements. The faults cut the Suminandig, Rangas and Cawayan volcanics, which may indicate that faulting took place between Middle Pliocene and <40,000 years B.P. These faults apparently control the southeastward flow of geothermal fluids (Panem and Alincastre, 1985).

A conjugate northeast fault set is also present, which is centered on 040°-050° (i.e., Cawayan Fault); however, this trend is less developed, but is known to channel acidic geothermal fluids (Reyes, 1985).

2.3.3 North-North Northeast Fault Set

The preferred orientation of the north-north northeast fault set lies between 010°-020°, and these faults have characteristic long surface traces bisecting the San Vicente-Linao Fault. This trend is regional in extent, which is observed across southern Luzon (Ferrer et al., 1986), and in Leyte Island (Delfin and Tebar, 1986).

The north-north northeast faults are mostly exposed in the WPM, which cross-cut the Lison, Kayabon and Cawayan volcanics. Thus, it is inferred that the inception of these faults occurred between 478,000 and 40,000 years B.P. Vertical fault displacements are dominant, and "horst and graben" features are common.

Moreover, the north-north northeast faults nowhere bisect the northwest and northeast faults.

2.4 SUMMARY OF GEOLOGIC HISTORY

In the Midddle Miocene, the Pocdol Mountains were occupied by the Bicol Basin (Zanoria *et al.*, 1984), and bathyal carbonaceous to calcareous siltstones and sandstones were deposited on pre-Tertiary ultramafic basement rocks. Most of the detrital materials were probably eroded from the Caramoan Ridge in the north, and the Western Bicol Range in the south.

Initiation of volcanic activity occurred in the WPM, and was probably accompanied by the inception of the San Vicente-Linao Fault during the Early Pliocene. At this time, the EPM was still submerged. Present exposures indicate a central vent region near Malobago ridge, and a probable satellite vent at Magaho area. These early submarine to subaerial eruptions were petrographically uniform and comprise the Malobago volcanics. Early eruptions constructed a steep cone of tuff breccias and minor lavas, which may have culminated in strombolian or phreatomagmatic eruptions.

A period of erosion followed, with attendant hydrothermal activity in the near-vent region. Prior to, or during this period, volcanic activity began in the EPM.

Volcanism in the EPM probably commenced in Early to Middle Pliocene times, from a vent or vents near the Matacla Dome and the Rangas microdiorite. Present outcrops of tuff breccias and minor lavas indicate steep southern slopes whereas moderately-dipping flows cover the eastern slopes. These rocks comprise the Suminandig volcanics, which interfinger with shallow marine to lagoonal sediments (Rangas conglomerate). The rock sequence indicates intermittent periods of volcanism and marine transgression.

A dacite dome (Matacla Dome) was later erupted onto the southern slopes of Suminandig volcano. This event was probably accompanied by the reactivation of San Vicente-Linao Fault, associated with sinistral movement along the Philippine Fault in Pliocene times (Allen, 1962). As a result, localised block faulting disrupted lenses of Rangas conglomerate. This phase of the volcano's history may have provided the first active hydrothermal system in the EPM.

Erosion of the Suminandig edifice and the Rangas conglomerate ultimately formed a subdued "ridge and basin" morphology. The topographic lows were later covered by younger volcanic flows, accounting for the sparse outcrops of the Suminandig volcanics.

Pangas volcanics were emplaced onto the northern slopes of an eroded Suminandig cone; the rocks were apparently erupted from a central vent, now occupied by the Pangas and Botong Domes. A period of faulting and erosion ensued, and surface thermal features were probably common. Initial vents were erupted on its northern slopes, forming the Matanga Dome; a satellite eruptive centre was also produced in Osiao, but was later plugged by the Osiao Dome, 1.7 Ma ago.

Succeeding activities of the Pangas volcano involved flank eruptions through to Middle Pleistocene times.

Two coeval eruptions followed; these took place on the western slopes of Pangas volcano, and formed the Palayang Bayan and Tanawon craters. These events were accompanied by hypabyssal intrusions (Pangas intrusives), and together with the cooling roots of the volcanic domes, probably resulted in the hydrothermal regime present today.

The final eruptions of Pangas volcano took place on its southeastern slopes, at Mt. Rangas peak, and the extrusives formed at that time now cover most of the traces of the vent regions of Suminandig volcano. During this period, renewed activity in the Palayang Bayan vent region was likely, on the basis of their similar youthful morphology.

Erosion of the Pangas edifice resulted in deposition of secondary mass flows, particularly in the southern slopes where laharic tuff breccias and conglomerates contain abundant travertine clasts.

Concurrently with or prior to the final eruptions of Pangas volcano, both Lison and Kayabon volcanics were unconformably emplaced onto the eastern slopes of an eroded Malobago volcano, 478,000 years B.P. Volcanic activity was probably associated with faulting along the San Vicente-Linao Fault zone, which were later displaced by north-trending normal faults (Panem and Alincastre, 1985).

Perhaps during or shortly after the emplacement of Lison and Kayabon volcanics, the Rangas microdiorite intruded both Suminandig and Mt. Rangas extrusives in the EPM, <65,000 years B.P.; succeeding faulting and erosion that exhumed the Rangas microdiorite indicate at least 20 m of vertical displacement.

Two eruptive events in the EPM (<40,000 years B.P.) signalled the end of active volcanism in the study area. The Cawayan volcanics were erupted near the Tanawon crater, forming voluminous lavas and tuff breccias as valley-filling deposits. Loose volcanic debris was transported by heavy rains as lahars, and dumped mainly at the distal margins near Manito. North-trending normal faulting was evident (Panem and Alincastre, 1985), and acted as pathways for both hydrothermal fluids and meteoric waters (Reyes, 1985). Solfataric activity in the crater region continues to the present-day.

Finally, the Pulog volcanics were emplaced onto the eastern slopes of the Pangas volcano probably 10^3-10^4 years later. Voluminous basaltic tuff breccias and lavas preferentially flowed towards the east. The deposit covered most of the traces of the San Vicente-Linao Fault, except on the southern slopes where incipient normal faulting has occurred (Panem and Alincastre, 1985).

CHAPTER III

PETROGRAPHY AND MINERALOGY

CHAPTER III

PETROGRAPHY AND MINERALOGY

3.1 INTRODUCTION

Prior to this work, there had been little petrologic study of the volcanic rocks of Pocdol Mountains, except for standard petrographic and clay mineral analyses. The lack of detailed data, combined with poor outcrop sections and absolute chronology, resulted in conflicting geological interpretations by previous workers (e.g., Obusan, 1977; Espiritu, 1979; Panem and Alincastre, 1985; KRTA, 1986).

Major goals of this section are, therefore, to present modal and mineralogical compositions and mineral stabilities of the volcanic rocks in the study area. In conjunction with stratigraphic relationships established in chapter II and bulk rock chemistry in chapter IV, the data are then used to constrain hypotheses on petrogenesis, with detailed discussions and qualitative models presented in chapter V, Petrogenesis.

Thirty rock specimens have been selected for detailed petrographic analysis, and from this suite, six specimens were examined for mineralogical compositions. Rock samples chosen are representative of the larger rock suites from both the WPM and EPM.

Electron microprobe analyses of minerals from six representative rock specimens of both WPM and EPM lava series were determined in the Analytical Facility of Victoria University, Wellington, using a **JEOL 733** Superprobe fitted with 3 wavelength dispersive spectrometers. Natural and synthetic oxides and silicates were used as standards and on line data reduction applied the Bence and Albee (1968) correction method. Instrumental setting conditions were accelerating potential of 15 KV and a specimen current of 1.2×10^{-8} amperes specimen current. The beam diameter was generally between 1 and 5 micrometres, although a reduction to 1 micrometre or less was made when grains were extremely small.

Full details of the analytical technique are reported in Watanabe *et al.* (1981).

3.2 NOMENCLATURE

Nearly 80 % of samples examined at PVF are andesites---aphanitic to porphyritic rocks containing phenocrysts of plagioclase, clinopyroxene, orthopyroxene, Fe-Ti oxide and occasional amphibole, which are readily observed with the naked eye. Olivine is absent in andesites, but is found in basaltic outcrops of the Malobago volcanics only. Texturally the volcanic rocks in the study area range from black vesicular hyalopilitic to grey glomeroporphyritic rocks. Pilotaxitic texture is common.

In thin section, feldspar is the most common phenocryst; bulk feldspar composition is labradorite, with subordinate andesine as microphenocryst and groundmass phases. Rare sanidines are present as microphenocrysts and groundmass constituents in high-K andesites and dacites. Two andesite types are recognised, on the basis of modal variations of ferromagnesian minerals (e.g., Gow, 1968) in these rocks. These are :

(i) Two pyroxene andesite---pyroxene >5 % (modal ratio of orthopyroxene to clinopyroxene is variable, but generally increases with increasing acidity of the magma), and

(ii) Hornblende andesite-------hornblende >1 %.

The two types of andesite grade into the other, but two pyroxene andesites are by far the most abundant whereas hornblende andesites are usually associated with rocks having >60 SiO_2 wt. %. It should also be noted that amphiboles (and rare biotites) only occur in a dome in the WPM (i.e., Lison Dome), and in older lavas and domes in the EPM (i.e., Matacla, Osiao and Matanga Domes; Suminandig and Pangas volcanics). Therefore, at PVF two pyroxene andesites and hornblende andesites may represent a "less-evolved" anhydrous magma and a "more-evolved" hydrous magma, respectively (see chapter V).

In addition, the suffix "**phyric**" is added to the rock name in order to emphasise their porphyritic texture (Mackenzie *et al.*, 1982); the term "**bearing**" is attached to a mineral name if present in trace amounts (<1 volume %). Thus, hornblende-bearing two pyroxene-phyric andesite implies that the rock is porphyritic, which contains <1 % hornblende and >5 % pyroxenes.

3.2.1 Volcanic Series of Pocdol Mountains

Geomorphic subdivisions established in chapter I (sect. 1.2.1) are used here for easy reference, as well as, to emphasise the close spatial relationships of lavas in the study area. Volcanic rocks in the Western Pocdol Mountains are therefore termed here as the "**WPM Series**" (Malobago, Kayabon and Lison volcanics) and those in the Eastern Pocdol Mountains, the "**EPM Series**" (Suminandig, Pangas, Cawayan and Pulog volcanics; however, no stratigraphic order is being implied in these groupings (see chapter II).

3.3 PETROGRAPHY

Modal compositions of both WPM and EPM lavas are compiled in Tables 3 and 4, respectively. Photomicrographs of representative rock specimens are shown in Figures 20 to 28. Petrographic terminology used here follows Mackenzie *et al.* (1982).

Detailed petrographic descriptions and other sampling data are given in appendix 1, and sample locations are shown in the attached geologic map.

3.3.1 Western Pocdol Mountains (WPM) Series

WPM lavas are holocrystalline and are largely porphyritic with total phenocryst (>0.2 mm) contents ranging from 44 to 61 volume percent. Plagioclase is the most abundant (27-35 %) followed by clinopyroxene (2-7 %), orthopyroxene (trace-5 %) and rare amphibole (trace-4 %); clinopyroxene phenocrysts are consistently more abundant than

FIELD NUMBER:	14	4	3	12	39	38	13
LITHOLOGIC UNIT:	Mgv	Knv	Knv	Lnv	Lnv	Lnv	Lnv
ROCK TYPE:	B(mk)	BA(hk)	A(mk)	A(mk)	A(mk)	A(mk)	A(hk)
PHENOCRYST MODE (Volume % ; 500 counts)							
Plagioclase	35.4	26.8	35.2	32.6	33.4	35.4	27.8
Clinopyroxene	2.4	5.8	7.0	2.4	6.2	4.6	2.6
Orthopyroxene	.2	1.8	5.0	1.4	5.2	2.6	2.6
Hornblende	-	-	-	1.2	.2	-	3.8
Olivine	3.4	-	-	-	-	-	-
Iron Oxide	2.2	3.2	3.6	2.4	2.0	1.4	1.8
GROUNDMASS:	56.4	62.4	49.2	59.8	53.0	56.0	61.4
Plg/(Plg+Px+hb)	86	78	74	87	74	83	75

TABLE 3 Modal compositions of WPM series lava obtained from at least 500 counts.

orthopyroxene phenocrysts (Table 3). Fe-Ti oxides range from 1.4 to 3.6 %, but are relatively lower in rocks containing >60 weight % SiO_2. Only the basalt specimen collected at Magaho area contains olivine crystals (<4 volume %).

All lavas appear fresh and unaltered, showing generally low volatile contents.

There is a poor correlation of plagioclase to total Fe-Mg silicate ratios from basalt to andesite in WPM lavas. This ratio is expected to increase with increasing acidity, due to decreasing abundances of Fe and Mg in the melt as SiO_2 increases (Ewart, 1982).

Several of the phenocryst phases are also present either as crystal clots or as megacrysts. Coarse crystalline aggregates, similar to those described here, are commonly found in calcalkaline rocks (e.g., Williams, 1942; Wilkinson *et al.*, 1964). Garcia and Jacobson (1979) also pointed out that crystal clots are common in island-arc tholeiites, oceanic island lavas and ocean-floor basalts. Some explanations for the origins of these clots are listed below :

(i) clusters of phenocrysts (Garcia and Jacobson, 1979);

(ii) anhydrous products formed by the breakdown of hornblende (Stewart, 1975);

(iii) accidental microxenoliths (Wilkinson *et al.*, 1964);

(iv) cognate magma chilled on wall rocks and subsequently dislodged and fragmented during eruption (Arculus, 1976);

(v) refractory residues carried up from the zone of partial melting (Flood *et al.*, 1977), and

(vi) cumulate material disrupted and incorporated into the host magma (Arculus and Wills, 1980).

FIG. 20 Olivine-phyric basalt, Magaho area (Malobago volcanics; Field No. 14). Anhedral bytownite-labradorite, olivine, titanomagnetite (note inclusion in olivine), and minor augite are set in a finer-grained hyalopilitic groundmass. Magnification: 10X

FIG. 21 Two pyroxene hornblende-phyric andesite, Lison Dome (Lison volcanics. Phenocrysts and microphenocrysts of subhedral-anhedral labradorite, opacite-rimmed hornblende, titanomagnetite and pyroxenes showing overgrowth textures, i.e., hypersthene core mantled with augite. Magnification: 10X

FIG. 22 Poikilitic amphibole (titanian magnesio-taramite) megacryst rimmed by minute oxides, occurring in a two pyroxene hornblende-phyric andesite (Field No. 13). Magnification: 10X

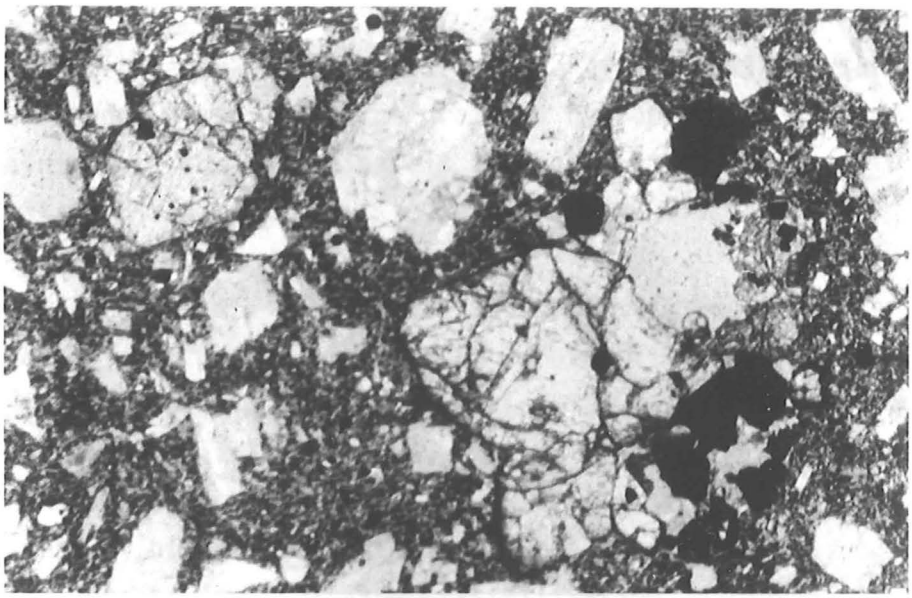

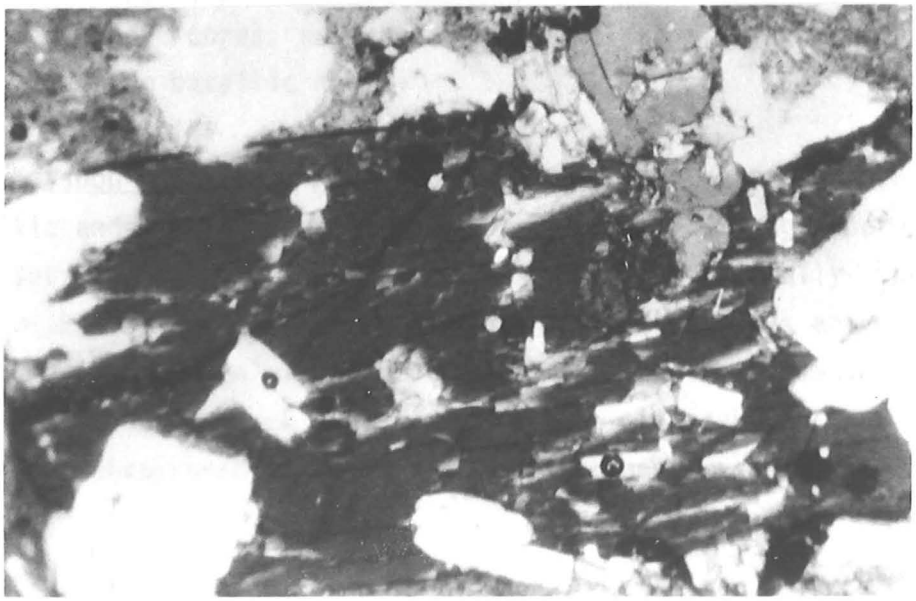

On the other hand, the megacrysts are often poikilitic, showing corroded and rounded rims. The fine grained hyalopilitic groundmass consists mainly of the same minerals as the phenocryst phases, with rare interstitial glass.

The preponderance of plagioclase phenocrysts and the common occurrence of titanomagnetite inclusions within olivine crystals, and the rare cases where olivines are in turn included within augite megacrysts indicate a crystallisation sequence of **titanomagnetite-olivine-clinopyroxene-orthopyroxene-amphibole, concurrent with plagioclase.** The disappearance of olivine in basaltic andesites and andesites of the WPM lavas suggests final olivine crystallisation in liquid compositions of <52 weight % SiO2, where it is replaced by orthopyroxene.

Petrographic data of each of the three lithologic units comprising the WPM lava series are summarised below :

(i) Malobago volcanics. The Malobago volcanics comprise basalt lava flows and tuff breccia clasts, which generally contain 35-45 % phenocrysts of labradorite-bytownite, olivine, titanomagnetite, augite and bronzite, with subordinate diopside and salite. These are the only rocks containing olivine crystals (<4 volume %), as euhedral to subhedral iddingsite-rimmed phenocrysts, microphenocrysts and groundmass phases (Fig. 20). Olivine glomerocrysts are also present, together with labradorite, augite and titanomagnetite. These olivines lack chrome spinel inclusions, are in equilibrium with coexisting pyroxene phenocryst cores, and represent the final stages of olivine crystallization from basaltic magma.

(ii) Kayabon volcanics. Lavas of the Kayabon volcanics range from basaltic andesite to andesite, and are commonly strongly porphyritic, but several specimens are weakly porphyritic. Generally these are dark rocks, enclosing large twinned feldspar crystals and minor mafic minerals. Modal analyses (Table 3) indicate that plagioclase feldspars are twice as much as mafic minerals; clinopyroxene is more abundant than orthopyroxene. Large plagioclase phenocrysts sometimes

FIELD NUMBER:	42B	23	30	40	19	33	34	35	22	29	25
LITHOLOGIC UNIT:	Pgv	Psv	Pgv	Pgv	Psv	Psv	Psv	Psv	Cnv	Psv	Cnv
PHENOCRYST MODE (Volume % ; 500 counts)											
Plagioclase	45.2	30.4	30.2	44.5	47.8	25.0	33.6	34.0	39.4	35.6	24.6
Clinopyroxene	5.8	2.0	4.2	8.0	2.2	4.2	5.6	4.8	8.2	2.6	5.0
Orthopyroxene	5.0	2.6	5.6	2.8	1.6	4.8	4.0	6.8	3.2	2.6	3.8
Hornblende	-	-	-	-	.2	-	-	-	-	-	-
Iron Oxide	3.6	1.2	2.4	6.6	3.0	2.0	1.0	2.0	3.2	3.0	2.4
GROUNDMASS	39.6	63.8	57.2	37.8	45.2	64.0	53.4	52.0	46.0	56.2	64.2
Plg/(Plg+Px+hb)	81	87	83	81	92	74	78	75	78	42	74

FIELD NUMBER:	7B	28A	28B	32	1	16	43	37	8	36	17	10C
LITHOLOGIC UNIT:	Psv	Psv	Psv	Psv	Cnv	Sgv	Sgv	Psv	Sgv	Psv	Sgv	Sgv
PHENOCRYST MODE (Volume % ; 500 counts)												
Plagioclase	32.8	24.4	22.8	21.4	31.6	16.4	21.4	27.0	23.4	33.6	32.4	35.4
Clinopyroxene	3.0	4.0	6.4	.2	4.0	3.0	3.4	3.4	3.2	4.8	1.2	.2
Orthopyroxene	6.6	1.6	4.4	.2	2.8	.4	1.4	5.2	2.4	3.8	3.4	1.8
Hornblende	.8	1.2	-	7.0	-	10.6	9.8	.8	1.0	.6	9.2	12.0
Iron Oxide	5.4	3.4	2.0	2.2	1.8	2.0	3.6	3.2	2.0	3.4	2.8	2.6
GROUNDMASS	51.2	62.8	63.0	69.0	59.8	67.6	60.4	59.4	68.0	51.6	49.8	42.8
Plg/(Plg+Px+hb)	76	98	68	74	82	54	59	74	78	79	70	65

TABLE 4 Modal compostions of EPM series lavas taken from a minimum of 500 points.

contain inclusions of hypersthene and augite, and have clear labradorite-andesine jackets (<0.5 mm) over clouded or dusty labradorite-bytownite core regions. Hornblende is absent in these rocks, as well as olivine. Fe-Ti oxides are dominated by subequant titanomagnetite occurring as microphenocrysts, as inclusions, or as groundmass phases. Matrix textures vary from hyalopilitic to strongly pilotaxitic.

(iii) Lison volcanics. Specimens of the Lison volcanics are mostly andesites, containing moderate amounts of subhedral to anhedral hornblende phenocrysts and microphenocrysts, which are always rimmed by minute oxides. Hornblende phases are abundant (~10 volume %) particurlarly in the youngest flows (i.e., Lison Dome). Pyroxenes are normally zoned and exhibit reaction relationships between Ca-rich and Ca-poor types, i.e., hypersthene core is jacketed by subhedral augite rim (<2 mm) in Fig. 21. Normally-zoned plagioclase feldspars show "clean" labradorite cores which are mantled by euhedral to subhedral andesine, and several plagioclases display resorbed crystal outlines. Subhedral titanomagnetite usually occurs as microphenocryst, as groundmass component and as minute inclusions in an aggregate of pyroxene and plagioclase.

Several subequant and rounded hornblende megacrysts (Fig. 22) are rimmed by opaque granules, which contain numerous subhedral labradorite, augite and titanomagnetite inclusions. These megacrysts are regarded here as phenocrysts grown in a shallow-level magma chamber and were subsequently resorbed during rapid ascent of magma to the surface (Miyashiro *et al.*, 1969). Groundmass mineralogy is essentially less basic in composition than phenocrysts and microphenocryst phases, and show pilotaxitic texture.

3.3.2 Eastern Pocdol Mountains (EPM) Series

EPM lavas comprise basaltic andesite to dacite, but the majority are andesites (n=16). These rocks range from strongly to weakly porphyritic. Groundmass textures vary from pilotaxitic-hyalopilitic to microgranular. Representative modal compositions are contained in Table 4.

FIG. 23 Two pyroxene basaltic andesite, Pulog volcanics (Field No. 40). Highly vesicular containg dark glassy matrix materials that enclose phenocrysts and microphenocrysts of subhedral dusty labradorite, titanomagnetite and pyroxenes. The large pyroxene in the centre exhibits an overgrowth texture (ie., hypersthene core jacketed by augite). Magnification: 10X

FIG. 24 Two pyroxene-phyric andesite (Pangas volcanics; Field No. 35) showing an aggregate of pyroxene + titanomagnetite. Fritted labradorite phenocryts are common, together with pyroxene overgrowth textures. Magnification: 10X

FIG. 25 Hornblende-phyric andesite (Pangas volcanics; Field No. 32). The opacite-rimmed amphibole minerals range from edenite to magnesio-taramite compositions. Magnification: 10X

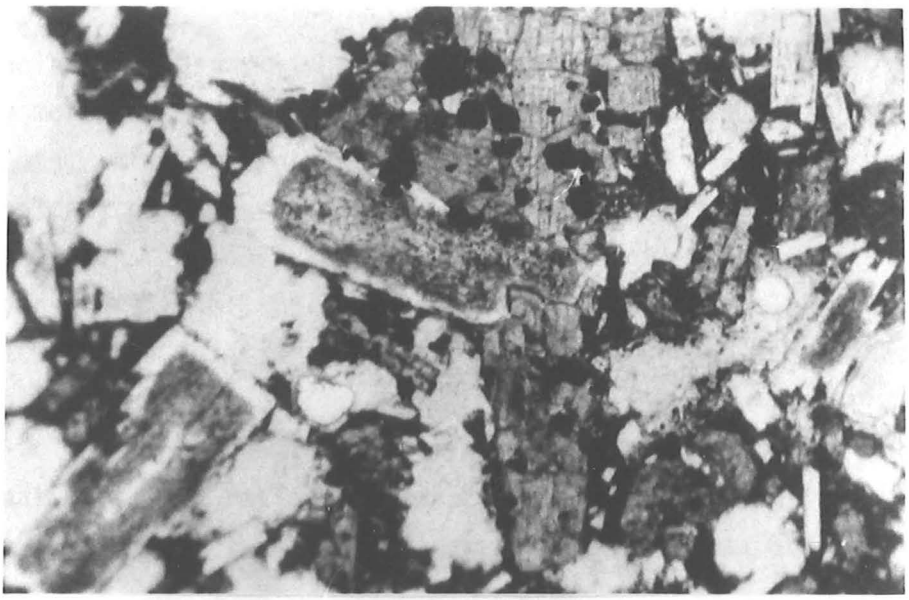

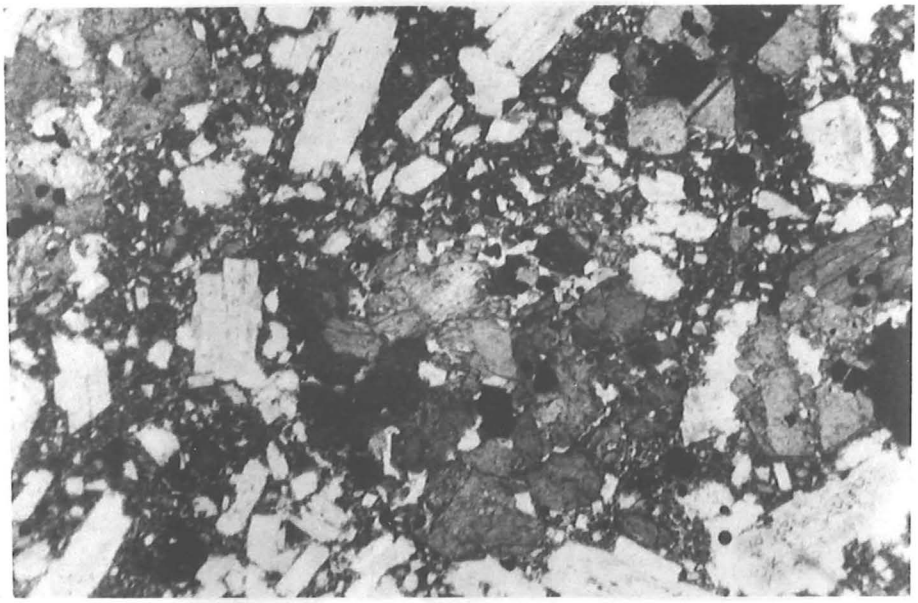

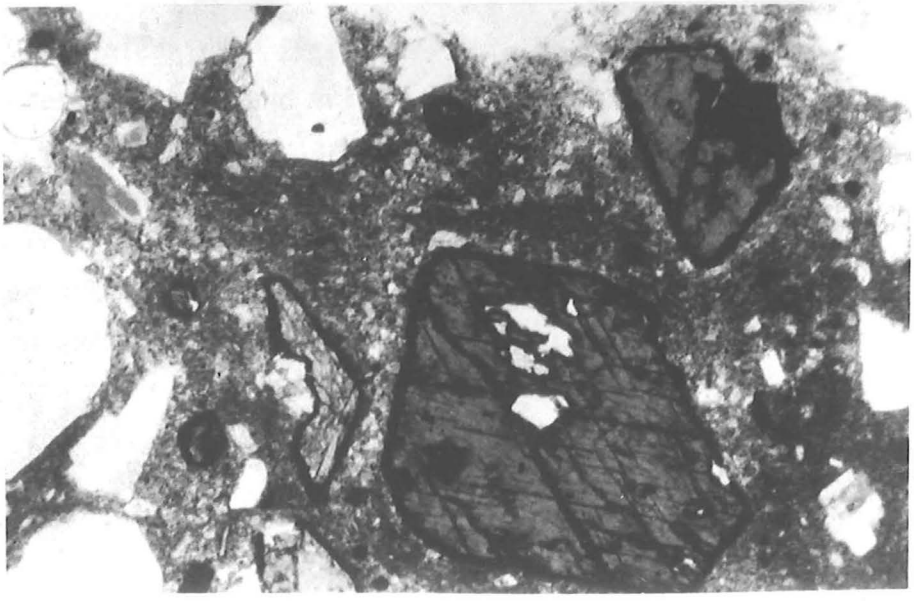

Plagioclase feldspar is the most dominant phase (21-45 %), and is typically more abundant than mafic minerals. Rare K-feldspars (trace amounts) are present as microphenocryst and matrix phases in andesites and dacites. Nearly 50 % of samples contain opacite-rimmed hornblendes, which are most abundant in rocks containing >60 % SiO_2. Pyroxene phases vary from 1 to 11 %; however, there is no clear relationship between the relative abundance of orthopyroxene and clinopyroxene, as silica increases.

Alternatively, the ratio of plagioclase to total Fe-Mg silicate phases has a poor correlation with increasing silica, as observed in WPM lavas.

Olivines are not found in these rocks, which may have been completely replaced by orthopyroxenes. Subhedral to anhedral titanomagnetites vary from 1 to 7 %, and occur as microphenocrysts, groundmass components, and inclusions within plagioclases and pyroxenes.

The ubiquity of plagioclase and titanomagnetite, which are both included in pyroxenes and amphiboles indicates an order of crystallisation of **titanomagnetite-pyroxene-amphibole, accompanied by plagioclase.** The highly variable orthopyroxene to clinopyroxene ratio, however, may suggests the near simultaneous appearance of both phases.

Brief descriptions of the four lithologic units comprising the EPM lava series are given below :

(i) <u>Pulog volcanics</u>. Extrusives of Mt. Pulog are generally basaltic andesite lavas and tuff breccias (Fig. 23), and majority of these are black highly vesicular rocks, consisting of 30-45 % plagioclase with fritted cores and are usually jacketed by anhedral andesine; large (<1 cm) normally zoned pyroxene grains and titanomagnetite are enclosed within a dark vitrophyric groundmass. Several pyroxenes exhibit overgrowth textures, i.e., hypersthene cores blanketed by augites.

FIG. 26 Two pyroxene andesite, Cawayan volcanics (Field No. 22). Large dusty labradorite grains are characteristic; few completely pseudomorped grains show aggregates of labradorite, titanomagnetite, augite and hypersthene. Magnification: 10X

FIG. 27 Two pyroxene hornblende microdiorite, Rangas microdiorite (Field No. 17). Magnification: 10X

FIG. 28 Hornblnde dacite, Matacla Dome (Field No. 10C). Abundant reddish brown opacite-rimmed to completely pseudomorphed oxyhornblende, subhedral hypersthene, titanomagnetite and minor quartz are set in a quartzofeldspathic groundmass. Magnification: 10X

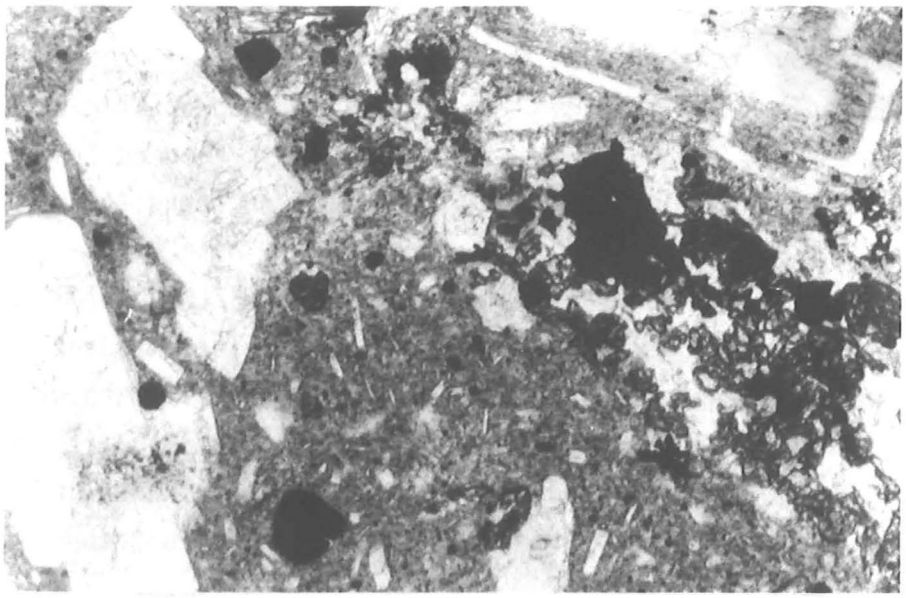

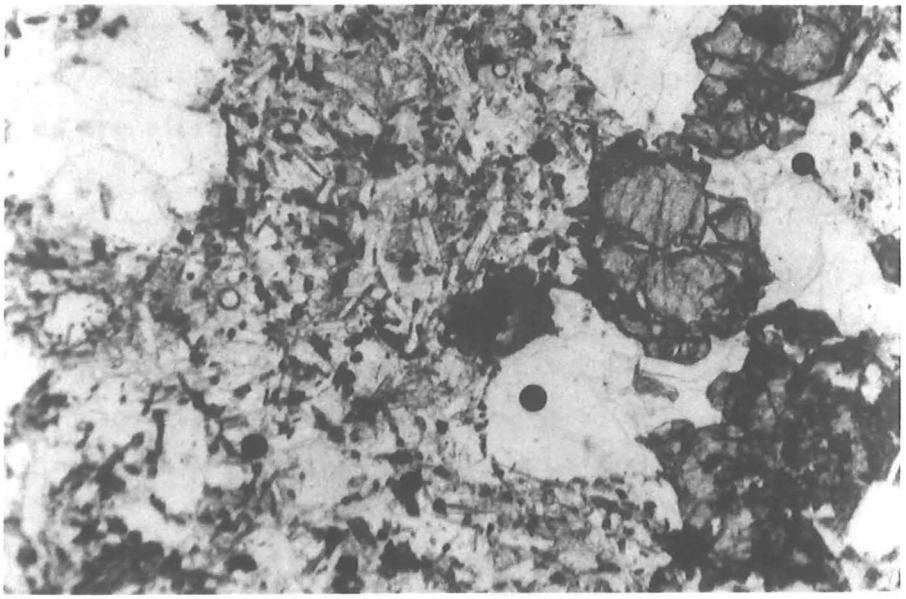

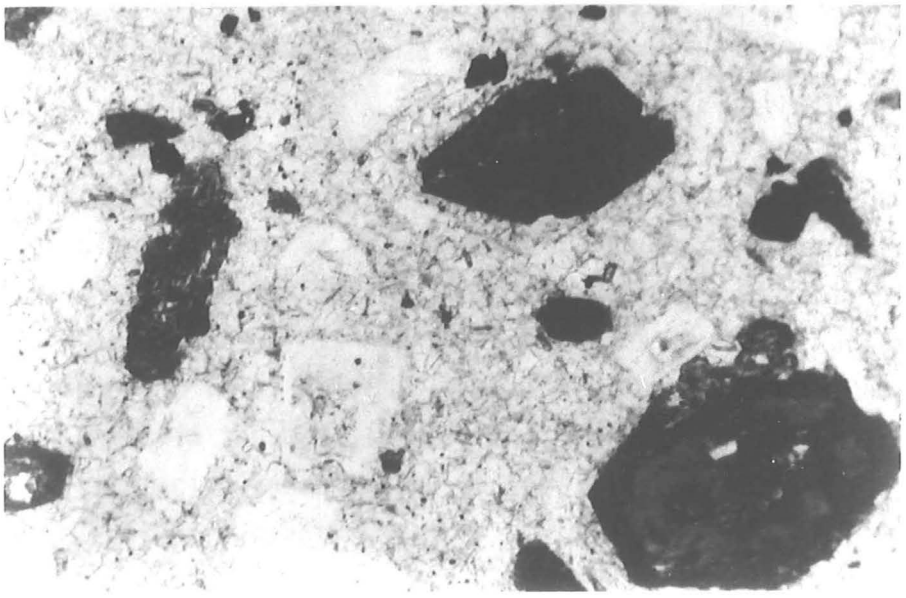

(ii) Pangas volcanics. Deposits of the Pangas volcanics are dominantly hornblende-bearing lavas and pyroclastics. These rocks show two "end member" types of andesite, i.e., a two pyroxene-phyric variety (Fig. 24) and a hornblende-phyric variety (Fig. 25).

In addition, two types of plagioclase phenocrysts (Fig. 26) are usually present, namely : (i) a relatively "clean" plagioclase crystal, which is normally-zoned (i.e., labradorite core with andesine rim), and (ii) a sieve-textured crystal, containing labradorite-andesine core which is usually overgrown with <2 microns of subhedral to euhedral andesine-labradorite rim ("dirty" variety).

The "dirty" plagioclase variety (sieve-textured) is often used as an indication for mixing of magmas (e.g., Sakuyama, 1979; 1981; 1984; Lofgren and Norris, 1981; Putirka and Weigand, 1987). Groundmass textures are vitrophyric to hyalopilitic.

(iii) Cawayan volcanics. Extrusives from the Cawayan crater are compositionally- and texturally-similar to the hornblende-free andesites of Pangas volcanics (Fig. 24). However, these rocks contain ubiquitous crystal aggregates of pyroxene + "cloudy" or fritted plagioclase + titanomagnetite; the pyroxenes and plagioclases are normally zoned (often oscillatory) and show overgrowth textures.

Inspection of crystal-clot phenocryst phases shows that a fixed ratio of minerals is not maintained. This observation is inconsistent with the hypothesis of Stewart (1975) and Boettcher (1977) that crystal clots have a fixed composition.

In all samples examined, the minerals in clots are also represented in the phenocryst or microphenocryst assemblage. The proportion of plagioclase is greater in the phenocryst assemblage than in crystal clots. The smaller proportion of plagioclase in clots may be the result of some of the clots having formed early at high pressures (Eggler and Burnham, 1973) prior to plagioclase becoming the dominant crystallising phase in the melt (Garcia and Jacobsen, 1979). Therefore, the crystal-clot phenocryst phases are treated here as more likely to be glomerophyric aggregates.

(iv) Suminandig volcanics. Products of the Suminandig volcanism represent the most evolved rocks in the study area, and consist of hornblende-phyric andesites (>60 % SiO2) and a dacite (Matacla Dome). These rocks are closely associated with a microdiorite dike (Fig. 27). Quartz and sanidine occur as microphenocrysts and as groundmass constituents in andesites and dacite, which show resorbed textures such as rounding, embayments and glass inclusions. Hornblende phenocrysts in dacites (Fig. 28) commonly show breakdown textures (Macgregor, 1938; Williams, 1942; Kuno, 1950; Stewart, 1975), and can be broadly categorised into two types (Garcia and Jacobsen, 1979). These are :

(i) a "black" type (Fig. 28); in which the amphibole is wholly or partly replaced by a very fine aggregate of minute iron ore and pyroxene minerals by dehydrogenation and oxidation during extrusion, caused by drastically increased fO_2/fH_2 and decreased f_{H2O}, and

(ii) a "gabbroic" type (Fig. 26); in which the amphibole is completely or partially replaced by a fine to medium grained aggregate of anhedral pyroxene, plagioclase and titanomagnetite as the result of dehydration within the magma chamber due to a decrease in f_{H2O} (Stewart, 1975).

The "black" type amphibole is consistently more abundant than the "gabbroic" type amphibole in andesites and dacite. Groundmass textures are usually hyalopilitic to microgranular.

3.4 SURVEY OF MINERAL CHEMISTRY IN LAVAS

3.4.1 Feldspars

Representative electron microprobe analyses of feldspars are contained in Table 5 and data are presented in terms of Ab-An-Or end-members in Fig. 29.

(i) Plagioclase is ubiquitous and is the most abundant mineral in all lavas, occurring as phenocrysts, microphenocrysts and groundmass phases. The compositional range is An_{93-43}, but the majority of crystals are labradorite.

ANAL. NO.	1409P	1409P	1409P	1415P	1415P	1402MP	1403G	1411I	1413P	4002P	4002P	4009G
SPEC	CORE	MID	RIM	CORE	RIM	CORE	MX	CPX	CORE	CORE	RIM	MX
OXIDE (wt.%)												
SiO2	48.14	50.99	51.28	46.60	52.80	50.35	55.47	46.12	48.84	51.10	54.89	53.79
TiO2	.05	.03	.10	.02	.08	.04	.09	.01	.02	.05	.12	.07
Al2O3	32.09	29.87	29.04	32.64	28.90	30.43	26.97	34.16	30.74	29.74	27.33	28.01
FeO	.62	.63	.70	.60	.79	.73	1.06	.51	.79	.66	.88	.76
MnO	.01	.00	.01	.06	.00	.03	.00	.04	.04	.00	.04	.01
MgO	.08	.07	.08	.07	.06	.09	.12	.04	.08	.06	.07	.12
CaO	16.12	14.24	13.91	17.13	12.42	14.45	10.49	18.23	15.46	13.92	11.16	12.20
Na2O	2.40	3.80	3.89	1.80	4.57	3.67	5.81	1.24	2.89	3.94	5.59	5.17
K2O	.11	.21	.19	.09	.30	.14	.46	.06	.14	.05	.15	.08
Cr2O3	.00	.00	.00	.00	.01	.00	.00	.01	.03	.00	.04	.00
NiO	.00	.03	.00	.00	.00	.00	.00	.00	.03	.02	.01	.00
Cl	.00	.00	.00	.01	.01	.00	.01	.02	.01	.01	.00	.00
TOTAL	99.62	99.87	99.20	99.00	99.94	99.93	100.48	100.44	99.07	99.55	100.28	100.21
NUMBER OF CATIONS ON THE BASIS OF 32 (O)												
Si	8.883	9.347	9.453	8.682	9.627	9.236	10.029	8.485	9.067	9.383	9.941	9.771
Ti	.006	.097	.014	.003	.012	.006	.013	.001	.002	.006	.017	.010
Al	6.979	6.453	6.311	7.168	6.210	6.578	5.747	7.407	6.726	6.435	5.834	5.996
Fe	.096	.097	.108	.094	.120	.112	.161	.078	.123	.101	.133	.115
Mn	.002	.000	.002	.009	.000	.004	.000	.006	.006	.000	.007	.002
Mg	.023	.020	.022	.019	.017	.024	.032	.010	.023	.017	.019	.033
Ca	3.187	2.797	2.749	3.420	2.426	2.839	2.032	3.593	3.075	2.739	2.166	2.374
Na	.859	1.350	1.392	.650	1.614	1.305	2.035	.442	1.042	1.403	1.961	1.820
K	.027	.048	.044	.022	.069	.033	.105	.014	.033	.012	.035	.020
Cr	.000	.004	.000	.000	.002	.000	.000	.002	.004	.000	.006	.000
Ni	.000	.000	.000	.000	.000	.000	.000	.000	.004	.003	.002	.000
Cl	.000	.000	.000	.003	.002	.000	.003	.006	.002	.002	.000	.000
TOTAL	20.064	20.120	20.095	20.069	20.099	20.138	20.157	20.043	20.106	20.102	20.120	20.141
An	78.25	66.68	65.69	83.58	59.04	67.97	48.71	88.74	74.10	65.94	52.04	56.34
Ab	21.09	32.18	33.26	15.89	39.28	31.24	48.78	10.92	25.12	33.78	47.12	43.19
Or	.66	1.14	1.05	.54	1.68	.79	2.52	.35	.80	.29	.84	.48

TABLE 5 Representative electron microprobe analyses of plagioclase feldspars.

Analysis number is coded such that "3205PX" refers to Field No. 32, and the "05" is for computer tabulation purposes only. The suffix letter "P" means phenocryst (>300 microns) analysis; "MP", microphenocryst (300-100 microns); "G", groundmass (70-20 microns); "I", inclusion; the "X" signifies that the analysed grain is occurring as an aggregate, an embayed grain, or a xenocryst. Mineral analyses are designated under "SPEC" as follows : (i) "CORE", phenocryst/microphenocryst core; (ii) "RIM", phenocryst/microphenocryst rim. If a mineral name is given under SPEC, the analysed grain was an inclusion in this mineral. A line connecting analyses indicates analyses on the same grain.

ANAL. NO.	4011MP	4012G	4013I	4014P	3202P	3203P	3203P	3203P	3205PX	3207PX	3208CX	3209G
SPEC	CORE	MX	PX	CORE	RIM	CORE	MID	RIM	CORE	CORE	CORE	MX
OXIDE (wt.%)												
SiO2	54.12	55.65	52.91	49.01	53.07	52.04	49.45	53.69	51.34	48.62	54.94	54.56
TiO2	.07	.06	.08	.00	.02	.02	.03	.04	.03	.03	.04	.02
Al2O3	27.86	27.72	28.75	31.62	29.18	29.65	31.07	28.54	30.33	31.70	28.22	28.50
FeO	.73	.72	.83	.60	.35	.37	.39	.41	.49	.29	.29	.23
MnO	.04	.07	.06	.00	.01	.00	.00	.00	.03	.04	.00	.01
MgO	.12	.10	.07	.04	.01	.00	.00	.04	.05	.01	.02	.05
CaO	11.57	11.06	12.99	15.86	12.41	13.43	15.30	11.96	14.09	15.84	11.23	11.67
Na2O	5.37	5.94	4.53	2.82	4.78	4.35	3.26	5.36	3.72	2.84	5.74	5.67
K2O	.09	.12	.09	.05	.14	.06	.07	.07	.01	.02	.08	.21
Cr2O3	.00	.00	.00	.00	.00	.00	.04	.00	.02	.00	.04	.00
NiO	.05	.00	.08	.06	.00	.00	.10	.00	.00	.04	.05	.00
Cl	.00	.01	.00	.00	.01	.00	.00	.00	.00	.01	.01	.00
TOTAL	100.02	101.45	100.39	100.06	99.98	99.92	99.71	100.11	100.11	99.44	100.66	100.92
NUMBER OF CATIONS ON THE BASIS OF 32 (O)												
Si	9.833	9.955	9.618	8.998	9.645	9.490	9.098	9.742	9.356	8.973	9.886	9.811
Ti	.009	.008	.011	.000	.002	.002	.004	.006	.004	.004	.005	.003
Al	5.965	5.844	6.158	6.842	6.249	6.373	6.737	6.103	6.514	6.896	5.984	6.040
Fe	.111	.108	.126	.091	.054	.057	.060	.062	.074	.045	.043	.035
Mn	.006	.011	.010	.000	.001	.000	.000	.001	.005	.006	.000	.001
Mg	.034	.027	.020	.011	.003	.001	.000	.010	.013	.002	.007	.014
Ca	2.253	2.120	2.529	3.120	2.415	2.623	3.016	2.325	2.752	3.133	2.165	2.249
Na	1.892	2.058	1.597	1.005	1.686	1.539	1.164	1.887	1.313	1.015	2.002	1.978
K	.021	.027	.020	.012	.033	.014	.016	.017	.003	.004	.018	.049
Cr	.000	.000	.000	.000	.000	.000	.006	.000	.004	.000	.006	.000
Ni	.007	.000	.012	.010	.000	.000	.015	.000	.000	.005	.007	.000
Cl	.000	.001	.000	.001	.002	.000	.000	.000	.000	.002	.004	.000
TOTAL	20.131	20.159	20.100	20.090	20.090	20.098	20.116	20.152	20.038	20.086	20.128	20.180
An	54.08	50.42	61.00	75.42	58.42	62.81	71.90	54.98	67.65	75.46	51.73	52.60
Ab	45.42	48.94	38.52	24.29	40.78	36.85	27.75	44.62	32.28	24.45	47.84	46.26
Or	.50	.64	.48	.29	.80	.34	.38	.40	.07	.10	.43	1.15

Table 5 (con't)

ANAL. NO.	3211P	3608PX	3609P	3609P	3610G	3611MP	3612G	3613P	3613R	1301I	1302G	1303I
SPEC	CORE	CORE	CORE———	RIM	MX	CORE	MX	CORE———	RIM	PX	MX	HB
OXIDE (wt.%)												
SiO2	48.81	50.77	44.44	56.04	51.63	54.98	56.99	57.39	56.58	55.95	53.56	55.24
TiO2	.01	.01	.02	.00	.02	.05	.01	.05	.04	.04	.02	.00
Al2O3	31.34	30.57	34.28	26.55	29.44	27.38	26.23	26.29	26.80	27.02	28.59	27.38
FeO	.38	.39	.41	.45	.70	.33	.37	.34	.49	.44	.44	.42
MnO	.00	.00	.00	.05	.05	.00	.01	.00	.03	.00	.00	.00
MgO	.02	.01	.05	.04	.04	.01	.02	.03	.04	.04	.07	.03
CaO	15.78	13.89	18.67	9.95	13.07	10.61	9.37	9.35	9.92	10.30	12.09	10.57
Na2O	79.00	3.76	.79	6.17	4.23	5.84	6.41	6.42	6.26	5.89	5.09	5.64
K2O	.05	.18	.04	.36	.28	.32	.57	.50	.44	.46	.31	.38
Cr2O3	.05	.01	.00	.00	.00	.00	.09	.00	.00	.02	.00	.00
NiO	.00	.00	.00	.03	.00	.00	.00	.00	.02	.00	.00	.00
Cl	.00	.00	.00	.00	.00	.01	.00	.00	.00	.01	.02	.00
TOTAL	99.36	99.59	98.70	99.64	99.46	99.53	100.07	100.37	100.62	100.17	100.12	99.66
NUMBER OF CATIONS ON THE BASIS OF 32 (O)												
Si	9.017	9.306	8.327	10.166	9.479	9.999	10.277	10.305	10.167	10.103	9.728	10.026
Ti	.002	.001	.003	.000	.002	.006	.002	.006	.006	.006	.003	.000
Al	6.823	6.604	7.570	5.677	6.371	5.868	5.575	5.564	5.674	5.750	6.120	5.856
Fe	.059	.060	.075	.068	.107	.050	.055	.052	.073	.067	.066	.064
Mn	.000	.000	.000	.008	.007	.000	.002	.000	.004	.000	.000	.000
Mg	.004	.003	.013	.009	.010	.004	.006	.008	.011	.010	.018	.008
Ca	3.124	2.727	3.748	1.934	2.572	2.067	1.810	1.798	1.911	1.993	2.353	2.056
Na	1.047	1.338	.288	2.171	1.504	2.060	2.241	2.234	2.180	2.060	1.770	1.985
K	.013	.042	.008	.084	.065	.073	.131	.115	.102	.105	.072	.088
Cr	.007	.001	.000	.000	.000	.000	.013	.000	.000	.003	.000	.000
Ni	.000	.000	.000	.005	.000	.000	.000	.000	.002	.000	.000	.000
Cl	.000	.000	.001	.002	.000	.001	.000	.000	.000	.003	.006	.000
TOTAL	20.096	20.081	20.034	20.124	20.117	20.128	20.113	20.082	20.130	20.100	20.136	20.083
An	74.67	66.40	92.68	46.17	62.09	49.210	43.28	43.36	45.58	47.93	56.09	49.79
Ab	25.02	32.58	7.12	51.83	36.32	49.050	53.59	53.87	51.99	49.54	42.19	48.07
Or	.31	1.02	.20	2.01	1.57	1.740	3.13	2.77	2.43	2.52	1.72	2.13

ANAL. NO.	1304G	1306MP	1308MP	1310G	1311P	1311P	1008MP	1009I	1012I	1013P	1013P
SPEC	MX	CORE	CORE	MX	CORE———	RIM	CORE	HB	HB	CORE--	---RIM
OXIDE (wt.%)											
SiO2	67.75	50.26	55.54	61.99	54.10	49.84	65.06	77.79	54.06	50.38	54.92
TiO2	.03	.01	.00	.07	.07	.01	.01	.08	.00	.03	.01
Al2O3	16.87	30.08	26.80	21.74	27.78	30.80	18.10	12.29	28.09	29.82	27.37
FeO	.60	.46	.36	.54	.39	.59	.17	.36	.33	.31	.2100
MnO	.00	.06	.08	.01	.01	.01	.00	.05	.00	.00	.00
MgO	.09	.01	.02	.02	.03	.07	.00	.04	.03	.08	.02
CaO	2.19	14.57	10.05	6.10	11.49	14.54	.48	.69	11.40	14.08	10.65
Na2O	5.36	3.64	5.98	6.15	5.14	3.40	4.24	3.19	5.30	3.88	5.81
K2O	5.36	.18	.48	2.38	.39	.18	10.23	5.08	.24	.13	.30
Cr2O3	.03	.00	.00	.04	.01	.00	.01	.00	.03	.07	.02
NiO	.02	.00	.02	.03	.00	.00	.05	.00	.00	.00	.00
Cl	.04	.00	.02	.02	.01	.01	.01	.13	.00	.01	.00
TOTAL	98.61	99.28	99.36	99.13	99.41	99.44	98.36	99.70	99.48	98.79	99.31
NUMBER OF CATIONS ON THE BASIS OF 32 (O)											
Si	12.220	9.274	10.112	11.200	9.873	9.181	12.001	13.464	9.850	9.322	10.003
Ti	.041	.001	.000	.010	.009	.001	.001	.010	.000	.005	.001
Al	3.587	6.541	5.751	4.629	5.975	6.686	3.934	2.506	6.031	6.505	5.874
Fe	.090	.071	.055	.087	.059	.091	.025	.052	.050	.048	.032
Mn	.000	.010	.012	.001	.002	.001	.000	.007	.000	.000	.000
Mg	.024	.003	.006	.007	.008	.019	111.000	.009	.007	.023	.006
Ca	.423	2.880	1.960	1.180	2.247	2.868	.094	.129	2.226	2.792	2.078
Na	1.873	1.303	2.111	2.155	1.820	1.213	1.518	1.070	1.872	1.392	2.052
K	1.234	.043	.112	.549	.092	.042	2.407	1.121	.057	.031	.070
Cr	.004	.000	.000	.005	.001	.000	.002	.000	.004	.011	.003
Ni	.002	.000	.003	.004	.000	.000	.008	.000	.000	.000	.000
Cl	.011	.000	.006	.007	.003	.002	.003	.037	.000	.004	.000
TOTAL	19.508	20.127	20.129	19.833	20.089	20.105	19.994	18.405	20.097	20.131	20.119
An	13.51	68.15	46.85	30.38	54.03	69.56	2.34	5.56	53.57	66.24	49.48
Ab	59.82	30.83	50.47	55.48	43.76	29.42	37.77	46.12	45.05	33.02	48.86
Or	39.41	1.02	2.68	14.14	2.21	1.02	59.89	48.32	1.37	.74	1.67

Table 5 (Con't)

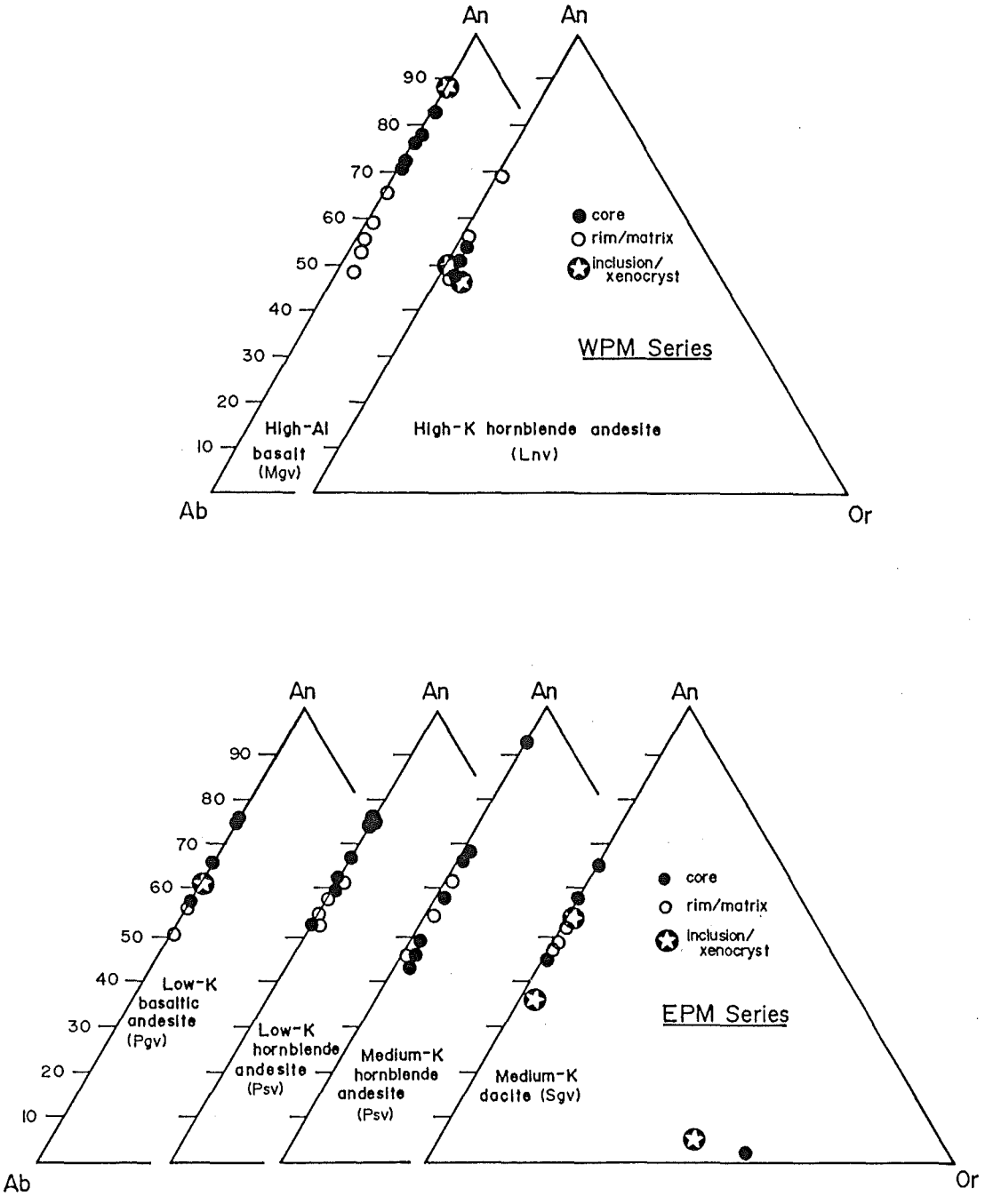

FIG. 29 Representative compositions of plagioclase feldspars.

Plagioclase crystals are often complexly zoned, but a general trend of Ca-rich cores and Na-rich rims is apparent. Most phenocrysts are nearly always oscillatory-zoned, particularly towards their grain boundaries. A thin (<3 microns) clear rim is always present, which generally lies within the compositional range of groundmass plagioclases. Inclusions of cryptocrystalline material, pyroxene and titanomagnetite are common (see Fig. 26), but apatite crystals were not observed as inclusions in plagioclases. Plagioclases also occur in aggregates, often coexisting with pyroxene and titanomagnetite.

Two types of disequilibrium texture can be observed in plagioclase phenocrysts. The first and the most conspicuous type is represented by crystals containing concentric dusty zones (see Fig. 26), which in a few cases are rimmed by a relatively more Ca-rich envelope (<2 microns) resulting in a euhedral to subhedral crystal morphology. This texture has been referred to as "fritted" or "sieve-like" texture (Gill, 1981). Fritted plagioclase phenocrysts are found occasionally in association with jacketed pyroxenes and unrimmed pyroxenes and/or plagioclases. The second type of disequilibrium texture is a resorption texture, which formed anhedral crystal outlines (see Fig. 21).

The zonation and textural features of plagioclases in these rocks therefore indicate at least three petrogenetic processes. These are :

(i) a close system plagioclase crystallisation, with attendant pyroxenes and oxides, from a liquid whose residue is represented by the groundmass phase;

(ii) entrainment of exotic crystalline material, or

(iii) magma mixing.

Experimental duplication of plagioclase sieve and overgrowth textures indicates that mixing of magmas is a viable mechanism (Lofgren and Norris, 1981), and the two above-mentioned disequilibrium textures have been successfully reproduced by Tsuchiyama (1985), who

notes that a dusty zone on the margin of plagioclase crystals only appears when plagioclase composition is more Ab-rich, compared with the plagioclase composition which is in equilibrium with the melt.

(ii) Alkali feldspars are rare, occurring as microphenocryst and groundmass phases in the more-evolved andesites and dacite. They also occur as quartz-orthoclase/sanidine intergrowths in the mesostasis of the Rangas microdiorite (see Fig. 27).

3.4.2 Pyroxenes

Pyroxenes are second only to plagioclase in phenocryst abundance. Augite and bronzite-hypersthene are the most commonly observed compositions, but rare diopside and salite occur, particularly in WPM lavas. The modal ratio of clinopyroxene to orthopyroxene is about 1.5 for both WPM and EPM andesites, but varies substantially in basaltic andesites where WPM lavas contain greater amounts of modal clinopyroxene than the EPM lavas; extreme values are shown by basalt and dacite specimens with clinopyroxene/orthopyroxene ratios of 12 and 0.4, respectively.

The proportion of plagioclase to $pyroxene_{(total)}$ phenocrysts varies widely in WPM lavas, however, a positive correlation with respect to increasing SiO_2 in bulk rocks is apparent in EPM lavas containing >61 % SiO_2 (Table 4). Positive correlations of $plagioclase/pyroxene_{(total)}$ and orthopyroxene/clinopyroxene ratios with respect to increasing bulk rock silica contents is considered to be an effect of fractional crystallisation, whereas abnormal ratios have been considered as resulting from accidental entrainment of igneous rock fragments from plutonic environment (Hackett, 1985).

Similarly, experimental studies on the phase relations of water-saturated and water-undersaturated melting of andesite compositions (Eggler, 1972; Eggler and Burnham, 1973; Green, 1982) have shown a very pronounced lowering of the plagioclase field of stability relative to the pyroxene phases with increasing X^{fluid} and P_{H2O}, together with a similar increase of the amphibole stability field.

Therefore, under anhydrous conditions, plagioclase is the liquidus phase; however, under increasing water pressures there will be a tendency for the interval between plagioclase and pyroxene (or amphibole) precipitation to be reduced, thereby favouring decreasing plagioclase/ferromagnesian ratios (Ewart, 1982).

Representative electron microprobe analyses of clinopyroxenes (Table 6) and orthopyroxenes (Table 7) are plotted in terms of Ca-Mg-Fe^{2}+Mn end-members (atomic %) in Fig. 30, together with coexisting olivines.

(i) Ca-rich pyroxenes. Clinopyroxene is an essential phenocryst mineral in all lavas, although it generally decreases in proportion to orthopyroxene with increasing bulk-rock silica contents in EPM lavas. It is found as euhedral to anhedral phenocrysts, microphenocrysts and groundmass phases. All crystals are pale-green to light-brown, commonly twinned and complexly zoned. Many of the larger crystals (megacrysts) are poikilitic with titanomagnetite and occasional plagioclase, glass and/or olivine inclusions.

Two types of zoning, normal and reverse, are observed in the phenocrysts of several rock specimens. The Ca and Mg contents at the rim of normally zoned clinopyroxene are lower than those at the core, whereas rare reversely zoned crystals show the opposite relationship, and are usually depleted in Ca. Both reverse and normal zonings are sometimes present in a single specimen. The reverse zoning on the rim of clinopyroxenes is attributed to the effects of magma mixing (Sakuyama, 1979; 1981; 1984; Gerlach and Grove, 1982).

Most Ca-rich pyroxenes are augites, except for WPM lavas which contain augite cores with diopside rims, and occasional salites in crystal clots. The limited Mg/Fe compositional range is a mineralogical reflection of the weak iron enrichment trend of bulk rocks (Gill, 1981).

Non-quadrilateral components such as Ti, Al, Fe^{+3} and Na of EPM lavas together comprise only 3-9 atomic % of total cations, and these

ANAL. NO.	1406P	1404MPX	4004P	4004P	4009P	4005G	4011P	1303MP	1303MP	1301I
SPEC	RIM	CORE	CORE	RIM	CORE	MX	RIM	CORE	RIM	CPX
OXIDE (wt.%)										
SiO2	49.54	49.01	50.85	51.79	52.25	51.61	49.30	51.95	52.30	52.34
TiO2	.90	1.00	.69	.45	.57	.68	.92	.36	.35	.54
Al2O3	4.68	4.94	2.92	1.57	1.97	2.42	5.57	1.60	1.77	2.22
FeO	8.30	8.36	10.24	9.54	9.39	9.17	8.91	8.01	7.50	7.64
MnO	.14	.29	.32	.39	.40	.34	.34	.43	.34	.33
MgO	14.97	14.50	14.14	14.72	15.02	14.63	13.85	15.06	15.27	14.99
CaO	20.29	21.09	20.06	19.53	20.04	20.25	20.46	21.40	21.41	21.56
Na2O	.44	.43	.33	.22	.26	.26	.40	.32	.37	.47
K2O	.00	.00	.00	.01	.00	.01	.00	.00	.01	.01
Cr2O3	.00	.00	.03	.00	.00	.00	.07	.00	.02	.08
NiO	.02	.06	.00	.00	.04	.01	.00	.00	.00	.07
Cl	.00	.01	.01	.00	.02	.00	.01	.00	.01	.01
TOTAL	99.28	99.69	99.59	98.22	99.96	99.38	99.83	99.13	99.35	100.26
NUMBER OF CATIONS ON THE BASIS OF 6 (O)										
Si	1.855	1.836	1.911	1.961	1.945	1.932	1.842	1.948	1.950	1.937
Ti	.025	.028	.020	.013	.016	.019	.026	.010	.010	.015
Al	.207	.218	.129	.070	.087	.107	.245	.071	.078	.097
Fe	.260	.262	.322	.302	.292	.287	.278	.251	.234	.237
Mn	.004	.009	.010	.012	.012	.011	.011	.014	.011	.010
Mg	.836	.810	.792	.831	.833	.817	.771	.842	.849	.827
Ca	.814	.840	.808	.792	.799	.812	.819	.860	.855	.855
Na	.032	.031	.024	.016	.019	.019	.029	.024	.027	.033
K	.000	.000	.000	.000	.000	.001	.000	.000	.001	.001
Cr	.000	.000	.001	.000	.000	.000	.002	.000	.001	.002
Ni	.000	.002	.000	.000	.001	.000	.000	.000	.000	.001
Cl	.000	.001	.001	.000	.001	.000	.001	.000	.000	.001
TOTAL	4.032	4.043	4.017	3.997	4.006	4.005	4.024	4.018	4.015	4.016
100Mg/Mg+Fe2	77	82	73	73	75	75	77	80	80	80
Ca	42.80	45.75	42.53	40.89	41.48	42.36	44.68	44.56	44.51	45.02
Mg	43.95	44.12	41.68	42.90	43.25	42.62	42.06	43.63	44.20	43.55
Fe2+Mn	13.25	10.13	15.79	16.21	15.27	15.02	13.26	11.81	12.29	11.43
Fe3	.012	.085	.032	-	.010	.010	.046	.037	.028	.030
Fe2	.248	.177	.290	.302	.282	.277	.232	.214	.206	.207
Al IV	.145	.164	.089	.039	.055	.068	.158	.052	.050	.063
Al VI	.115	.054	.040	.031	.032	.039	.087	.019	.028	.034

TABLE 6 Representative electron microprobe analyses of clinopyroxene (explanation as in TABLE 5).

ANAL. NO.	4009PX	4002MP	4005G	3606P	3605MP	3602G	3201PX	1302G	1304I	1001P	1003MP	1004I
SPEC	CORE	CORE	MX	CORE	CORE	MX	CORE	MX	PLG	CORE	CORE	PLG
OXIDE (wt.%)												
SiO2	54.48	53.12	53.67	53.66	53.71	53.37	53.44	53.16	54.03	53.25	53.04	52.84
TiO2	.22	.23	.27	.21	.12	.18	.16	.25	.16	.09	.13	.08
Al2O3	.65	.90	.67	.74	.58	.74	1.28	1.94	.58	.49	.47	.92
FeO	16.80	18.36	17.19	18.61	17.98	18.56	18.09	15.69	17.06	19.74	19.63	19.89
MnO	.53	.59	.60	.79	1.12	.88	1.13	.70	.91	1.28	1.24	1.26
MgO	25.67	24.43	25.23	24.78	24.56	24.65	24.61	25.88	25.31	24.73	24.09	24.50
CaO	1.61	1.45	1.79	1.15	1.07	.98	.64	1.35	1.18	.44	1.23	.59
Na2O	.03	.03	.00	.00	.04	.02	.01	.00	.00	.00	.04	.00
K2O	.01	.01	.01	.00	.02	.00	.00	.03	.00	.02	.00	.03
Cr2O3	.00	.03	.00	.00	.06	.07	.00	.06	.00	.00	.00	.00
NiO	.00	.00	.00	.08	.00	.00	.01	.00	.01	.00	.03	.00
Cl	.00	.00	.00	.01	.00	.05	.00	.01	.00	.00	.01	.00
TOTAL	100.00	99.25	99.43	100.03	99.26	100.31	99.37	99.07	99.24	100.04	99.91	100.11
NUMBER OF CATIONS ON THE BASIS OF 6 (O)												
Si	1.980	1.967	1.971	1.970	1.983	1.971	1.969	1.945	1.984	1.967	1.966	1.953
Ti	.006	.007	.007	.006	.003	.005	.004	.007	.004	.002	.004	.002
Al	.028	.039	.029	.032	.025	.032	.056	.084	.025	.021	.020	.040
Fe	.512	.568	.528	.571	.555	.573	.556	.480	.524	.610	.609	.615
Mn	.016	.018	.019	.024	.035	.027	.035	.022	.028	.040	.039	1.350
Mg	1.393	1.348	1.382	1.356	1.352	1.357	1.351	1.412	1.386	1.362	1.331	.023
Ca	.063	.058	.071	.045	.042	.039	.025	.053	.046	.017	.049	.000
Na	.063	.002	.000	.000	.003	.002	.001	.000	.000	.000	.003	.000
K	.002	.001	.000	.000	.001	.000	.000	.001	.000	.001	.000	.001
Cr	.000	.001	.000	.000	.002	.002	.000	.002	.000	.000	.000	.000
Ni	.000	.000	.000	.002	.000	.000	.000	.000	.000	.000	.001	.000
Cl	.000	.000	.000	.001	.000	.003	.000	.001	.000	.000	.001	.000
TOTAL	4.001	4.008	4.007	4.009	4.002	4.011	4.000	4.006	3.999	4.021	4.022	4.025
Mg#	76	71	73	71	70	71	71	75	73	70	69	69
Ca	3.28	2.93	3.58	2.27	2.10	1.97	1.27	2.71	2.32	.85	2.43	1.13
Mg	72.51	68.15	69.62	68.49	67.74	68.54	68.65	72.15	69.86	67.69	66.12	66.57
Fe2+Mn	24.21	28.92	26.80	29.24	30.16	29.49	30.08	25.14	27.82	31.46	31.45	32.30
Fe3	.063	.014	.015	.016	.004	.016	-	.010	-	.017	.015	-
Fe2	.449	.554	.513	.555	.567	.557	.556	.470	.524	.593	.594	.615
Al IV	.020	.033	.029	.030	.017	.029	.031	.055	.016	.021	.020	.040
Al VI	.008	.006	-	.002	.008	.003	.025	.029	.009	-	-	-

TABLE 7 Representative electron microprobe analyses of orthopyroxene (explanation as in TABLE 5).

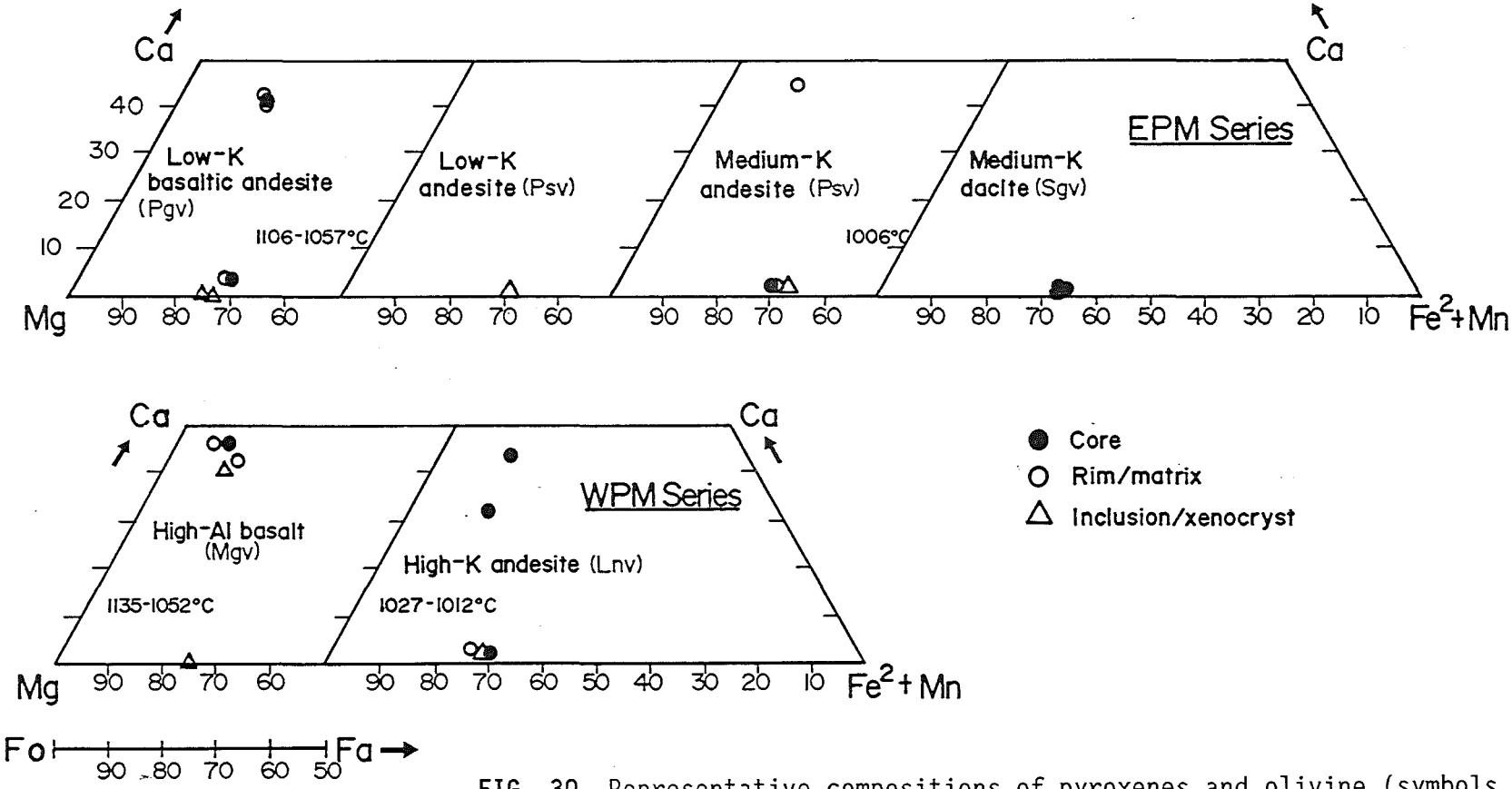

FIG. 30 Representative compositions of pyroxenes and olivine (symbols as in FIG. 29). Calculated equilibration temperatures of clinopyroxene-orthopyroxene pairs are also indicated.

values are totally within the range of WPM lavas, 1-10 atomic % of total cations. Aluminium is always sufficient to fill tetrahedral sites with Si, and the remaining octahedrally-coordinated Al is generally <3 % of total cations. No consistent trends of Al and Ti are apparent, and weak sector zonation with respect to Al and Ti probably accounts for most individual crystal variations.

Endiopside, subcalcic augite or pigeonite are not observed in these rocks.

(ii) <u>Ca-poor pyroxenes</u>. Orthopyroxene phenocrysts are elongate-prismatic and are pleochroic from pale pink to pale greyish-green. In basaltic andesites and andesites, orthopyroxene replaces olivines as the major calcium-poor ferromagnesian phenocrysts. All WPM lavas contain bronzites, occurring as phenocrysts, microphenocrysts and groundmass constituents, whereas EPM lavas consist of bronzites and/or hypersthenes. Several orthopyroxenes are also found in crystal aggregates and as inclusions in plagioclases.

Al_2O_3 ranges between 0.5 to 2 %, and most of it being tetrahedrally-coordinated. No consistent core to rim Al zonation is apparent. Since orthopyroxene has no 8-fold site, Al and Na values are lower than in coexisting clinopyroxene.

Orthopyroxene is normally zoned, but in some lavas fritted-skeletal cores are overgrown by Mg-rich jackets up to several microns wide and/or overgrowth of one pyroxene on another; pyroxene overgrowths are often more magnesian than the cores (see Fig. 23).

Overgrowth textures range from tiny augite crystals attached on the columnar surface parallel to the C-axis to anhedral orthopyroxenes jacketed by euhedral augite crystals. Although this texture indicates a reaction relationship between orthopyroxene and augite, it cannot be reproduced by simple fractional crystallisation because orthopyroxene and augite have a cotectic relationship in normal andesitic to dacitic system (Nakamura and Kushiro, 1970; Grove *et al.*, 1982).

The compositional reversals and overgrowth patterns in pyroxenes therefore are inferred to have resulted from magma mixing and/or entrainment of exotic crystals (Anderson, 1976; Sakuyama, 1979; 1981; 1984; Gerlach and Grove, 1982).

Likewise, euhedral to subhedral orthopyroxene phenocrysts without an augite rim commonly coexist with rimmed orthopyroxenes in a single rock specimen; this is also observed among clinopyroxenes and plagioclases. This textural type is common in EPM lavas, and has been suggested to indicate a complex change of melt composition and temperature (Sakuyama, 1984).

3.4.3 Fe-Ti Oxides

Representative electron microprobe analyses of titanomagnetites are given Table 8. Ulvospinel (Usp) contents have been calculated according to the method of Carmichael (1967).

The only recognisable primary Fe-Ti oxide phase is titanomagnetite, occurring as equant microphenocrysts (<0.3 mm), which are also observed as inclusions in all silicate phases, and as groundmass constituents. Titanomagnetites of the WPM lavas range from 9 to 11 % TiO_2 (25-32 mol % Usp), whereas EPM lavas show 6 to 7 % TiO_2 (18-20 mol % Usp), but titanomagnetites occurring as inclusions in silicate phenocrysts generally contain lower values ranging from 4 to 11 % TiO_2 (11-26 mol % Usp). The low TiO_2 content of these rocks, combined with the absence of ilmenite phase, reflects the Ti-poor bulk compositions of host rocks (Buddington and Lindsley, 1964), as well as, the effects of increasing acidity and oxygen fugacity during groundmass crsytallisation (Haggerty, 1976).

The absence of coexisting ilmenite and titanomagnetite phases precluded an estimate of magmatic temperature and oxygen fugacity in section 3.5.

ANAL. NO.	1402MPX	3203P	1405I	1409I	4006I	1006I
SPEC	CORE	CORE	OL	CPX	OPX	PLG
MINERAL	TMT	TMT	TMT	TMT	TMT	TMT
OXIDE (wt.%)						
SiO2	.05	.05	.04	.01	.12	.17
TiO2	8.62	7.25	9.11	8.66	11.29	5.16
Al2O3	5.09	2.18	5.52	4.33	3.11	1.94
FeO	76.14	82.71	74.99	74.58	78.36	84.17
MnO	.41	.58	.38	.35	.34	.51
MgO	3.77	1.44	4.53	4.99	1.84	1.24
CaO	.00	.01	.00	.06	.01	.15
Na2O	.00	.00	.00	.00	.00	.00
K2O	.00	.00	.00	.00	.00	.00
Cr2O3	.06	.00	.07	.08	.01	.00
NiO	.04	.00	.00	.03	.00	.00
Cl	.01	.00	.01	.00	.00	.01
TOTAL	94.49	94.22	94.65	93.09	95.08	93.35
RECALCULATED ANALYSES : Ulvospinel Basis (after Carmichael, 1967)						
Fe2O3	47.45	52.74	46.71	48.32	43.86	56.34
FeO	33.45	35.25	32.96	31.11	38.90	33.48
TOTAL	99.25	99.50	99.33	99.94	99.48	99.00
Usp (mol%)	24.56	20.80	25.70	24.65	32.23	14.92
NUMBER OF CATIONS ON THE BASIS OF 32 (O)						
Si	.014	.015	.011	.003	.036	.052
Ti	1.892	1.638	1.975	1.909	2.520	1.176
Al	1.750	.773	1.875	1.496	1.088	.693
Fe3	10.417	11.922	10.133	10.657	9.796	12.848
Fe2	8.163	8.856	7.945	7.626	9.656	8.485
Mn	.102	.148	.094	.086	.086	.131
Mg	1.639	.644	1.947	2.180	.813	.561
Ca	.000	.004	.000	.019	.004	.049
Na	.000	.000	.000	.000	.000	.000
K	.000	.000	.000	.000	.000	.000
Cr	.014	.000	.016	.019	.004	.000
Ni	.009	.000	.000	.007	.000	.000
Cl	.005	.000	.005	.000	.000	.006
TOTAL	24.005	24.000	24.001	24.002	24.003	24.001

TABLE 8 Representative electron microprobe analyses of Fe-Ti Oxides (explanation as in TABLE 5).

3.4.4 Olivine

Olivine is only found in the lavas of the Malobago volcanics, occurring as euhedral to subhedral phenocrysts, microphenecrysts and groundmass phases. This mineral also occurs as one of the primary constituents of crystal clots (see Fig. 20), together with augite and titanomagnetite in basalts. Several olivine microphenocrysts are subhedral inclusions in a zoned augite megacryst.

In most cases, olivine shows a reaction rim of dark reddish brown cryptocrystalline alteration product (iddingsite ?), which is similar to "type 1" iddingsite-rimmed olivine described by Baker and Haggerty (1967) to have formed as a low-temperature ($<140^{o}$) post-deuteric alteration product under oxidising conditions. The reaction rim is always thin (<5 microns).

Representative chemical compositions of olivines are given in Table 9.

The observed chemical compositions of the cores of phenocrysts and microphenocrysts range from Fo_{76-77}; those occurring in clots have less-magnesian cores (Fo_{75}), and the most-magnesian cores (Fo_{79-77}) are represented by olivine inclusions in augite megacryst. As a rule, olivine phenocrysts are unzoned though some of the larger crystals may show a slight normal zonation; olivine inclusions in augite megacryst, however, have more-magnesian rims with respect to their cores (<5 mol percent).

Olivine phenocrysts are associated with An-rich plagioclase (An_{83}), and glomeroporphyritic aggregates of An-rich plagioclase, olivine (Fo_{75}) and titanomagnetite (Usp_{25}). Although olivines in clots appear to be rounded and show resorption features, their forsterite contents are too low (Fo <82) to be interpreted as mantle xenocrysts (Gill, 1981). Most of the magnesian olivine (Fo >70) phenocrysts contain titanomagnetite inclusions, and chromian spinel phases were not observed.

ANAL. NO.	1401P	1407P	1403PX	1404PX	1405I
SPEC	CORE	CORE	CORE	CORE	CPX
OXIDE (wt.%)					
SiO2	37.87	38.05	37.96	37.65	38.60
TiO2	.03	.05	.00	.04	.01
Al2O3	.01	.06	.02	.04	.01
FeO	22.22	20.89	22.51	23.25	19.64
MnO	.42	.47	.51	.46	.31
MgO	38.75	39.56	38.58	38.68	40.90
CaO	.14	.19	.17	.16	.11
NaO	.00	.02	.00	.00	.04
K2O	.00	.04	.00	.00	.00
Cr2O3	.00	.00	.05	.00	.01
NiO	.03	.06	.00	.03	.04
Cl	.01	.02	.02	.01	.01
TOTAL	99.48	99.41	99.82	100.32	99.68
NUMBER OF CATIONS ON THE BASIS OF 4(O)					
Si	.992	.992	.993	.984	.996
Ti	.001	.001	.000	.001	.000
Al	.000	.002	.000	.001	.000
Fe	.487	.456	.492	.508	.424
Mn	.009	.010	.011	.010	.007
Mg	1.513	1.537	1.504	1.506	1.573
Ca	.004	.005	.005	.004	.003
Na	.000	.001	.000	.000	.002
K	.000	.001	.000	.000	.000
Cr	.000	.000	.001	.000	.000
Ni	.001	.001	.000	.001	.001
Cl	.000	.001	.001	.000	.000
TOTAL	3.007	3.008	3.007	3.015	3.005
Fo	76	77	75	75	79

TABLE 9 Representative electron microprobe analyses of olivine (explanation as in TABLE 5).

Calcium contents in olivine phenocrysts and microphenocrysts lie between 0.14 to 0.20 % (average = 0.18 %); those included in augite megacryst, 0.11 to 0.17 %, and those in clots have relatively constant values (0.16-0.17 %) from cores towards the rims.

The role of pressure as a control on Ca in olivine is debatable (Stormer, 1973), but absence of a clear Ca zonation in olivine and its coexistence with plagioclase suggest low pressures (<9 kb) olivine crystallisation. Indeed, the observed range of CaO values in olivine is consistent with 1 atmosphere crystallisation of olivine from melts having the 6 to 10 % CaO contents of basalts (Watson, 1979).

3.4.5 Amphiboles

Strongly pleochroic pale green amphibole (<10 volume %) occurs as phenocrysts and microphenocrysts (see Fig. 21), and as megacrysts (see Fig. 22), but never as groundmass constituent or inclusion in other silicate phases. It is often found in the extrusives of dome eruptions, and appears as a significant mafic phase (>1 volume %) in bulk rock compositions of >58 % SiO_2; it is the dominant ferromagnesian phase (12 volume %) in dacite (see Table 4). However, the amphibole in dacite is a reddish brown variety (oxyhornblende, basaltic hornblende or lamprobolite), which indicates a higher Fe_2O_3/FeO ratio (Gill, 1981).

Coronas of opaque material (opacite) are always present (see Figs. 22, 25 and 26), and in several cases, the amphiboles are wholly or partially replaced by opaque minerals. Opacite rims in rocks suggest resorption (or oxidation), which are formed either in magmatic environments due to reduction of P_{H2O} and/or increase in temperature or during eruption (Gill, 1981), or at the Earth's surface (Larsen et al., 1937).

Representative electron microprobe analyses of amphiboles are contained in Table 10.

ANAL. NO. SPEC	3203P CORE	3211P CORE	3205P CORE	3205P RIM	3207P CORE	3207P RIM	3204MP CORE	3601MP CORE	1301P CORE	1011P CORE	1001P RIM	1004PX CORE	1004PX RIM	1006PX CORE	1002P RIM
OXIDE (wt.%)															
SiO2	42.67	43.99	41.71	43.55	44.84	46.20	45.27	45.86	43.75	46.44	43.15	46.91	47.09	46.67	47.15
TiO2	1.96	1.62	1.95	1.78	1.36	1.60	1.84	1.90	3.09	1.82	1.18	1.79	1.31	1.30	.96
Al2O3	12.92	10.79	13.16	11.86	10.14	9.11	9.45	7.53	9.87	7.70	8.38	7.82	7.82	7.59	6.63
FeO	9.95	12.59	10.96	10.53	12.99	12.45	12.48	11.26	11.50	12.41	11.34	12.29	12.26	11.96	12.21
MnO	.16	.25	.16	.25	.50	.38	.33	.40	.22	.50	.44	.40	.40	.40	.73
MgO	15.01	14.36	14.31	15.75	14.67	14.87	14.75	15.46	14.32	15.42	18.25	15.69	15.82	15.54	16.34
CaO	12.01	11.11	11.67	11.64	10.60	10.69	10.80	11.41	11.47	11.04	10.46	11.10	10.74	10.64	10.66
Na2O	2.53	2.23	2.74	2.64	2.14	1.91	2.43	2.80	2.36	1.67	3.40	1.40	1.52	2.65	2.74
K2O	.28	.19	.23	.21	.16	.15	.12	.61	.96	.35	.28	.30	.29	.33	.20
Cr2O3	.05	.03	.07	.02	.00	.04	.00	.00	.03	.04	.01	.03	.00	.10	.00
NiO	.00	.00	.01	.01	.00	.00	.03	.00	.00	.01	.00	.02	.00	.00	.00
Cl	.03	.03	.03	.02	.04	.02	.03	.12	.09	.06	.09	.08	.04	.08	.04
H2O	2.05	2.03	2.03	2.06	2.04	2.05	2.04	2.03	2.03	2.04	2.01	2.06	2.05	2.04	2.04
TOTAL	99.62	99.22	99.03	100.32	99.48	99.47	99.57	99.38	99.69	99.50	98.99	99.86	99.34	99.30	99.70
NUMBER OF CATIONS ON THE BASIS OF 23 (O)															
Si	6.230	6.491	6.163	6.322	6.597	6.757	6.642	6.761	6.452	6.814	6.418	6.836	6.884	6.858	6.913
Ti	.215	.180	.217	.194	.151	.176	.203	.210	.342	.200	.132	.196	.144	.143	.106
Al	2.222	1.877	2.292	2.029	1.759	1.570	1.634	1.308	1.715	1.332	1.469	1.343	1.347	1.315	1.148
Fe	1.215	1.554	1.355	1.279	1.598	1.522	1.532	1.388	1.419	1.523	1.411	1.498	1.499	1.470	1.470
Mn	.020	.031	.020	.031	.062	.047	.041	.049	.028	.063	.056	.049	.049	.049	.046
Mg	3.268	3.160	3.152	3.409	3.217	3.242	3.227	3.397	3.149	3.373	4.046	3.408	3.447	3.404	3.511
Ca	1.878	1.756	1.848	1.810	1.671	1.675	1.697	1.803	1.812	1.736	1.667	1.733	1.683	1.675	1.704
Na	.717	.637	.785	.743	.610	.542	.690	.800	.673	.474	.980	.395	.432	.756	.333
K	.052	.036	.044	.038	.030	.027	.023	.115	.180	.066	.052	.056	.054	.062	.048
Cr	.006	.004	.008	.002	.000	.005	.000	.000	.004	.004	.001	.003	.000	.012	.002
Ni	.000	.000	.001	.001	.000	.000	.004	.001	.000	.001	.000	.002	.000	.000	.000
Cl	.006	.008	.007	.006	.009	.006	.008	.029	.022	.015	.023	.021	.010	.019	.009
OH	2.000	2.000	2.000	2.000	2.000	2.000	2.000	2.000	2.000	2.000	2.000	2.000	2.000	2.000	2.000
TOTAL	17.830	17.733	17.892	17.864	17.703	17.570	17.703	17.861	17.796	17.602	18.254	17.541	17.551	17.764	17.826
Mg/Mg+Fe2	.75	.69	.72	.75	.68	.68	.71	.71	.69	.70	.80	.72	.72	.72	.70
Al IV	1.770	1.509	1.837	1.678	1.403	1.243	1.358	1.239	1.548	1.186	1.582	1.164	1.116	1.142	1.087
Al VI	.452	.368	.455	.351	.356	.327	.276	.069	.167	.146	-.113	.179	.231	.173	.059
Fe3	.119	.108	.119	.158	.105	-	.239	-	-	.100	.399	.142	.155	.135	-
Fe2	1.096	1.446	1.236	1.121	1.493	1.552	1.293	1.388	1.419	1.423	1.012	1.356	1.344	1.335	1.596

TABLE 10 Representative electron microprobe analyses of amphibole (explanation as in TABLE 5).

Two types of amphiboles are identified (Table 11), according to the classification of Leake (1978). WPM lavas contain calcic amphiboles only, typically ferroan to titanian pargasitic hornblende, whereas EPM lavas consist of both calcic and sodic-calcic types; andesites largely show normally-zoned ferroan pargasitic hornblende to edenite (calcic) and unzoned magnesio-taramite (sodic-calcic), whereas the dacite has edenite to magnesio-hornblende (calcic) and magnesio-taramite to magnesio-katophorite (sodic-calcic).

Amphiboles are generally silica-undersaturated, typically containing 42 to 47 % SiO_2, with Si contents ranging from 6.2 to 6.9 (average = 6.6) per 23 O. Thus, amphibole precipitation is an effective mechanism to increase silica and normative quartz in magma (Bowen, 1928). Nearly 65 % of analyses are considered high-Si (>6.5 Si per 23 O) amphiboles, and hence, are atypical for island arc andesites (Jakes and White, 1972).

Aluminium is always sufficient to supplement Si in filling the **Z** group, and the Al^{vi} values are generally <0.46 per 23 O. Based on experimental data (Green, 1972; Allen *et al.*, 1975; Allen and Boettcher, 1978), the low Al^{vi} contents (<0.5 per 23 O) suggest their extrusion at P_{H2O} < 9 kb.

The $100.Mg/Mg+Fe^2$ ratios of amphiboles range between 66.8 to 74.1 (mol %), which are less magnesian than coexisting clinopyroxenes, but lie within the Mg/Fe range of orthopyroxenes. Such variation has been reported in other island arc andesites (e.g., Ewart, 1971; Nicholls, 1971; Jakes and White, 1972). The positive correlation of Mg/Fe ratios between pyroxene and amphibole indicates that the amphibole will cause Fe-enrichment in a magma, although enrichment particularly with respect to silica, is lesser compared to pyroxene or olivine fractionation (Gill, 1981).

Several amphiboles show reverse zoning; the rim has a higher Mg/Fe ratio than the core, and is more enriched in Al and Na (in dacite, but is depleted in Ca and K (in dacite) and in Al, Na and K (in andesite). Si contents widely vary and show no clear correlation. The reverse Mg/Fe zoning in amphiboles can result from magma mixing

SAMPLE NO. (Rock type)	SPECIFICATION (n)	CALCIC $(Ca+Na)_B>1.34;Na_A<0.67$	PRESSURE (Kb)	SODIC-CALCIC $(Ca+Na)_B>1.34;0.67<Na_A<1.34$
A: WPM-Series 13 (High-K andesite)	Ph/Mp core (1)	Ferroan Pargasitic hornblende $(Na+K)_A>0.50;Ti<0.50;Fe^3<Al^{IV}$	4.71	-
	Xenocryst (1)	Titinian Pargasitic hornblende $(Na+K)_A>0.50;Ti<0.50;Fe^3<Al^{IV}$	4.9	-
B: EPM-Series 32 (Low-K andesite)	Phe/Mp core (6)	Ferroan Pargasitic to Edenitic hornblende	5.52 4.62	Magnesio-taramite $(Na+K)_B>0.50$
	Phe/Mp rim (2)	Edenite $(Na+K)_A>0.50;Ti<0.50;Fe^3<Al^{IV}$	3.98	Magnesio-taramite $(Na+K)_A>0.50$
36 (Medium-K andesite)	Phe/Mp core (1)	Edenite	2.66	-
10 (Medium-K dacite)	Phe/Mp core (1)	Edenite	2.78	-
	Phe/Mp rim (2)	-	-	Magnesio-taramite to Magnesio-katophorite
	Xenocryst (2)	Magnesio-hornblende	2.85	Magnesio-katophorite

TABLE 11 Classification of amphiboles (after Leake, 1978) and pressure estimates (after Hammarstrom and Zen, 1986).

(Sakuyama, 1978) or increase in oxygen fugacity (Mason, 1978) probably due to influx of volatiles (Gill, 1981). Similar reversely-zoned amphiboles have been reported in Haruna volcano (Oshima, 1975) and Shirouma-Oike volcano (Sakuyama, 1978).

Thus, using the mineral compositions and assemblages, some qualitative evaluations of crystallisation temperature, pressure and water content are possible. These estimates will be the first for the volcanic rocks of Pocdol Mountains.

3.5 T-P-X_{H2O} RELATIONS

3.6.1 Temperature

Crystallisation temperature estimates (Table 12) are taken from coexisting pyroxenes and the most An-rich plagioclases. The absence of phenocrystic ilmenite phases in both WPM and EPM lavas precluded the use of coexisting Fe-Ti oxides (Buddington and Lindsley, 1964).

The results of two-pyroxene thermometry, following the method of Kretz (1982), yield crystallisation temperatures ranging from 1135°C (in basalt) to 1006°C (in andesite); no temperature estimate is given for dacite because hypersthene is the only pyroxene phase present. In contrast, higher temperature estimates are observed when using the plagioclase thermometry (Kudo and Weill, 1971 and Mathez, 1973), which probably reflects the earlier precipitation of plagioclase phases in the melt. Crystallisation temperature estimates of plagioclases at 1 kb are as follows : 1415°C (in basalt), 1239°C (in basaltic andesite), 1217°C (in low-K andesite), 1205°C (in medium-K andesite), 1179°C (in high-K andesite), and 1009°C (in dacite).

Similarly, Ringwood has implied that the high temperature of crystallisation of plagioclase and the broad temperature interval through which plagioclase crystallises alone (Ringwood, 1977, see Table 2) effectively constitute a thermal barrier between basalt and rhyodacite. However, several workers (e.g., Kuno, 1950) have shown that a crystallisation path exists through these compositions.

	Tempera ture (°C)	
	Pyroxenes (1 atm)	Plagioclase (1 kb)
A: WPM SERIES		
High-Al basalt	1052-1135	1169-1415
High-K andesite	1012-1027	908-1179
B: EPM SERIES		
Low-K basic andesite	1060-1106	1136-1239
Medium-K andesite	1006	1020-1217
Medium-K dacite	-	968-1009

TABLE 12 Results of two pyroxene (Kretz, 1982) and plagioclase (Kudo and Weill, 1970; Mathez, 1973) geothermometry.

3.6.2 Pressure and Water Content

The Al^T content of calcic amphiboles has been shown to be directly related to the depth of emplacement of plutonic rocks, and hence, is regarded as an indicator of pressure (Hammarstrom and Zen, 1986).

Following the treatment of Hammarstrom and Zen (1986), low pressure (<6 kb) crystallisation in subcrustal reservoirs (see Table 10) is indicated by the Al^T contents of calcic amphiboles in both WPM and EPM andesites and dacite. WPM series andesites show an average pressure of 4.8 kb whereas EPM series andesites have variable pressure ranging from 5.1 for andesites to 2.8 kb for dacite.

In addition the following aspects of the observed mineralogy also indicate low pressure (<7 kb) crystallisation :

(i) The coexistence of olivine and plagioclase in andesite lavas requires crystallisation pressures of <7 kb, because at higher pressures these phases will react to form aluminous pyroxenes + spinel (Green and Hibberson, 1969);

(ii) The calcium content of olivine is generally low, and is almost constant from cores to rims, which indicates a low pressure, nearly isobaric olivine crystallisation (Gill, 1981), and

(iii) The observed concentrations of Al, Na, and Ti in pyroxenes, although dependent also on temperature, cooling rate, silica activity, and coexisting minerals, are low enough to at least eliminate pressures of >10 kb (Green, 1972).

Both WPM and EPM lavas were probably H_2O-undersatured, but not completely anhydrous, during phenocryst precipitation, based on comparison with experimental results of other studies. For example, Gill (1981; see Table 4.1 and Fig. 4.1) suggested that about 2-5 % H_2O is required to achieve reasonable agreement between observed eruptive temperatures and experimentally-determined andesite liquidus temperatures, and Eggler (1972) concluded that most andesite magmas must contain <3 % H_2O to contain plagioclase phenocrysts.

CHAPTER IV

BULK ROCK CHEMISTRY

CHAPTER IV

BULK ROCK CHEMISTRY

4.1 INTRODUCTION

There are few bulk rock analyses of volcanic rocks at Pocdol Mountains, and where published, are usually quoted as average values and seldom discussed in detail. For example, in a study of extrusive rocks in the Bicol arc, Divis (1980, see Table 1) presented an average andesite composition (n=8) from Pocdol Mountains; however, no sampling information is given. Reyes (1985) analysed several "fresh" rocks in order to quantify metasomatism in hydrothermally-altered rocks in the field area.

The primary aim of this section is therefore to present bulk rock major oxide and trace element concentrations, combined with petrogaphy and mineralogy (see chapter III). The data will then be used to constrain petrogenetic models of the volcanic rocks at Pocdol Mountains in chapter V.

Major oxide and trace element analyses reported in this study were carried out in the X-Ray Spectrometry Laboratory of the Department of Geology, University of Canterbury, Christchurch, using a **Philips PW 1400** X-ray spectrometer. Major oxides were determined on fused glass beads, following the techniques outlined by Norrish and Hutton (1969), with modifications after Harvey *et al.* (1973) and Schroeder *et al.* (1980).

Analyses of international standard rocks are listed in Table 13.

Trace elements were obtained on pressed powder pellets which were analysed for Zr, Nb, Ba, Ni, Cr, V, Nd, Ce, La and Zn, using a 3 KW Au tube; for Y, Rb, Sr, Ga, Pb and Th, using a 3 KW Mo tube. Both tubes were run at 40 KV and 50 MA. Mass absorption corrections were made using Compton and Rayleigh tube lines.

	AGV-1		G2		GA		GSP-1		MRG-1		NIM-D	
	DET	REC	DET	REC	DET	REC	DET	REC	DET	REC	DET	REC
SiO_2	59.74	59.72	68.27	69.19	70.00	69.96	67.20	67.31	39.23	39.14	38.96	38.88
TiO_2	1.05	1.05	.48	.50	.35	.38	.66	.66	3.77	3.75	.02	.02
Al_2O_3	17.35	17.22	15.20	15.35	14.76	14.51	15.13	15.19	8.49	8.56	.28	.32
tFe_2O_3	6.77	6.88	2.58	2.62	2.71	2.83	4.31	4.34	17.86	17.79	17.02	16.97
MnO	.10	.10	.04	.04	.08	.09	.04	.04	.18	.17	.22	.22
MgO	1.54	1.55	.71	.77	.87	.95	.95	.96	13.53	13.51	43.66	43.56
CaO	4.95	5.00	1.91	1.98	2.46	2.45	2.02	2.02	14.89	14.72	.27	.28
Na_2O	4.36	4.31	3.99	4.06	3.51	3.55	2.72	2.80	.75	.71	$<.10$	.05
K_2O	2.95	2.93	4.44	4.52	4.10	4.03	5.49	5.53	.19	.18	$<.01$	.01
P_2O	.50	.50	.13	.14	.13	.12	.28	.28	.06	.07	$<.05$	.02

	NIM-G		NIM-L		NIM-N		NIM-S		SY2		SiO_2	
	DET	REC	DET	REC	DET	REC	DET	REC	DET	REC	DET	REC
SiO_2	75.65	75.72	52.45	52.45	52.66	52.56	63.55	63.65	60.43	60.09	100.16	100.00
TiO_2	.09	.09	.49	.49	.19	.20	.04	.04	.14	.15	$<.01$	$<.01$
Al_2O_3	12.12	12.09	13.60	13.59	16.72	16.54	17.36	17.37	12.14	12.15	$<.20$	$<.01$
tFe_2O_3	1.96	2.02	9.99	9.94	8.97	8.87	1.39	1.40	6.28	6.29	$<.01$	$<.01$
MnO	.01	.02	.75	.76	.19	.18	.01	.01	.32	.32	$<.01$	$<.01$
MgO	$<.10$	.04	.29	.28	7.51	7.48	.34	.46	2.70	2.69	$<.10$	$<.01$
CaO	.78	.78	3.15	3.24	11.56	11.46	.68	.66	7.99	8.00	$<.01$	$<.01$
Na_2O	3.24	3.30	8.58	8.30	2.56	2.46	.28	.42	4.50	4.35	$<.10$	$<.01$
K_2O	5.00	5.00	5.45	5.46	.24	.25	15.41	15.38	4.48	4.50	$<.01$	$<.01$
P_2O_5	$<.05$	.02	.05	.06	$<.05$	.03	.12	.12	.44	.44	$<.05$	$<.01$

DET: Determined value, X-ray Laboratory, Geology Department, University of Canterbury

REC: Recommended value of International Standard. SiO_2 = specpure silica

TABLE 13 Analyses of international rock standards for major element determinations (analyst: Dr. S.D. Weaver, June, 1987).

Detection limits (in ppm) for trace elements are the following : Sr (2), Zr (3), Nb (2), Ba (30), V (<5), Cr (<5), Nd (<5), Ce (<5), Zn (<3), Ni (<5) and La (<5). In cases where results fall below these limits, above values are retained in the analyses.

4.2 CLASSIFICATION

Since all the lavas examined are porphyritic, a classification scheme based on chemical composition is preferred and the method of Peccerillo and Taylor (1976), modified by Ewart (1982), is adopted in this study. Ewart (1982) classified extrusive rocks on their silica and potash contents (Fig. 31) into :

(i)	basalt	<52 wt.% SiO_2
(ii)	basaltic (basic; low-Si) andesite	52-56 wt.% SiO_2
(iii)	andesite (or acid andesite)	52-63 wt.% SiO_2
(iv)	dacite	63-70 wt.% SiO_2

In addition, lines on the K_2O divisions mark boundaries between the following rock suites :

(i) I, "arc tholeiitic series";
(ii) II, "calc-alkaline series";
(iii) III, "high-K calcalkaline series", and
(iv) IV, "shoshonitic series".

Moreover, rock suites I to III correspond to "low-K", "medium-K" and "high-K series" of Gill (1981) and these terms are used interchangeably in this study.

The above classification, however, is only an attempt to subdivide a continuum, and hence, boundaries are not rigid. All plots used are based on data which were first recast to 100 % (anhydrous basis), with Fe_2O_3/FeO normalised to 0.3 (Gill, 1981).

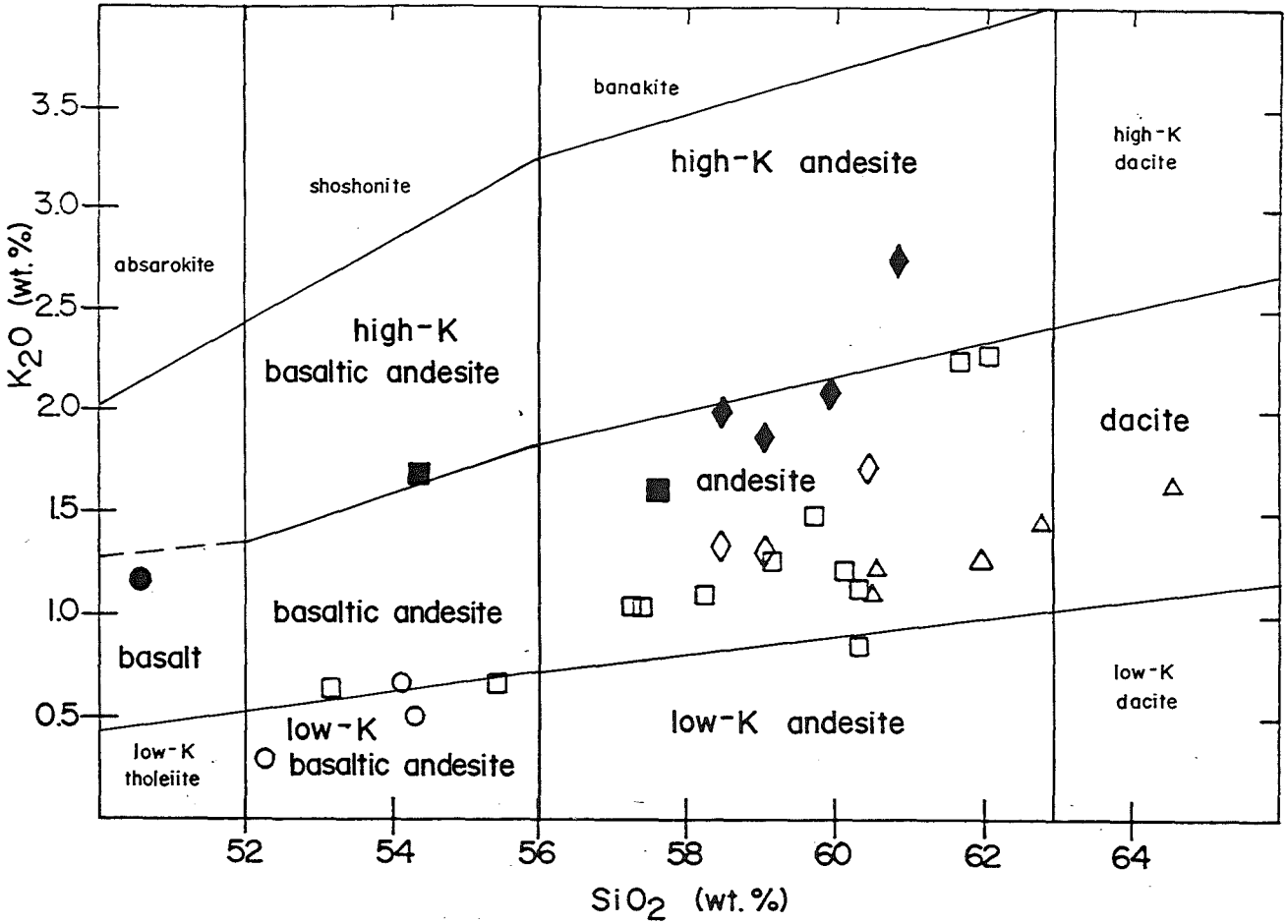

FIG. 31 Chemical nomenclature of volcanic rocks according to Peccerillo and Taylor (1976), as modified by Ewart (1982). Filled symbols denote WPM rocks : Malobago (circle), Kayabon (square), and Lison volcanics (diamond); and open symbols, EPM lavas : Pulog (circle), Pangas (square), Cawayan (diamond), and Suminandig volcanics (triangle).

In retrospect the two groups of lavas, discussed in chapters II and III, again are clearly differentiated on the basis of the silica versus potash diagram (Fig. 31), such that :

(i) the **WPM series** consist of medium-K high alumina basalt to high-K basaltic andesite to medium- and high-K andesite, which lie entirely in the field of "calcalkaline series" (Jakes and Gill, 1970, see Fig. 2), and

(ii) the **EPM series** comprise low-K basaltic andesite to medium-K andesite to medium-K dacite, and rocks containng <56 % SiO_2 plot in the field of "island-arc tholeiitic series", but the bulk of EPM rocks (57.3-64.6 % SiO_2) plots within the "transition zone" between calc-alkaline and island-arc tholeiitic series (see discussion in chapter V).

Similarly, pronounced variations in abundances of high field strength (HFS) ions and large-ion lithophile (LIL) elements are apparent between WPM and EPM series lavas (section 4.4).

Major oxide compositions of WPM and EPM lavas are contained in Tables 14 and 15, respectively. Data are plotted on silica-oxide variation diagrams (Harker diagrams) in Fig. 32. Average major oxide compositions of the different rock suites in both WPM and EPM lavas are listed in Table 16.

The use of silica content as an abscissa and as an implicit measure of relative differentiation is particularly effective in andesites due to the following features :

(i) silica variance in andesites greatly exceeds the sum of other oxide variances (Chayes, 1964);

(ii) silica dominates the primary factor in factor analyses of andesites (Le Maitre, 1976), and

(iii) silica correlates positively and significantly with measures of differentiation (Gill, 1981).

FIELD NUMBER:	14	4	3	12	39	38	13
LITHOLOGIC UNIT:	Mgv	Knv	Knv	Lnv	Lnv	Lnv	Lnv
MAJOR ELEMENTS (Weight %)							
SiO2	50.58	54.30	57.63	58.51	59.05	60.01	60.86
TiO2	1.08	.79	.68	.64	.65	.61	.62
Al2O3	20.46	18.94	18.29	18.43	17.87	17.67	17.44
Fe2O3	2.03	1.75	1.63	1.49	1.52	1.40	1.27
FeO	6.77	5.83	5.44	4.97	5.06	4.69	4.23
MnO	.13	.13	.12	.11	.12	.12	.10
MgO	4.69	4.09	3.44	2.84	3.06	3.08	2.75
CaO	9.37	8.94	7.56	7.06	7.01	6.64	6.05
Na2O	3.36	3.24	3.43	3.65	3.56	3.55	3.72
K2O	1.12	1.61	1.56	1.95	1.84	2.03	2.68
P2O5	.40	.36	.12	.34	.25	.19	.28
LOI	.44	.93	.22	-1.35	.04	-1.27	.52
SUM	99.98	100.25	99.87	98.42	98.72	98.24	100.01
Mg Number	51	51	49	46	47	50	49
FeO*/MgO	1.83	1.81	2.01	2.22	2.10	1.93	1.96
CIPW NORMS (mol%)							
Q	-	2.25	7.64	8.18	9.21	10.38	10.19
Or	6.51	9.33	9.10	11.40	10.63	11.81	15.64
Ab	27.88	26.90	28.59	30.46	29.44	29.62	31.07
An	36.71	31.76	29.44	27.77	26.65	25.87	22.62
Di	5.20	7.80	5.08	3.84	4.71	4.45	4.26
Hy	8.47	16.54	15.74	14.04	14.14	13.82	12.14
Ol	8.98	-	-	-	-	-	-
Mt	2.87	2.48	2.31	2.12	2.14	2.00	1.80
Il	2.02	1.48	1.27	1.21	1.21	1.14	1.16
Ap	.87	.79	.46	.74	.55	.42	.61
TRACE ELEMENTS (ppm)							
Rb	9	32	31	40	39	42	60
Ba	447	612	460	765	541	518	875
Sr	988	838	526	827	611	483	708
Pb	5	5	8	8	9	7	9
La	23	25	22	27	15	17	32
Ce	49	45	32	45	30	35	57
Nd	40	33	30	27	25	27	34
Th	3	3	3	7	3	5	9
Y	26	35	30	21	24	23	28
Zr	101	124	104	133	119	129	182
Nb	7	8	8	8	9	7	10
V	301	235	192	156	173	170	145
Cr	25	12	11	5	10	8	20
Ni	21	14	8	7	7	7	11
Zn	73	79	61	62	61	56	48
Ga	19	18	17	16	18	19	17
K/Rb	1033	418	418	405	392	401	371
Rb/Sr	.01	.04	.06	.05	.06	.09	.08

TABLE 14 Major and trace element concentrations and CIPW norms of WPM series lavas. Oxide values were recast to 100% (anhydrous basis), assuming $Fe_2O_3/FeO = 0.3$ (Gill, 1981). Loss on ignition (LOI) were obtained after 24 hrs at 1000°C. SUM indicates the original total of oxides + LOI.

FIELD NUMBER:	428	23	30	40	19	33	34	35	22	29	25	78
LITHOLOGIC UNIT:	Pgv	Psv	Pgv	Pgv	Psv	Psv	Psv	Psv	Cnv	Psv	Cnv	Psv
MAJOR ELEMENTS (Weight %)												
SiO2	52.30	53.21	54.17	54.31	55.48	57.27	57.41	58.26	58.46	59.14	59.15	59.73
TiO2	.68	.80	.75	.98	.65	.69	.65	.63	.74	.63	.78	.66
Al2O3	20.42	18.98	20.15	18.91	19.33	18.72	18.54	18.48	17.75	18.05	17.42	17.14
Fe2O3	2.13	1.99	1.89	2.00	1.83	1.64	1.60	1.56	1.58	1.55	1.60	1.44
FeO	6.59	6.62	6.30	6.68	6.11	5.47	5.35	5.21	5.27	5.17	5.35	4.82
MnO	.18	.15	.14	.15	.20	.12	.12	.13	.14	.12	.13	.11
MgO	5.56	4.81	4.82	4.47	3.88	3.98	3.82	3.67	3.34	3.17	3.19	3.78
CaO	9.28	9.62	8.01	8.41	8.68	7.41	7.81	7.51	7.52	7.23	7.14	7.13
Na2O	2.47	3.04	3.00	3.46	3.08	3.53	3.51	3.32	3.74	3.52	3.72	3.61
K2O	.27	.62	.64	.47	.64	1.02	1.02	1.08	1.31	1.22	1.31	1.42
P2O5	.12	.15	.14	.15	.12	.16	.16	.15	.16	.19	.20	.16
LOI	2.94	.16	-.35	.15	1.02	.46	.59	.55	-1.67	-.12	-1.17	-.34
SUM	99.75	99.31	98.92	100.17	100.37	99.98	100.46	100.44	98.35	100.35	99.09	99.93
Mg Number	56	52	53	50	49	52	52	51	49	48	47	54
FeO*/MgO	1.53	1.75	1.66	1.90	2.00	1.74	1.78	1.80	2.00	2.07	2.13	1.62
CIPW NORMS (mol%)												
Q	3.07	2.45	4.93	3.87	6.83	7.55	7.80	10.03	8.46	10.92	10.05	10.49
Or	1.52	3.58	3.69	2.75	3.69	5.93	5.93	6.28	7.63	7.16	7.69	8.34
Ab	19.80	25.10	24.86	28.88	25.54	29.34	29.34	27.75	31.28	29.60	31.19	30.29
An	41.58	35.53	38.00	34.17	36.32	31.71	31.41	31.93	27.48	29.64	26.70	26.16
Di	1.15	8.41	-	4.98	4.25	2.84	4.80	3.21	6.95	3.98	5.91	6.54
Hy	25.31	19.47	23.11	20.36	18.65	18.20	16.71	16.95	14.22	15.34	14.50	14.79
Mt	2.92	2.80	2.66	2.85	2.59	2.32	2.28	2.23	2.25	2.22	2.29	2.07
Il	1.23	1.49	1.40	1.83	1.21	1.29	1.23	1.19	1.40	1.19	1.48	1.25
Ap	.24	.33	.31	.33	.26	.35	.35	.33	.35	.42	.44	.35
TRACE ELEMENTS (ppm)												
Rb	1	10	11	7	11	20	19	21	26	25	26	30
Ba	103	162	166	68	134	257	240	266	317	314	375	371
Sr	355	499	413	280	381	397	407	399	430	524	404	427
Pb	5	6	4	5	5	5	6	9	6	9	7	6
La	5	5	5	5	5	5	7	5	8	9	9	12
Ce	16	16	13	11	16	18	13	19	22	23	30	24
Nd	9	12	22	25	16	15	17	21	23	18	27	21
Th	1	1	1	1	1	2	2	2	2	3	2	2
Y	15	20	21	26	22	22	20	20	23	22	28	24
Zr	46	61	70	88	58	85	93	88	105	100	121	123
Nb	4	5	4	7	5	6	6	5	8	5	8	6
V	220	263	216	239	186	171	179	161	179	175	178	166
Cr	26	23	19	23	19	39	16	14	7	7	5	7
Ni	14	13	12	12	11	14	13	11	9	9	6	30
Zn	77	76	74	87	67	63	64	66	61	62	66	56
Ga	18	19	19	19	17	19	19	17	19	17	19	16
K/Rb	2241	515	483	557	483	423	446	427	418	405	418	393
Rb/Sr	.00	.02	.03	.03	.03	.05	.05	.05	.06	.05	.06	.07

TABLE 15 Major and trace element concentrations and CIPW norms of EPM series lavas. Oxide values were recast to 100% (anhydrous basis), assuming $Fe_2O_3/FeO = 0.3$ (Gill, 1981). Loss on ignition (LOI) were obtained after 24 hrs at 1000°C. SUM indicates the original total of oxides + LOI.

FIELD NUMBER:	28A	28B	32	1	16	43	37	8	36	17	10C
LITHOLOGIC UNIT:	Psv	Psv	Psv	Cnv	Sgv	Sgv	Psv	Sgv	Psv	Sgv	Sgv
MAJOR ELEMENTS (Weight %)											
SiO2	60.13	60.32	60.36	60.47	60.52	60.54	61.67	61.98	62.07	62.80	64.56
TiO2	.59	.64	.58	.64	.65	.68	.59	.70	.59	.55	.50
Al2O3	17.54	18.37	18.73	17.58	17.03	16.49	19.30	18.67	17.28	16.97	16.65
Fe2O3	1.46	1.47	1.40	1.37	1.46	1.53	1.32	1.47	1.29	1.24	1.13
FeO	4.86	4.90	4.67	4.57	4.88	5.10	4.39	4.91	4.29	4.14	3.77
MnO	.13	.10	.10	.10	.12	.13	.11	.11	.11	.12	.10
MgO	3.47	3.16	2.65	2.91	3.48	3.69	2.56	2.91	2.38	2.69	2.34
CaO	7.01	6.37	6.66	6.69	7.18	7.31	6.05	4.76	5.85	6.20	5.56
Na2O	3.46	3.41	3.86	3.84	3.49	3.25	3.64	3.10	3.73	3.77	3.69
K2O	1.19	1.09	.84	1.68	1.08	1.17	2.20	1.23	2.23	1.41	1.59
P2O5	.15	.17	.15	.15	.11	.11	.17	.15	.19	.12	.11
LOI	-.03	1.30	.89	.76	-.29	-.13	-.06	1.94	.41	.03	-.11
SUM	100.04	100.26	100.70	100.23	99.22	99.06	99.64	100.03	100.16	100.55	100.04
Mg Number	52	49	46	49	52	52	47	47	45	49	48
FeO*/MgO	1.78	1.97	2.24	2.00	1.78	1.76	2.18	2.14	2.29	1.95	2.05
CIPW NORMS (mol%)											
Q	12.51	14.09	13.03	10.93	13.12	13.67	12.99	20.47	13.48	16.05	19.24
Or	6.99	6.28	4.88	9.75	6.28	6.75	12.81	7.05	12.99	8.29	9.35
Ab	29.02	28.26	32.22	31.98	29.11	27.00	30.39	25.48	31.15	31.74	30.99
An	28.50	29.82	30.96	25.41	27.15	26.45	24.08	21.96	23.57	25.15	24.00
Di	4.10	-	.60	5.26	5.96	6.98	3.73	-	3.23	3.93	2.24
Hy	15.44	16.46	14.69	12.68	14.37	14.70	12.34	15.64	11.96	12.28	11.51
Mt	2.08	2.08	2.00	1.95	2.08	2.16	1.87	2.06	1.83	1.78	1.62
Il	1.12	1.19	1.10	1.19	1.21	1.27	1.29	1.29	1.12	1.04	.95
Ap	.33	.37	.33	.33	.24	.24	.33	.33	.42	.26	.24
TRACE ELEMENTS (ppm)											
Rb	21	22	15	34	18	23	48	12	47	29	33
Ba	327	276	191	422	320	288	580	389	661	398	398
Sr	415	392	359	453	331	318	487	283	480	317	323
Pb	7	7	5	5	7	6	9	7	9	7	5
La	7	6	5	14	7	8	16	19	70	10	9
Ce	19	17	9	25	20	17	31	22	36	22	26
Nd	25	26	28	27	22	15	32	27	31	16	27
Th	4	2	2	4	2	2	4	3	5	2	4
Y	18	20	19	24	18	20	24	18	25	18	17
Zr	94	98	86	116	90	86	148	134	158	93	104
Nb	5	4	5	6	5	4	8	5	6	6	5
V	143	173	143	185	167	176	138	139	154	126	109
Cr	33	35	17	9	38	34	6	6	8	9	8
Ni	13	13	11	8	11	13	6	8	11	8	8
Zn	59	67	65	55	59	60	43	55	49	53	47
Ga	18	17	17	18	16	17	16	17	17	16	15
K/Rb	470	411	465	410	498	422	381	851	394	404	400
Rb/Sr	.05	.06	.04	.08	.05	.07	.10	.04	.10	.10	.10

Table 15 (Con't)

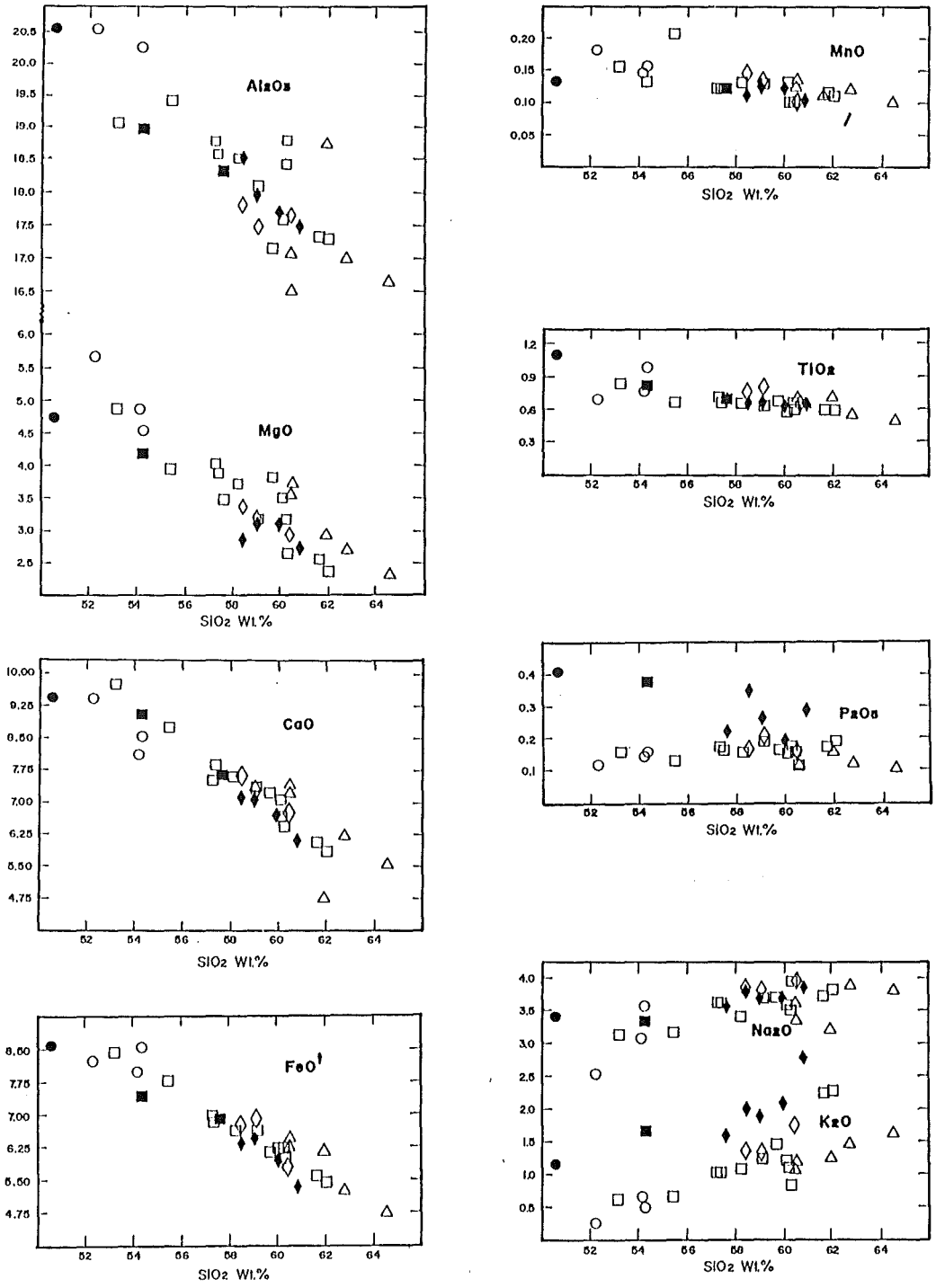

FIG. 32 Silica-major oxide variation diagrams (symbols as in FIG. 31).

Major Oxide (wt.%) (n)	WPM High-Al basalt (1)	WPM High-K basic andesite (1)	WPM Medium-K andesite (4)	WPM High-K andesite (1)	EPM Low-K basic andesite (3)	EPM Medium-K basic andesite (2)	EPM Low-K andesite (1)	EPM Medium-K andesite (15)	EPM Medium-K dacite (1)
SiO2	50.58	54.30	58.80	60.86	54.03	53.69	60.36	59.81	64.56
TiO2	1.08	.79	.64	.62	.77	.78	.58	.66	.50
Al2O3	20.46	18.94	18.06	17.44	19.53	19.56	18.73	17.89	16.65
Fe2O3	2.03	1.75	1.51	1.27	1.99	1.94	1.40	1.49	1.13
FeO	6.77	5.83	5.04	4.23	6.46	6.46	4.67	4.97	3.77
MnO	.13	.13	.12	.10	.18	.14	.10	.12	.10
MgO	4.69	4.09	3.11	2.75	4.64	4.82	2.65	3.30	2.34
CaO	9.37	8.94	7.07	6.05	8.79	8.82	6.66	6.86	5.56
Na2O	3.36	3.24	3.55	3.72	3.00	3.02	3.86	3.52	3.69
K2O	1.12	1.61	1.84	2.68	.46	.63	.84	1.35	1.59
P2O5	.40	.36	.22	.28	.13	.14	.15	.15	.11

TABLE 16 Representative major element compositions of WPM and EPM series lavas.

However, Chayes (1960) noted that the major handicap of Harker diagrams is its tendency to introduce negative correlation in some oxide plots in the diagram; but this does not affect their use as a graphical test of compositional changes in the magma, resulting from crystal fractionation (Wilcox, 1979).

4.3. MAJOR ELEMENTS

4.3.1 Silica

Silica values of volcanic rocks in the field area range from 50 to 65 %, and therefore according to the above classification scheme, the rocks belong to the **"basalt-andesite-dacite"** suite common in island arc settings (Chayes, 1969; Le Maitre, 1976; Ewart, 1982). Most rocks have silica contents between 57 and 62 %, which reflects the predominance of andesites in the sample population.

The compositional range of andesites also show the greatest scatter, particularly for Al_2O_3, MgO, K_2O and P_2O_5. Precipitation of plagioclase, pyroxene and occasionally hornblende, with subordinate titanomagnetite phases will decrease Al_2O_3, CaO, MgO, MnO, FeO^t, TiO_2 and P_2O_5 concentrations of the silicate melt, thus accounting for the expected negative correlations with SiO_2 contents from basalt to dacite (Fig. 31).

Silica typically shows a good correlation with most other oxides due to its abundance (as explained in the preceding section). However, there seems to be a generally poor correlation for EPM lavas, which may reflect their more porphyritic texture compared to WPM lavas (see Tables 3 and 4).

Although both lava groups show a nearly continuous variation from basalt to dacite, a compositional gap is apparent between 55.5 to 57.3 % SiO_2. This gap may have resulted from the small sample population (n=30). Some oxides show distinct changes at >57.3 % SiO_2, i.e.,

two trends for K_2O (in EPM lavas) are apparent at higher silica contents, and for TiO_2 (in WPM lavas), there is a slight change in slope at 54 % SiO_2. In both instances, there is an abrupt decline in modal plagioclase, clinopyroxene and opaque oxide phases at the change (see Table 3).

4.3.2 Aluminium, Calcium, Magnesium, Total Iron, Titanium and Phosphorous

Aluminium content is high in all rocks, ranging from 16.65 to 20.46 %. Some EPM lavas (57.3-62.0 % SiO_2) exhibit constant Al_2O_3 values with increasing silica content, which is different from the usual negative trend. These rocks also show constant modal plagioclase phenocrysts (23-25 volume %; see Table 4), and are distinctive from the normally increasing plagioclase modes in these rocks.

Calcium behaves similarly to Al_2O_3, and ranges from 6.05-9.37 % in WPM lavas and 4.76-9.62 % in EPM lavas. The trend is a strong indication that clinopyroxene and plagioclase fractionation (e.g., Gill, 1981) occurs in both WPM and EPM lavas.

Magnesium contents are consistently lower in WPM (4.69-2.75 %) than EPM (5.56-2.34 %) lavas. EPM rocks also show more scatter and a greater decrease with increasing silica than WPM lavas, which probably reflect the greater abundance of modal pyroxenes in EPM rocks.

Total iron ($FeO^t = FeO + 0.9Fe_2O_3$) also behaves similarly to MgO, and ranges from 4.7-8.7 %; FeO^t contents are comparable to CaO, which is typical of calcalkaline volcanic suites (Gill, 1981). Petrography indicates that fractionation of pyroxenes, olivine and subordinate titanomagnetite (+ amphibole ?) is the mechanism for the suppresion of iron enrichment in both rock series.

Titanium contents of WPM (0.61-1.08 %) and EPM (0.50-0.98 %) lavas are generally low (<1.3 % TiO_2), and are typical of rocks at convergent plate margins (Jakes and White, 1971); TiO_2 and FeO^t contents usually correlate positively with each other and negatively with silica in orogenic andesites (Gill, 1981, p.111).

EPM lavas exhibit more scatter than WPM lavas, particularly in the basaltic andesite range, which probably reflects the extreme modal contents of titanomagnetite (1.0-6.5 volume %) in these rocks (see Table 4). Similarly, there is an indication that TiO_2 (so does FeO^t) peaks at 54 % SiO_2, which suggests titanomagnetite precipitation. WPM lavas also show an inflection at 54-56 % SiO_2, and this point may correspond to the peak of modal titanomagnetite contents (3.0-3.5 volume %; see Table 3) in these lavas.

Phosphorous contents in orogenic andesites are typically low, between 0.05-0.30 % (Gill, 1981, p.112), and values reported here vary from 0.11-0.40 % P_2O_5. EPM lavas have generally lower P_2O_5 contents (0.11-0.20 %), which remains almost constant, and then decrease in bulk rocks >62 % SiO2. In contrast, WPM lavas have higher P_2O_5 values (0.12-0.40 %), showing considerable scatter particularly in andesites. This feature indicates apatite precipitation, but this mineral was not observed in these lavas.

4.3.3 Alkalies

Potassium contents vary more between andesite suites than any other oxide contents (e.g., Gill, 1981), and hence, these variations have tectonic (e.g., Dickinson, 1968; 1975), as well as petrogenetic significance (e.g., Taylor, 1969).

In both WPM and EPM lavas K_2O correlates positively with SiO_2, which implies that potassium is strongly incompatible through the entire compositional range. The two lava series have already been separated using silica-potash diagram (section 4.2), but EPM lavas also display two distinct trends :

(i) a low-K basaltic andesite to medium-K andesite trend, which is refferred to here as the "**EPM andesite trend**", and

(ii) a low to medium-K andesite to medium-K dacite trend, called here as the "**EPM dacite trend**".

The EPM dacite trend is typified by distinct changes in phenocryst modal proportions such as : **(i)** increasing plagioclase (20-35 volume %); **(ii)** increasing hornblende (6-12 volume %); **(iii)** decreasing clinopyroxene (4 volume % - trace), and **(iv)** decreasing titanomagnetite (3.75-2.75 volume %).

Most WPM lavas follow a smooth positive correlation with silica, but four analyses within the andesite compositional range are anomalous (Fig. 31). These are typified by : **(i)** high modal plagioclase (~35 volume %); **(ii)** extreme values of pyroxene modes (7.0-2.5 volume % clinopyroxene; 6.0-1.5 volume % orthopyroxene); **(iii)** <2 volume % hornblende crystals, and **(iv)** decreasing titanomagnetite mode (3.5-1.5 volume %).

Sodium is contained in plagioclase (0.5-7.5 % Na_2O; see Table 5), and hence, is more compatible than potassium. WPM lavas are more strongly correlated with SiO_2 than EPM lavas, which may reflect the narrow modal proportions of plagioclase (26-38 volume %) in WPM rocks compared to wider variations in EPM lavas (15-50 volume %).

4.4 TRACE ELEMENTS

Trace element concentrations are listed in Table 14 (WPM series) and 15 (EPM series), and selected data are plotted against SiO_2 in Fig. 33; average trace element abundances of the various rock suites in both WPM and EPM lavas are contained in Table 17.

4.4.1 Rubidium , Barium and Strontium

These elements have large cations (Whittaker and Muntus, 1970), and follow K during geochemical processes (Ewart, 1982); their concentrations therefore generally correlate positively with K_2O and SiO_2 in most andesites (Gill, 1981).

In the Pocdol Mountains, the abundances of these large-ion lithophile (LIL) elements are consistently higher in WPM than EPM lavas, usually by 1.5 to 2.0 times.

Trace Element (ppm) (n)	WPM High-Al basalt (1)	WPM High-K basic andesite (1)	WPM Medium-K andesite (4)	WPM High-K andesite (1)	EPM Low-K basic andesite (3)	EPM Medium-K basic andesite (2)	EPM Low-K andesite (1)	EPM Medium-K andesite (15)	EPM Medium-K dacite (1)
Rb	9	32	38	60	6	10	15	26	33
Ba	447	612	571	875	102	164	191	360	398
Sr	988	838	612	708	339	456	359	410	323
Pb	5	5	8	9	5	5	5	7	9
La	23	25	20	32	5	5	5	13	9
Ce	49	45	31	57	14	14	9	22	26
Nd	40	33	27	34	17	17	28	23	27
Y	26	35	25	28	21	20	19	22	17
Th	3	3	5	9	1	1	2	3	4
Zr	101	124	121	182	64	66	86	109	104
Nb	7	8	8	10	5	4	5	6	5
Zn	73	79	60	48	77	75	65	59	47
Ni	21	14	7	11	12	12	11	12	8
V	301	235	173	145	215	240	143	166	109
Cr	25	12	9	20	23	21	17	18	8
Ga	19	18	18	17	18	19	17	17	15
K/Rb	1033	418	404	371	1094	499	465	451	400
Rb/Sr	.01	.04	.07	.08	.02	.02	.04	.07	.10

TABLE 17 Representative trace element compositions of WPM and EPM series lavas.

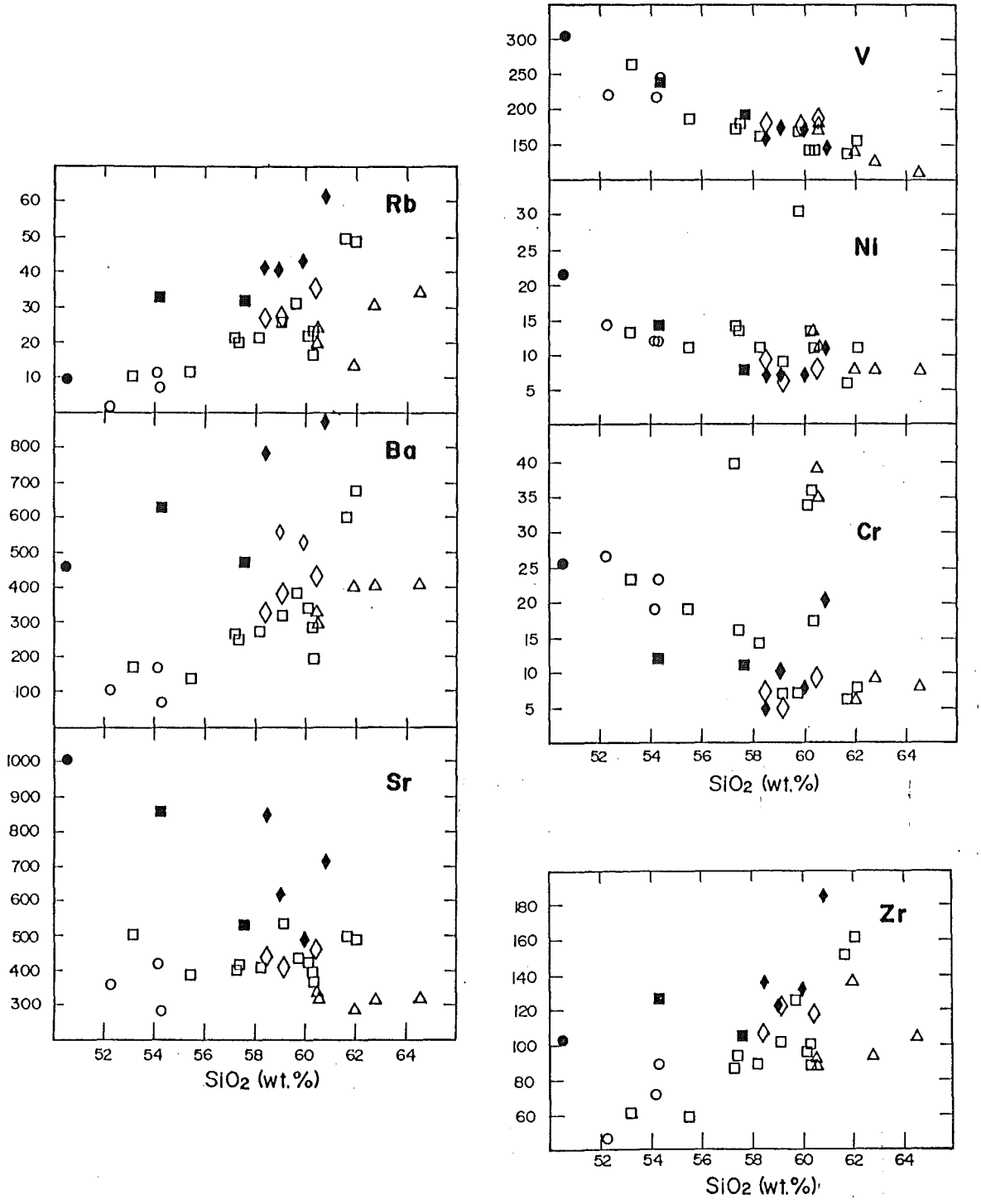

FIG. 33 Selected silica-trace element varaition diagrams (symbols as in FIG. 31).

Rubidium and barium show almost identical patterns to K_2O. Both EPM andesite and dacite trends, described in the silica-potash diagram in Fig. 31 (section 4.3), are still present. In addition, the EPM dacite trend exhibit an abrupt decrease in concentration of Rb (10 ppm) and Ba (150 ppm), as well as Sr (100 ppm), at 60.5 % SiO_2. This point also correspond to equivalent drops in modal abundances of primary phenocryst phases, such as plagioclase (10 %); clinopyroxene (4.5 %), orthopyroxene (2 %); amphibole (4 %), and titanomagnetite (1.5 %).

The scatter in the andesite range of both Rb and Ba in WPM lavas is associated to large modal variations of clinopyroxenes (2-7 %) and orthopyroxenes (1.5-5.5 %) in these rocks.

Strontium trends are opposite Rb and Ba because Sr is a compatible element, which preferentially goes to plagioclase feldspars. The Sr scatter in the basaltic andesite range (EPM andesite trend) defines considerable variations in modal plagioclase (30-50 %), orthopyroxene (1-6 %) and clinopyroxene (2-8 %) whereas the constant slope at >61 % SiO_2 (EPM dacite trend) corresponds to increasing modal plagioclase (20-37 %) and hornblende (7-12 %), and decreasing clinopyroxene (4%-trace) and orthopyroxene (7-2 %).

4.4.3 Zirconium

Zirconium is an incompatible, high field strength (HFS) cation, which behaves similarly to Rb and Ba.

4.4.4 Vanadium, Nickel and Chromium

These are strongly compatible elements that usually decrease regularly with increasing SiO_2, and follow the trend of Feo^t and TiO_2 (Gill, 1981). Abundances of the ferromagnesian elements in both lava series are characteristically low, i.e., in WPM lavas (V, 301-145 ppm; Ni, 21-7 ppm; Cr, 25-5 ppm) and in EPM lavas (V, 220-109 ppm; Ni, 30-6 ppm; Cr, 39-5 ppm). These concentrations are too low for liquids in equilibrium with mantle peridotite (Gill, 1981, see Fig. 5.14).

Two additional points are stressed with respect to the variation of ferromagnesian elements and silica contents. These are :

(i) an inflection for V, Ni and Cr, between 56-58 % SiO_2, as observed in TiO_2, occur in WPM lavas and is related to the decrease in modal clinopyroxene (5 %) and titanomagnetite (2 %), and

(ii) an abrupt decrease at 60.5 % SiO_2 (section 4.4.1) is present, with Cr showing the largest drop, 35 ppm; second is V, 50 ppm, and lastly Ni, 10 ppm.

CHAPTER V

PETROGENESIS

CHAPTER V

PETROGENESIS

In this section petrogenetic models are based on the detailed petrologic, chemical and stratigraphic data presented in chapters II to IV. A brief review of recent models of volcanic arc-trench systems is outlined, followed by a discussion of the tectonic setting and volcanic rock associations of the Pocdol Mountains.

5.1 ROCK ASSOCIATIONS OF VOLCANIC ARC - TRENCH SYSTEMS

Volcanic rocks in island-arc setting can be subdivided (Fig. 34) into three rock associations (Jakes and White, 1969; Jakes and Gill, 1970) :

(i) "tholeiitic" rocks lie in the oceanic side, and are followed away from the trench by
(ii) "calcalkaline (or calcalkalic)" and
(iii) "shoshonitic (or alkalic)" rocks.

The spatial sequence of volcanic rock associations in island arcs has been well documented in Japan (Kuno, 1959; 1966; Sugimura, 1960), and is essentially similar to the pattern described earlier by Rittmann (1953) from Indonesia.

Jakes and his coworkers elaborated some important points on their generalised arc model, and these are summarised below :

(i) Each of the three recognised associations has a dominant rock type. Basalt (<54 wt.% SiO_2) is the most common rock of the island-arc tholeiitic and shoshonitic associations. In contrast, andesite (54-63 wt.% SiO_2) dominates the calcalkaline association.

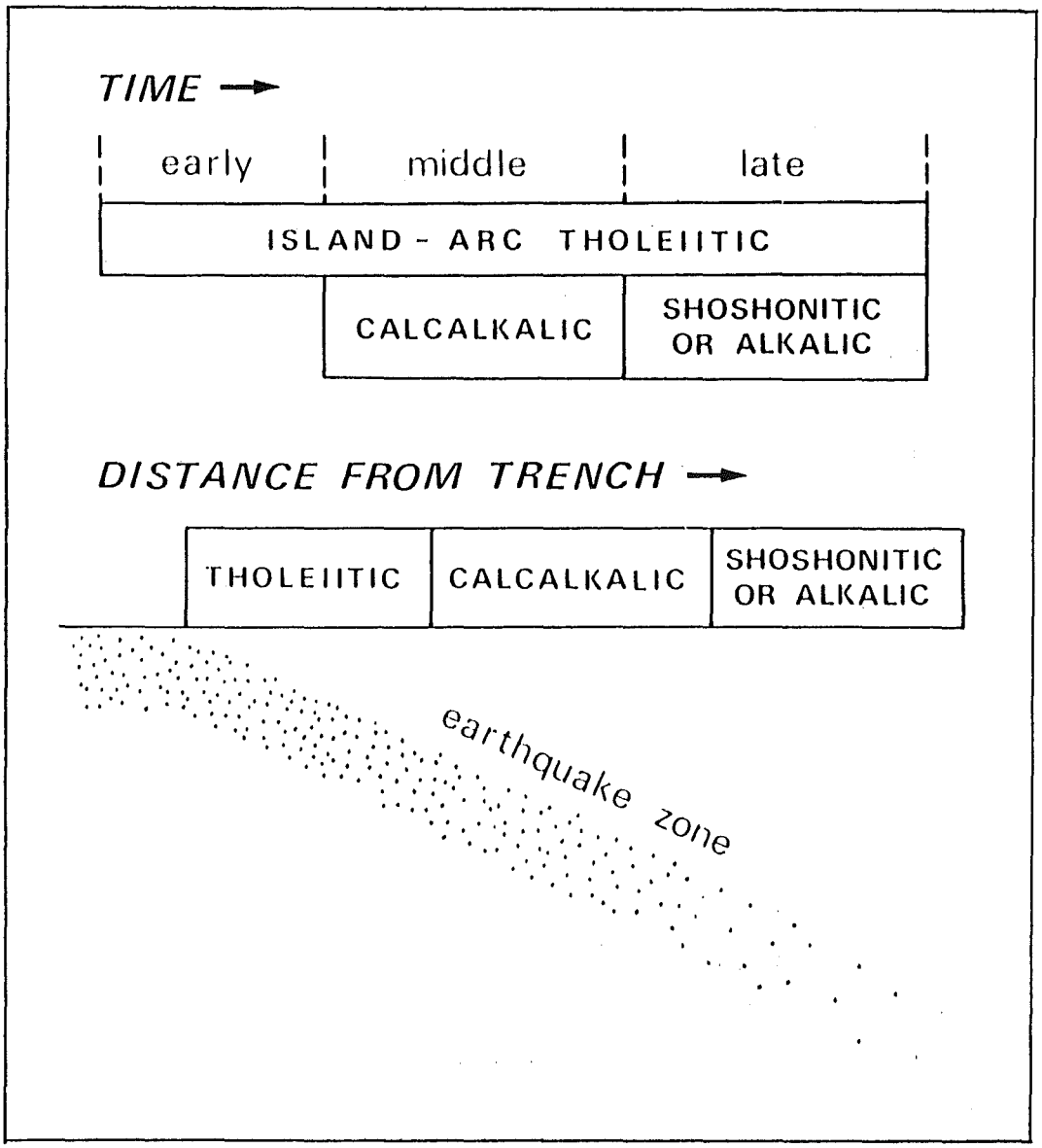

FIG. 34 Summary of spatial and temporal relationships between volcanic rock associations in arc-trench systems (after Jakes and White, 1969; 1972; Jakes and Gill, 1970).

(ii) Abundances of K_2O, Rb, Ba, Sr, Pb, Cs, Th, and U, as well as Th/U and K/Na ratios increase as depths to Benioff zone (h) increase. TiO_2 and Zr concentrations are higher in some shoshonitic rocks, compared with calcalkaline and tholeiitic ones. The degree of "iron enrichment" is reported to decrease as h increases.

(iii) The associations also imply a variation in composition with time and stratigraphic level, such that the earliest rocks are tholeiitic, followed away from the trench by calcalkaline rocks along with tholeiites, and in the latest stage shoshonites appear with tholeiitic and calcalkaline rocks (Fig. 34).

Thus, Jakes and White (1971; 1972) have proposed that the crust of island arcs has primary stratification with respect to K, Rb, Ba, Sr, REE, SiO_2, FeO^t/MgO and K_2O/Na_2O.

Although subsequent studies have demonstrated that many exceptions to this evolutionary scheme exist (Johnson *et al.*, 1971; Donnelly *et al.*, 1971; De Long *et al.*, 1975; Brown *et al.*, 1977; Foden and Varne, 1980), Ringwood (1974; 1977) considers the model to provide important boundary contraints for theories of petrogenesis (section 5.3), if viewed in a broader perspective rather than a rigorous sequential development.

Arculus and Johnson (1978) consider that too much emphasis has been given on similarities between arcs. They note that broad similarities in arcs should be accompanied by critical assessment of unique features before controlling factors of arc evolution can be ascertained.

5.2 VOLCANIC ARCS OF THE CENTRAL PHILIPPINES

The Central Philippines lies between two oppositely dipping zones of seismicity, which are marked by trenches-- the Manila Trench in the west and the Philippine Trench in the east (see Fig. 1).

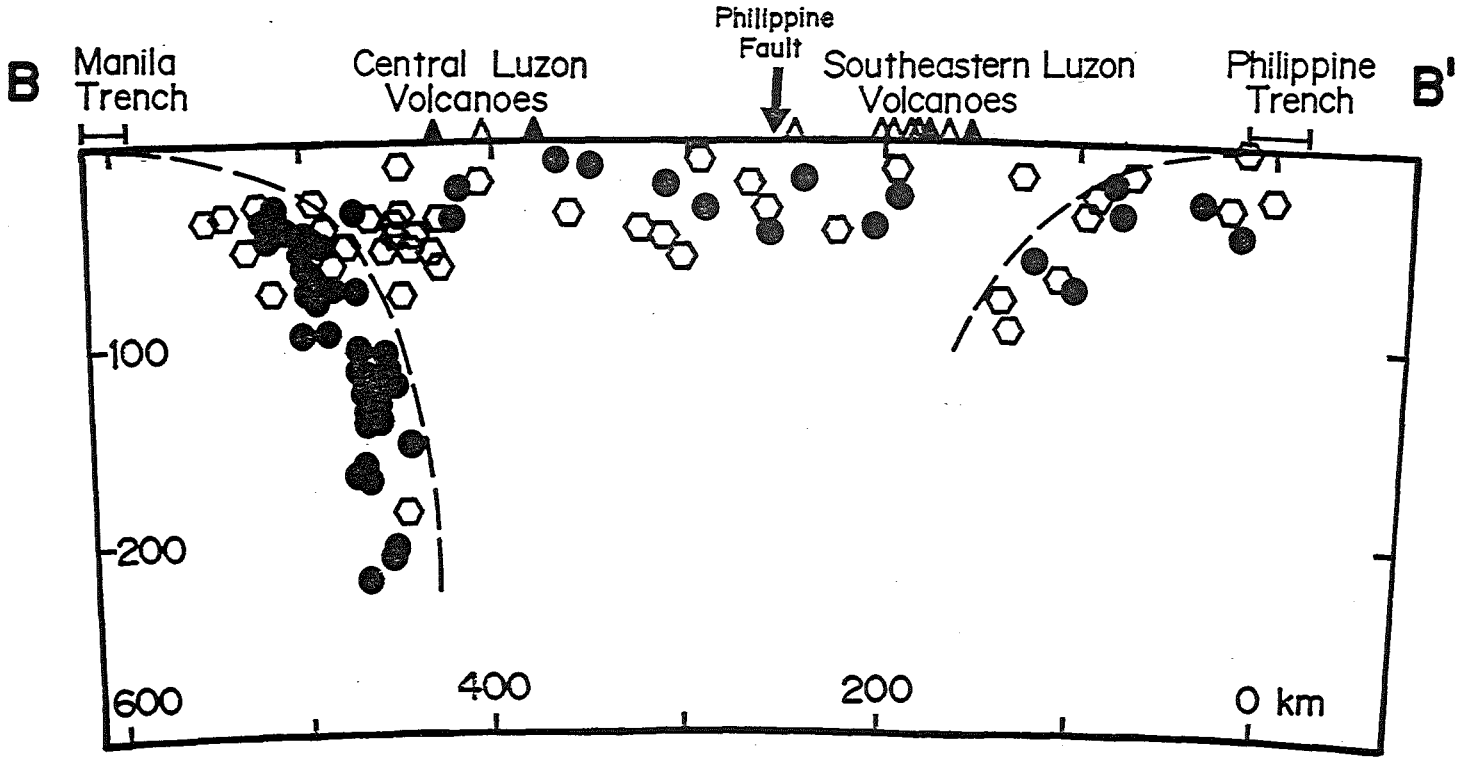

FIG. 35 Schematic section across northern Palawan and SE Luzon (line BB′ in FIG. 1) showing intermediate earthquake hypocentres (modified from Cardwell *et al.*, 1980). Filled circles and open hexagons represent good and fair quality earthquake hypocentres, respectively. The dashed line approximates the surface of the downgoing slab. Historically active volcanoes are shown as solid triangles, and volcanoes of inferred Quaternary age are shown as open triangles.

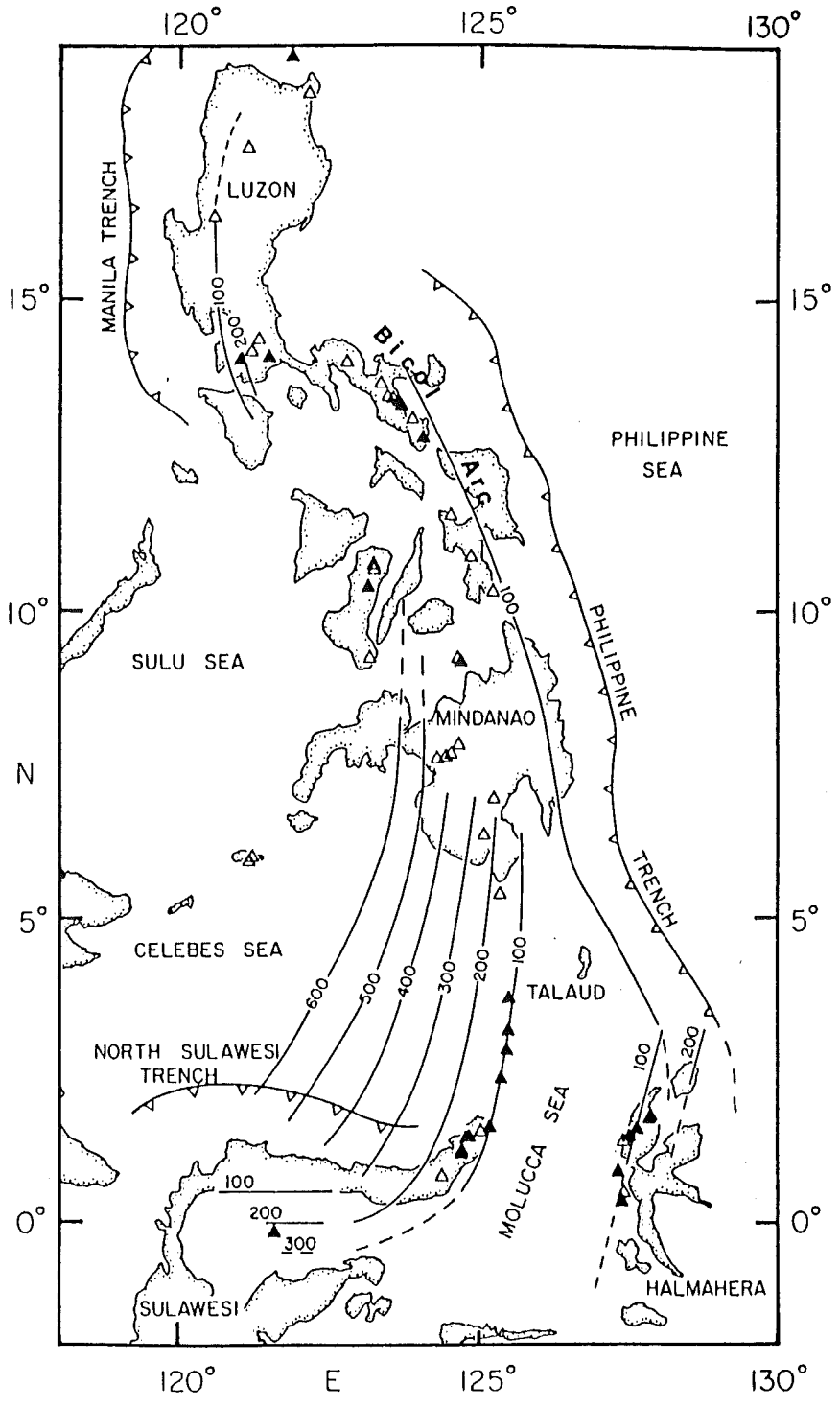

FIG. 36 Depth contours to the tops of the subducting slab in the Philippine and NE Indonesian region (after Cardwell *et al.*, 1980).

Except for the western Central Philippines where the North Palawan continental terrane has collided with the islands (McCabe *et al.*, 1985), the oppositely-dipping seismic zones (Fig. 35) are well-defined to depths of 200-250 kms and 100-150 kms beneath western- and eastern Luzon, respectively (Cardwell *et al.*, 1980). The western and eastern volcanic belts associated with each subduction zones are called the "**Western Central Luzon arc**" and "**Bicol arc**", respectively (Defant *et al.*, 1988; Knittel and Defant, 1988).

5.2.1 The Western Central Luzon Arc

The Western Central Luzon arc comprises tholeiitic, calcalkaline, and shoshonitic lavas with increasing distance from the Manila Trench (De Boer *et al.*, 1980; Ragland and Defant, 1983). The arc can be subdivided broadly into the Bataan and Mindoro arc segments, which are separated by a narrow NE-SW "cross-arc" zone of intense volcanism (**Macolod Corridor**), and perhaps delineating a transform structure between the Manila and Philippine Trenches (Defant, 1985; Defant *et al.*, 1988).

5.2.2 The Bicol Arc

The Bicol arc comprises 14 Pliocene to Recent stratovolcanoes (Newhall, 1979; Divis, 1980; Datuin, 1982; Bogie and Lawless, 1986), extending for about 250 kms through southern Luzon, and appears to continue southwards across Leyte Island towards eastern Mindanao (Divis, 1980; Hawkins *et al.*, 1985). Only Mayon and Bulusan volcanoes are presently active within this chain, with hypersthene augite andesite the dominant effusive, and minor basalt and basaltic andesite, dacite domes and rare rhyolitic ignimbrites (Divis, 1980). All volcanoes lie above the 100 kms contour of the Benioff zone descending from the Philippine Trench (Fig. 36).

Sr isotopic compositions of andesites in the Bicol arc range from 0.7034 to 0.7037 and correlate with Rb/Sr ratios (Divis, 1980). Rhyolite flows exposed on the eastern slope of Mt. Malinao have slightly higher $^{87}Sr/^{86}Sr$ (0.70377-0.70397) and Rb/Sr ratios (Weber,

1984). Mukasa *et al.* (1986) have reported that these rocks also contain low $^{206}Pb/^{204}Pb$ and high $^{208}Pb/^{204}Pb$ with respect to MORB, and are similar to the rocks in Taiwan (Sun, 1980) and northeast Indonesia (Morris *et al.*, 1983). However, the rocks fall within the MORB field on $^{207}Pb/^{204}Pb$ versus $^{206}Pb/^{204}Pb$ correlation diagrams, which they reckoned as unusual, because most arc materials have $^{207}Pb/^{204}Pb$ ratios higher than those of MORB.

Unlike the Western Luzon arc, the Bicol arc has not developed a clear rock/tectonic association. Divis (1980) has reported the predominance of calcalkaline effusives, but Mukasa *et al.* (1986) have indicated that the Bicol arc is characterised by high-K tholeiitic basalts and andesites, rather than calcalkaline rocks.

The absence of a clear zonation of volcanic rocks in the Bicol arc is probably related to the younger age of the Philippine Trench subduction complex in general (Lewis and Hayes, 1983). The subduction of the Philippine Sea plate along the Philippine Trench adjacent southern Luzon however, is probably not as young as suggested by Hawkins *et al.* (1985) in the region near eastern Mindanao, where the absence of associated active volcanoes is well-documented.

The volumetric dominance of andesite over basalt, constant Fe/Mg ratio, trace element data, and the parallelism of volcanic centres in the Bicol arc to the Philippine Trench led Divis (1980) to propose that the Bicol arc andesitic magmas were probably derived by a "two stage" process (Figs. 37 and 38), similar to that proposed by Ringwood (1974; 1977). In addition, Divis (1980) noted that crystal fractionation has occurred in the Bicol volcanic rocks, but has not been extreme enough to result in substantial modification of trace element abundances with increasing SiO_2.

On the contrary, Newhall (1979) has indicated that low pressure crystal fractionation of anhydrous silicate minerals and hornblende account for much of the chemical variations observed in the lavas of Mayon volcano.

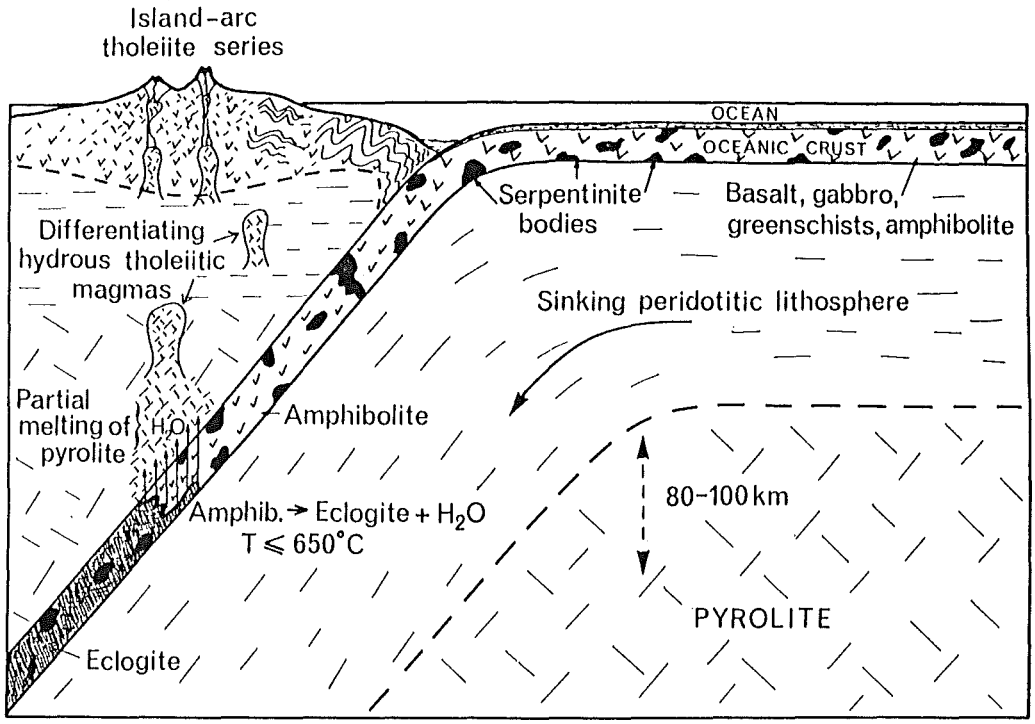

FIG. 37 Early phase of an island arc development involving dehydration of amphibolite in subducted oceanic crust, introduction of water into the overlying wedge and generation of "island arc tholeiite" igneous series (after Ringwood, 1974; 1977).

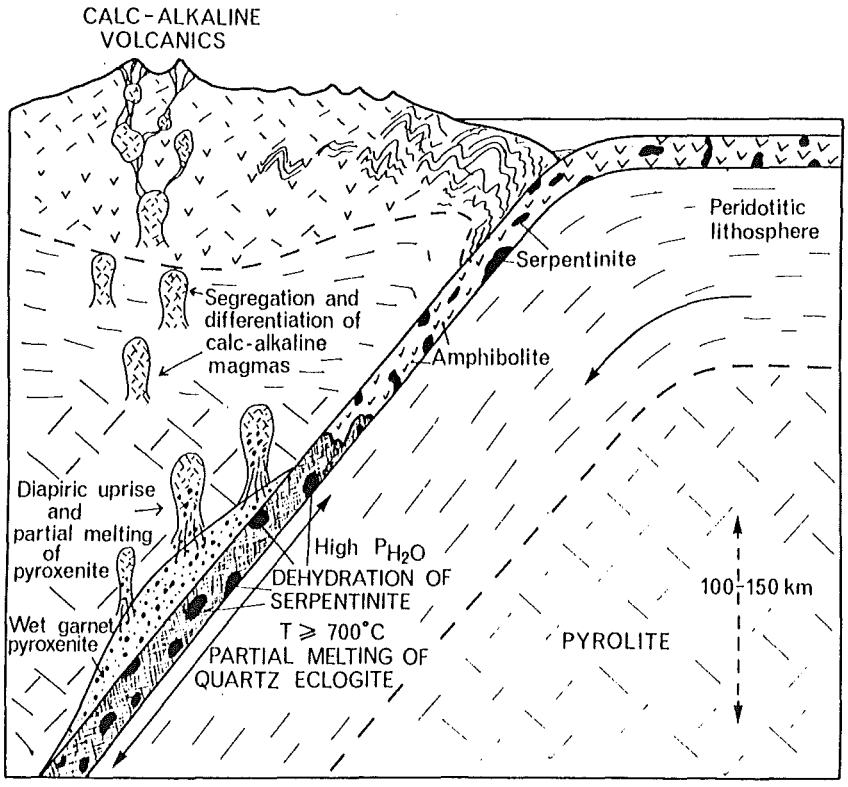

FIG. 38 Later phase of island arc development involving partial melting of subducted oceanic crust and reaction of liquids with mantle wedge, leading to diapiric uprise and formation of calcalkaline-type magmas (after Ringwood, 1974; 1977).

5.3 MAGMA GENESIS OF VOLCANIC ROCKS FROM THE POCDOL MOUNTAINS

The Bicol arc is an oceanic island arc, and therefore, the volcanic rocks of Pocdol Mountains must have been derived from the upper mantle or from subducted oceanic crust (Ringwood, 1974; 1977), as proposed by Divis (1980). Contamination by sialic crustal material (e.g., De Paolo, 1981) is assumed to have played an insignificant role in this region (Divis, 1980).

Both WPM and EPM lavas show typical characteristics of island-arc rocks. The eruptives are calcalkalic in character and are generally quartz-hypersthene normative, except for the Malobago volcanics (WPM series). Thus, there is little iron enrichment (Figs. 39 and 40).

Both rock series however have undergone extensive fractionation, as indicated by low concentrations (in ppm) of trace elements, such as Ni (21-7, WPM; 30-6, EPM) and Cr (25-5, WPM; 39-5, EPM), as well as low $Mg/(Mg + Fe^2) = <0.56$ (see Tables 14 and 15). For primary mantle-derived basaltic magmas in equilibrium with mantle olivine ($\sim Fo_{88}$), expected values are approximately Ni = 200-250 and Cr = 500-800 (Nicholls, 1978), and $Mg/(Mg + Fe^2) = 0.69$ (Nicholls and Whitford, 1976).

The greater abundances of large-ion lithophile (LIL) elements, light rare earth elements (LREE), high field strength (HFS) ions and potassium contents of WPM lavas than EPM lavas may indicate their possible derivation from sources that have undergone different degrees of partial melting and/or contamination (i.e., the "IRS" fluid of Gill, 1981) within the overlying mantle wedge and/or the subducted slab. The generally high radiogenic Sr and Pb isotope concentrations of Mid-Tertiary plutonic and Pliocene-Recent volcanic rocks in the Bicol arc led Mukasa *et al.* (1986) and Knittel and Defant (1988) to invoke inhomogeneities in the source regions.

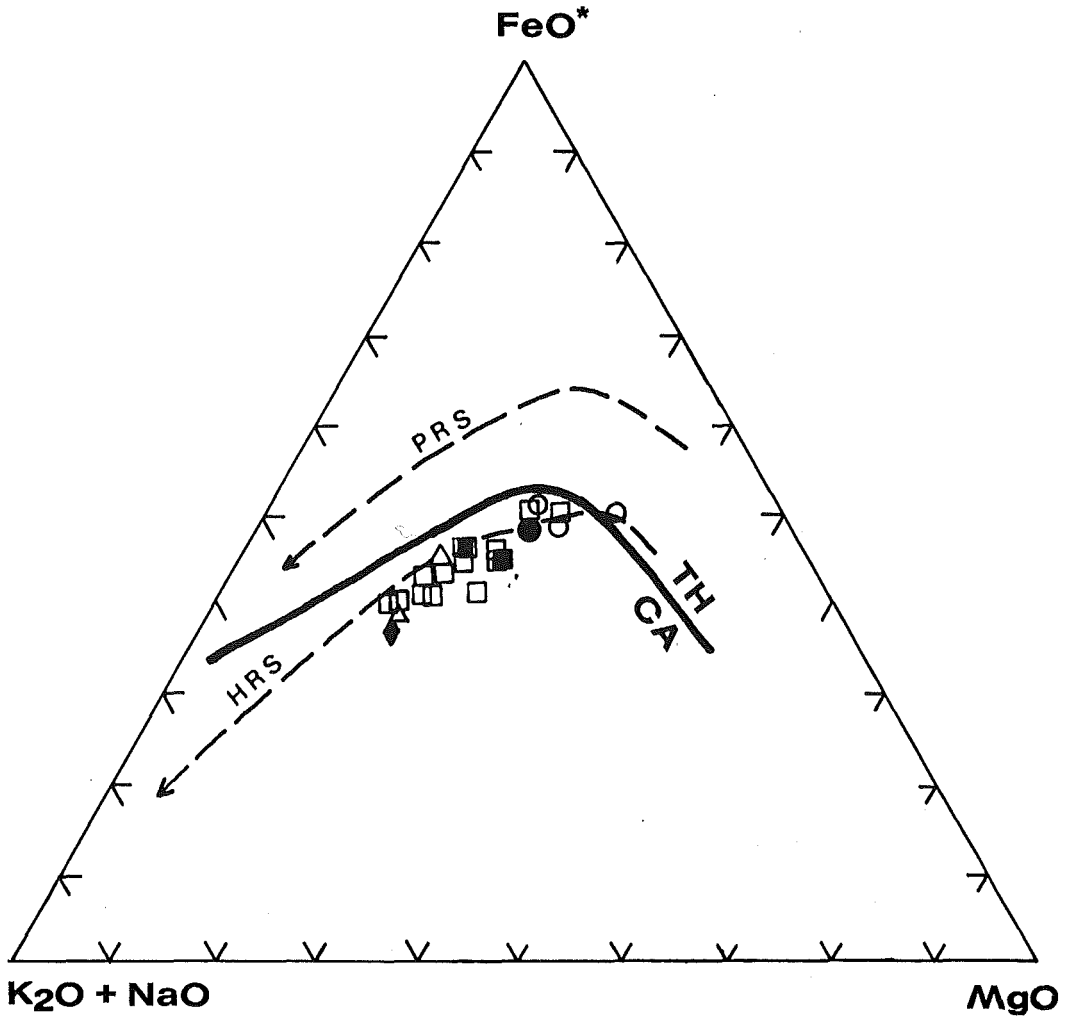

FIG. 39 AFM diagram of WPM and EPM lavas (symbols as in FIG. 31). A, $Na_2O + K_2O$; F, $FeO + 0.9Fe_2O_3$; M, Mgo. Heavy solid line separates tholeiitic (TH) from calcalkaline (CA) suites using the criteria of Irvine and Baragar (1971). Dashed lines connect Kuno's (1968) average compositions of pigeonitic (PRS) and hypersthenic rock series (HRS) in Japan.

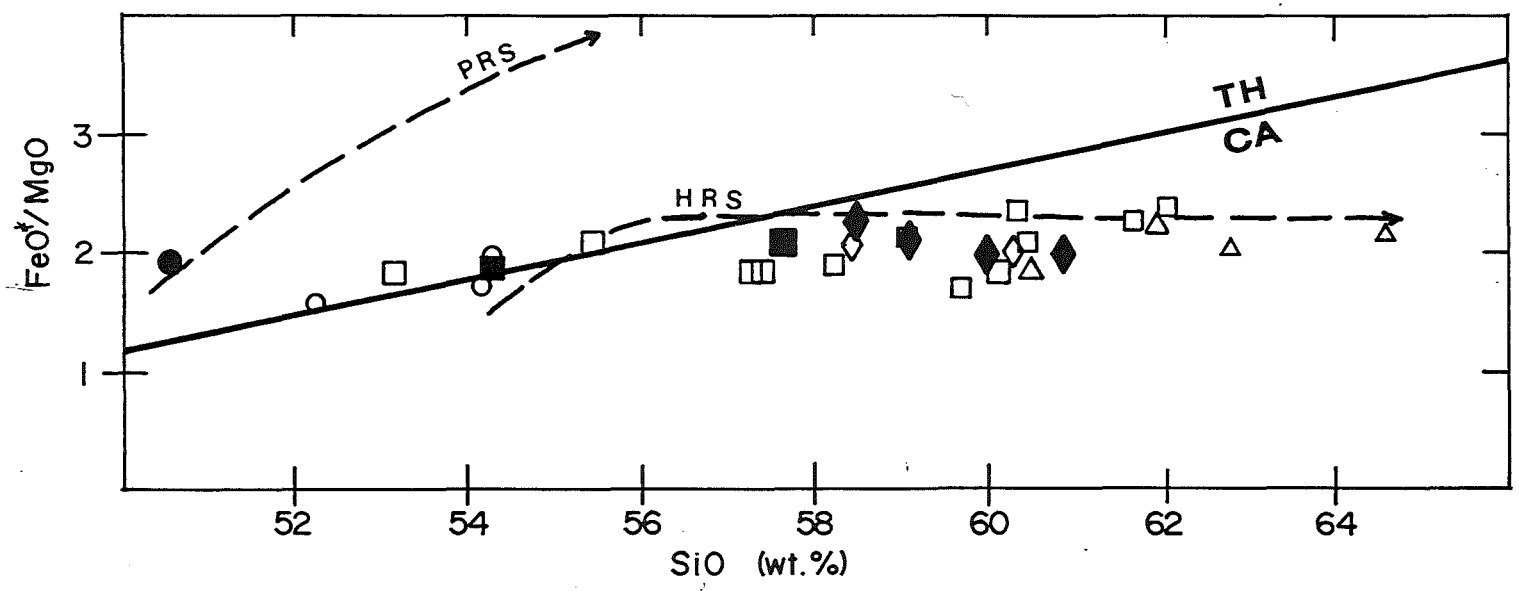

FIG. 40 Definition of tholeiitic (TH) and calcalkaline (CA) rocks, following Miyashiro (1974). Dashed lines show rock suites as in FIG. 39 Symbols as in FIG> 31).

Similar "enrichments" have been reported in the Sunda arc (Foden and Varne, 1980), in Iceland (Wood *et al.*, 1979) and in the Antarctic Peninsula and the South Shetland Islands (Saunders *et al.*, 1980).

The most likely mechanism to account for the highly evolved compositions of both WPM and EPM series involves the "**plagioclase + orthopyroxene or olivine + augite + magnetite (POAM) fractionation model**" proposed by Gill (1981). This process operates under low pressure (<10 kb) crustal environments. Other processes may have occurred concurrently with POAM fractionation, i.e., magma mixing (O'Hara, 1977). However, petrologic evidences for mixing in these rocks, such as the disequilibrium features described by Sakuyama (1979; 1981; 1983; 1984), are either absent or rare. In cases where reverse zoning is implied, i.e., in pyroxenes (see Tables 6 and 7), the crystals are usually megacrysts, and therefore, local changes in P-T conditions may easily produce such zoning during settling, and not because of the influx of a totally different magma batch.

Major element variation diagrams (see Fig. 32) indicate that the EPM lavas are crystal fractionates of a basic parent similar to the basaltic andesite of the Pulog volcanics, and the WPM series, from high-alumina basalt of the Malobago volcanics. Another argument for two separate magma sources in the Pocdol Mountains is largely based on spatial distribution between the two lava series. It is possible, using a least-squares mixing programme (Geist *et al.*, 1985), to derive both dacite and andesite trends (Fig. 41 and Table 18) of the EPM by subtracting plagioclase, orthopyroxene, clinopyroxene and titanomagnetite phases from the basaltic andesite source (Pulog volcanics).

In contrast, modelling of WPM series by crystal fractionation yields a much inferior model, giving R^2 values of >1. The presence of large residuals, particularly in the alkalies and TiO_2, suggests that POAM fractionation is an inadequate petrogenetic model. The high residuals for alkalies support the idea of an "IRS" metasomatic fluid, being invoked by Knittel and Defant (1988) to be present within the sub-Bicol arc mantle wedge.

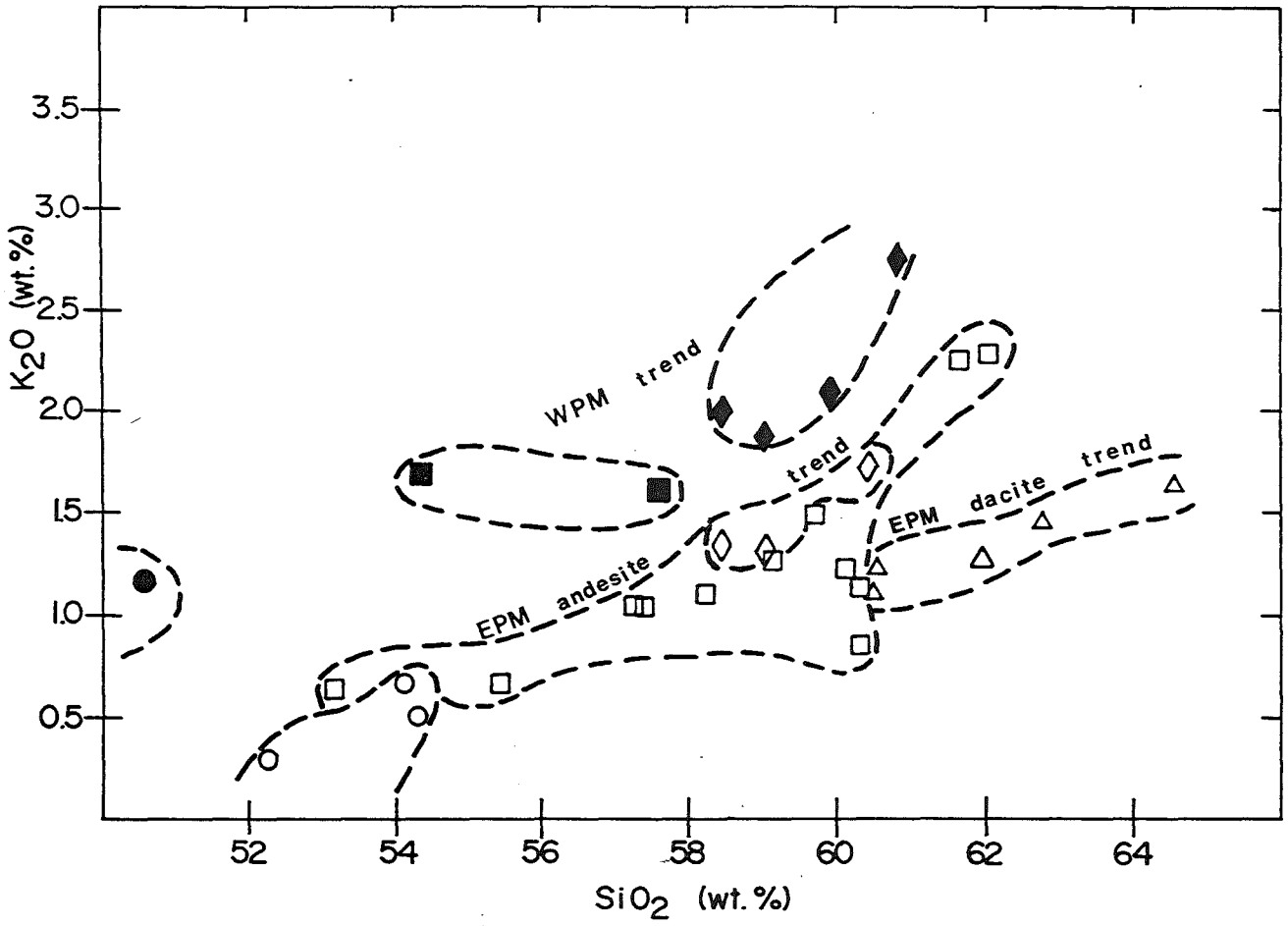

FIG. 41 Inferred fractionation trends of WPM and EPM lavas (symbols as in FIG. 31).

	PARENT (40)	DAUGHTER (34)	MODEL	RESIDUAL	PHASE	PERCENT
SiO2	54.51	57.60	57.61	-.01		
TiO2	.98	.65	.86	-.21		
Al2O3	18.98	18.60	18.63	-.03		
FeO	8.51	6.81	6.78	.03		
MnO	.15	.12	.14	-.02		
MgO	4.49	3.83	3.83	.00	Plg	67.75
CaO	8.44	7.84	7.83	.01	opx	17.00
Na2O	3.47	3.52	3.34	.18	Tmt	8.83
K2O	.47	1.02	.72	.30	Cpx	6.42

R SQUARED = .168

	PARENT (40)	DAUGHTER (32)	MODEL	RESIDUAL	PHASE	PERCENT
SiO2	54.51	60.54	60.50	.03		
TiO2	.98	.58	.82	-.24		
Al2O3	18.98	18.78	18.78	.00		
FeO	8.51	5.95	5.91	.04		
MnO	.15	.10	.14	-.04		
MgO	4.49	2.66	2.74	-.09	Plg	61.91
CaO	8.44	6.68	6.69	-.01	Opx	20.87
Na2O	3.47	3.87	4.27	-.40	Tmt	8.76
K2O	.47	.84	.82	.02	Cpx	8.46

R SQUARED = .228

	PARENT (32)	DAUGHTER (10C)	MODEL	RESIDUAL	PHASE	PERCENT
SiO2	60.56	64.71	64.71	.00		
TiO2	.59	.50	.59	-.09		
Al2O3	18.80	16.69	16.73	-.05		
FeO	5.91	4.79	4.78	.01		
MnO	.10	.10	.06	.04		
MgO	2.66	2.34	2.35	-.01		
CaO	6.69	5.58	5.40	.17	Plg	79.61
Na2O	3.87	3.70	3.87	-.17	Opx	13.43
K2O	.84	1.60	1.11	.49	Tmt	6.96

R SQUARED = .309

TABLE 18 Least-squares mixing calculations for EPM lavas, assuming simple crystal fractionation.

If it is assumed that the dacitic melt forming the Suminandig volcanics occurred in the top of the reservoir, then the traditional concept of a differentiating magma chamber, wherein a basaltic magma undergoes POAM fractional crystallisation as it solidifies and causing the residual liquid to become progressively more SiO_2-rich with time, is inadequate to account for the order of eruption of the EPM series lavas; however, this could satisfactorily account for the genesis and order of eruption of the WPM series lavas.

Recent experimental and theoretical analysis of evolving magma chambers seem to account better for the volcanic stratigraphy and geochemistry of the EPM series lavas. Cooling around the margins and roof of a closed-system magma chamber would lead to fractional crystallisation in the sheath of magma near the walls (McBirney, 1980; Turner, 1980; McBirney *et al.*, 1985), but would not significantly affect the composition of the main mass of magma in the core of the chamber (Sparks *et al.*, 1984). Fractionated liquids would then escape upwards by boundary layer convection, because their density is less than the unfractionated magma, and pond near the roof to form a highly differentiated cap available for eruption. This process could have taken place soon after emplacement of the magma chamber (Sparks *et al.*, 1984).

Dacites and hornblende-phyric andesites of the Suminandig volcanics could have been produced in this way in a shallow (<20 kms) basaltic andesite magma chamber beneath the EPM. The "dacite" cap is probably thin because of the sparse dacite outcrops, and the eruptions were probably "mild" that culminated in the effusion of the Matacla Dome near the southern slopes of Suminandig volcano. Successive tapping of the reservoir produced increasingly more basic eruptives, i.e., from two pyroxene and hornblende andesites (Pangas volcanics) to two pyroxene andesites (Cawayan volcanics), until the core of the magma chamber was emptied, and produced the low-K basaltic andesites of Pulog volcanics <30,000 years ago.

This model is the reverse of the traditional volcanic evolutionary cycle-- the more SiO_2-rich liquids are erupted first and the basic magmas last. This pattern is similar to that produced within relatively short periods of time during eruption of pyroclastic rock deposits zoned compositionally from SiO_2-rich at the base to SiO_2-poor at the top (e.g., Ritchey, 1980; Worner and Schmincke, 1984).

CHAPTER VI

CONCLUSIONS

CHAPTER VI

CONCLUSIONS

Results of recent volcano-stratigraphic studies, five new potassium-argon ages and detailed petrographic, mineralogic and petrochemical analyses of 30 rock specimens lead to new interpretations on the volcanic geology of Pocdol Mountains. These are outlined below :

6.1 VOLCANIC STRATIGRAPHY

(i) Volcanic rocks of Pocdol Mountains were produced over a period of 3 Ma, and the deposits formed seven distinct lithostratigraphic units, namely : (1) Malobago volcanics (Early Pliocene); (2) Suminandig volcanics (Middle Pliocene); (3) Pangas volcanics (Middle Pliocene to Early Pleistocene); Middle Pliocene to Early Pleistocene (4) Lison volcanics (0.478 Ma) and (5) Kayabon volcanics (<0.065 Ma), and Late Pleistocene to Recent (6) Cawayan volcanics (<0.04 Ma) and (7) Pulog volcanics (<0.03 Ma).

(ii) Volcanic rocks are group into : (1) a Western Pocdol Mountains (WPM) series and (2) an Eastern Pocdol Mountains (EPM) series, based on petrologic and geochemical constraints, and a clear geographic separation as well. WPM series comprise the Malobago, Lison and Kayabon volcanic units, whereas the EPM eruptives consist of the Suminandig, Pangas, Cawayan and Pulog volcanic units.

(iii) Hydrothermal activity appears to be associated with the Suminandig and Pangas volcanism in the eastern Pocdol Mountains, which are characterised essentially by "more-evolved" effusives, with associated domes, intrusive phases and active faulting. The Rangas conglomerate may provide the "stratigraphic permeability", but their discontinuous outcrops pose some difficulties. The San Vicente-Linao Fault zone could well be initially giving vertical discontinuity for hydrothermal fluid flow in the area. Both Cawayan and Pulog volcanics may have acted as a "capping mechanism" of the geothermal system.

6.2 PETROLOGY AND GEOCHEMISTRY

(i) Both WPM and EPM lavas are plagioclase-phyric, with subordinate clinopyroxene, orthopyroxene, titanomagnetite and amphibole. Olivine is only found in the Malobago volcanics. The inferred order of crystallisation of WPM rocks is titanomagnetite-olivine-pyroxene-amphibole, accompanied by plagioclase; it is essentially the same in EPM lavas, but without olivine. Phenocrysts phases and textures indicate normal crystal fractionation processes, and rare disequilibrium textures are explained by localised P-T changes related to crystal settling or magma convection, rather than the effects of magma mixing.

(ii) The overall mineralogy of lavas suggests low pressure (<9 kb) crystallisation, and estimated equilibration temperatures range from 1006^{o} to 1135^{o}, using the clinopyroxene-orthopyroxene geothermometer.

(iii) Both WPM and EPM eruptives are typical calcalkaline volcanic rocks, showing little iron enrichment, and are mainly quartz and hypersthene normative. WPM lavas comprise medium-K high-alumina basalt (Malobago volcanics) to medium-K and high-K basaltic andesite and andesite (Lison and Kayabon volcanics), whereas the EPM rocks consist of low-K basaltic andesite (Pulog volcanics) to medium-K andesite and dacite (Pangas, Cawayan and Suminandig volcanics).

(iv) Major oxide and trace element variations suggest at least two possible parental liquids, each generating WPM and EPM series. However, these liquids have been extensively modified by crystal fractionation processes resulting in low Ni, Cr and $Mg/(Mg+Fe^{2})$ abundances.

(v) Two distinct liquid lines of descent (a dacite and an andesite) are displayed by EPM series lavas; however, a scatter is evident between 56 to 62 % SiO_2, perhaps reflecting the accumulation of phenocrysts.

6.3 MAGMA GENESIS

(i) Volcanic rocks of Pocdol Mountains represent magmas initially derived by high degrees of partial melting within the mantle wedge and/or the subducted slab. Source regions may have experienced some degree of mantle metasomatism due to influx of K-rich aqueous fluids from the downgoing slab, i.e., the "IRS" fluid of Gill (1981). The petrologic characteristics of both WPM and EPM lavas indicate substantial modifications of primary magma compositions by low-pressure POAM fractionation (Gill, 1981).

(ii) Stratigraphic criteria and least-squares mixing calculations indicate that by fractionating plagioclase, orthopyroxene, titanomagnetite and clinopyroxene, both Lison and Kayabon andesites were probably derived from a high-alumina basaltic source (Malobago volcanics), whereas the Suminandig, Pangas and Cawayan volcanics originate from a low-K basaltic andesite liquid (Pulog volcanics).

(iii) Assuming that dacitic melt was ponded on top of the EPM magma chamber, it is necessary to invoke liquid fractionation (McBirney **et al.**, 1985), whereby fractionated liquids move upward along the walls or sides of the reservoir and collect at the roof, due to differences in densities of fractionated and unfractionated liquids.

ACKNOWLEDGEMENTS

I am grateful to Professor J.W. Cole and Dr. S.D. Weaver for their critical reviews and useful suggestions; to Dr. C.J. Adams (Institute of Nuclear Sciences, DSIR) for providing five potassium-argon age determinations; to Arthur Alloway (Geology Department, University of Canterbury) for generating high precision XRF results; to Dr. J.A. Gamble, Ken Palmer and Kifle Khasai (Geology Department, Victoria University) for their assistance with the operation of the **JEOL 733** Superprobe microanalyser, and to the staff (David Jones, Albert Downing, and Lee Leonard) and graduate students (Sutikno Bronto, Malcolm Warnes, Martin Kirkbride, and Mark Lawrence) of the Department of Geology, University of Canterbury, for their extra help.

The assistance of Mr. R.S. Alincastre in the field is very much appreciated, and also the support of PNOC-EDC Geoscientific staff : to Mr. C.C. Panem for discussion relating to the structural framework of the area; to Miss A.G. Reyes for facilitating thin section processing, and Mr. H.P. Ferrer, who originally suggested the study area.

Finally I would like to mention the support and encouragement given by Annie (my wife), Aisa (my daughter) and Lisa (my sister-in-law) during the course of this study.

Preparation of this thesis was supported by the Republic of the Philippines - New Zealand Bilateral Aide Programme and by the Philippine National Oil Company - Energy Development Corporation (PNOC-EDC).

REFERENCES

REFERENCES

Abella, E.C., 1885. Emanaciones volcanicas subordinadas al Malinao (Filipinas). *Boletin de la Comision del mapa geologico de Espana,* 11, 136.

Abella, E.C., and Vera, J., 1893. Estudio descriptivo de algunos manatiales minerales de Filipinas. *Boletin de la Comision del mapa geologico de Espana,* 28, 12.

Acharya, H.K., 1980. Seismic slip on the Philippine fault and its tectonic implications. *Geology,* 8, 40-42.

Adams, G.I., and Pratt, W.E., 1910. Geologic reconnaissance of southeastern Luzon. *Phil. J. Sci., Sec. A,* 449-481.

Alcaraz, A.P., 1963. Progress in geology and geophysics in the Philippines since the first Pacific Science Congress in 1920, in MacDonald, G.A., chairman, Geology and Solid Earth Geophysics of the Pacific Basin; Report of the Standing Committee. University of Hawaii, Honolulu, pp. 1-5.

Alcaraz, A.P., 1976. Geothermal exploration and development in the Philippines--Summary, in Halbouty, M.T., Maher, J.C., and Lian, H.M., eds., Circum-Pacific Energy and Mineral Resources, *Assoc. Amer. Petrol. Geol. Mem. 25,* 140-145.

Alincastre, R.S., 1983. Geology of eastern Bacon-Manito geothermal project. *Unpublished PNOC-EDC Report,* 45 pp.

Allen, C.R., 1962. Circum-Pacific faulting in the Philippines-Taiwan region. *J. Geophys. Res.,* 67, 4795-4811.

Allen, J.C., and Boettcher, A.L., 1978. Amphiboles in andesite and basalt II. Stability as a function of P-T-fO_2. *Amer. Mineral.,* 63, 1074-1087.

Allen, J.C., Boettcher, A.L., and Marland, G., 1975. Amphiboles in andesite and basalt: I. Stability as a function of P-T-fO_2. *Amer. Mineral.,* 60, 1068-1085.

Anderson, A.T., 1976. Magma mixing: petrological process and volcanological tool. *J. Volcanol. Geotherm. Res.,* 1, 3-33.

Aniceto, H.G., 1982. Petrology of Mo-1, Bacon-Manito geothermal field, southeastern Luzon, Philippines. *Diploma in Energy Technology (Geothermal) Report 82.02,* University of Auckland, New Zealand, 45 pp.

Arculus, R.J., 1976. Geology and geochemistry of the alkali basalt-andesite association of Grenada, Lesser Antilles island arc. *Geol. Soc. Amer. Bull.,* 87, 612-624.

Arculus, R.J., and Johnson, R.W., 1978. Criticism of generalized models for the magmatic evolution of arc-trench systems. *Earth Planet. Sci. Lett.,* 39, 118-126.

Arculus, R.J., and Wills, K.J.A., 1980. The petrology of plutonic blocks and inclusions from the Lesser Antilles island arc. *J. Petrol.,* 21, 743-799.

Ashley, G.H., Cheney, M.G., Galloway, J.J., *et al.,* 1933. Classification and nomenclature of rock units. *Geol. Soc. Amer. Bull.,* 44, 423-459.

Baker, I., and Haggerty, S.E., 1967. The alteration of olivine in basaltic and associated lavas, Part II: Intermediate and low temperature alteration. *Contrib. Mineral. Petrol.,* 16, 258-273.

Balce, G.R., Magpantay, A.L., and Zanoria, A.S., 1979. Tectonic scenarios of the Philippines and northern Indonesian region. Paper presented at the ESCAP CCOP-IOC Ad Hoc Working Group on the Geology and Tectonics of Eastern Indonesia, Bandung, Indonesia.

Baltazar, A.S.J., 1987. Geochemical survey of the western sector of the Bacon-Manito geothermal project. *Unpublished PNOC-EDC Report*, 12pp.

Becker, G.F., 1901. Report on the geology of the Philippine Islands. *U.S.G.S. 21st Ann. Rep. Part 3* , 487-614.

Bence, A.E., and Albee, A.L., 1968. Empirical correction factors for the electron microanalysis of silicates and oxides, *J. Geol.*, 76, 382-403.

Boettcher, A.L., 1977. The role of amphibole and water in circum-Pacific volcanism, in Manghnani, M.H., and Akimoto, S., eds., High pressure research applications in geophysics. Academic Press, London New York, pp. 107-126.

Bogie, I., and Lawless,J.V., 1986. The relationship between volcanic centres and active hydrothermal systems of the Bicol Peninsula, Luzon, Philippines. *Proc. 8th NZ Geothermal Workshop*, 123-127.

Brown, G.M., Holland, J.G., Sigurdsson, H., Tomblin, J.F., and Arculus, P.J., 1977. Geochemistry of Lesser Antilles volcanic island arc. *Geochim. Cosmochim. Acta*, 41, 785-801.

Bruinsma, J.W., 1983. Results of potassium-argon dating on twenty rock samples from the Pinatubo, southeast Tongonan, Bacon-Manito, southern Negros and Tongonan, Leyte, Philippines. Unpublished PNOC-EDC Report, 25 pp.

Buddington, A.F., and Lindsley, D.H., 1964. Iron-titanium oxide minerals and synthetic equivalents. *J. Petrol.*, 5, 310-357.

Bueza, E.L., 1983. Petrographic and XRD results of northeast Bacon-Manito surface rock samples. *Unpublished PNOC-EDC Report*, 37 pp.

Cardwell, R.K., Isacks, B.L. and Karig, D.E., 1980. The spatial distribution of earthquakes, focal mechanism solutions, and subducted lithosphere in the Philippines and northeastern Indonesian Islands, in Hayes, D.E., ed., The tectonic and geologic evolution of Southeast Asian seas and islands, *Geophys. Monogr. 23*, AGU, Washington, D.C., pp. 1-36.

Carmichael, I.S.E., 1967. The iron-titanium oxides of salic volcanic rocks and their associated ferromagnesian silicates. *Contrib. Mineral. Petrol.*, 14, 36-44.

Centeno, J., 1889. Estudio geologico del volcan Taal. *Boletin de la Comision del mapa geologico de Espana*, 12, 24.

Chayes, F., 1960. On correlation between variables of constant sum. *J. Geophys. Res.*, 65, 4185-4193.

Chayes, F., 1964. Variance-covariance relations in some published Harker diagrams of volcanic suites. *J. Petrol.*, 5, 219-237.

Chayes, F., 1969. The chemical composition of Cenozoic andesite, in McBirney, A.R., ed., *Proc. Andesite Conf. Dep. Geol. Min. Res. Oreg. Bull.*, 65, 1-11.

Cook, E.F., 1965. Stratigraphy of Tertiary volcanic rocks in eastern Nevada. *Nevada Bureau of Mines Report 11*, 61 pp.

Datuin, R., 1982. An insight on Quaternary volcanoes and volcanic rocks of the Philippines. *J. Geol. Soc. Phil.*, 36, 1-10.

De Boer, J.Z., Odom, L.A., Ragland, P.C., Snider, F.G., and Tilford, N.R., 1980. The Bataan orogene: eastward subduction, tectonic rotations, and volcanism in the western Pacific (Philippines). *Tectonophysics*, 67, 251-282.

De Leon, M.M., Lawless, J.V., and Licup, A.C., 1983. Structures and stratigraphy of Bacon-Manito geothermal area. *Unpublished PNOC-EDC Report*, 56 pp.

De Long, S.E., Hodges, F.N., and Arculus, R.J., 1975. Ultramafic and mafic inclusions, Kanaga Island, Alaska, and the occurrence of alkaline rocks in island arcs. *J. Geol.*, 83, 721-736.

De Paolo, D.J., 1981. Trace element and isotopic effects of combined wallrock assimilation and fractional crystallisation. *Earth Planet. Sci. Lett.*, 53, 189-202.

Defant, M.J., 1985. The potential origin of the potassium-depth relationship in the Bataan orogene, the Philippines. *Unpublished Ph.D. thesis*, Florida State University, Fla., 622 pp.

Defant, M.J., De Boer, J.Z., and Oles, D., 1988. The western Central Luzon volcanic arc, the Philippines: two arcs divided by rifting? *Tectonophysics*, 145, 305-317.

Delfin, F.G., and Tebar, H.J., 1986. Geologic structures at the Mahiao, Sambaloran and Malitbog sectors of the Tongonan geothermal field, Leyte, Philippines. *Proc. 8th NZ Geotherm. Workshop*, 129-134.

Dickinson, W.R., 1968. Circum-Pacific andesite types. *J. Geophys. Res.*, 73, 2261-2269.

Dickinson, W.R., 1975. Potash-depth (K-h) relations in continental margin and intra-ocean magmatic arcs. *Geology*, 3, 53-56.

Divis, A.F., 1980. The petrology and tectonics of recent volcanism in the central Philippine Islands, in Hayes, D.E., ed., The tectonic and geologic evolution of Southeast Asian seas and islands, *Geophys. Monogr. 23*, AGU, Washington, D.C., pp. 127-144.

Donnelly, T.W., Rogers, J.J.W., Pushkar, P., and Armstrong, R.L., 1971. Chemical evolution of the igneous rocks of the eastern West Indies: an investigation of thorium, uranium, and potassium distributions, and lead and strontium isotope ratios. *Geol. Soc. Amer. Mem..*, 130, 181-224.

Eggler, D.H., 1972. Water-saturated and undersaturated melting relations in a Paricutin andesite and an estimate of water content in the natural magma. *Contrib. Mineral. Petrol.*, 34, 261-271.

Eggler, D.H., and Burnham, C.W., 1973. Crystallization and fractionation trends in the system andesite-H_2O-CO_2-O_2 at pressures to 10 kb. *Geol. Soc. Amer. Bull.*, 84, 2517-2532.

Espiritu, D.D., 1979. Geology and geothermal potential of Inang Maharang and Puting Bato areas. *Unpublished PNOC-EDC Report*, 35pp.

Ewart, A., 1971. Notes on the chemistry of ferromagnesian phenocrysts from selected volcanic rocks, Central Volcanic Region. *N.Z. J. Geol. Geophys.*, 14, 323-340.

Ewart, A., 1982. The mineralogy and petrology of Tertiary-Recent orogenic volcanic rocks: with special reference to the andesitic-basaltic compositional range, in Thorpe, R.S., ed., Andesites, John Wiley & Sons, pp. 25-95.

Ferrer, H.P., Bate, E.S, Guerrero, D.R. and Ferrer, A.P., 1986. LANDSAT-assisted geostructural analysis of the Bacon-Manito geothermal field, southeastern Luzon, Philippines. *Geotherm. Res. Council Bull.*, May issue, 8-14.

Fisher, R.V., 1961. Proposed classification of volcaniclastic sediments and rocks. *Geol. Soc. Amer. Bull.*, 72, 1409-1414.

Fisher, R.V., 1963. Classification of volcanic breccias : A reply. *Geol. Soc. Amer. Bull.*, 74, 87-88.

Fisher, R.V., 1966. Rocks composed of volcanic fragments and their classification. *Earth Sci. Rev.*, 1, 287-298.

Fisher, R.V, and Schmincke, H.-U., 1984. Pyroclastic rocks. Springer-Verlag. 472 pp.

Flood, R.H., Vernon, R.H., Shaw, S.E., and Chapell, B.W., 1977. Origin of pyroxene plagioclase aggregates in a rhyodacite. *Contrib. Mineral. Petrol.*, 60, 299-306.

Foden, J.D., and Varne, R., 1980. The petrology and tectonic setting of Quaternary-Recent volcanic centres of Lombok and Sumbawa, Sunda arc. *Chem. Geol.*, 30, 201-226.

Garcia, M.O., and Jacobson, S.A., 1979. Crystal clots, amphibole fractionation and the evolution of calc-alkaline magmas. *Contrib. Mineral. Petrol.*, 69, 319-327.

Geist, D.J., Baker, B.H., and McBirney, A.R., 1985. A program package for creating and using geochemical data files (Version for IBM-PC and compatible microcomputers). Center for Volcanology, University of Oregon, Eugene, Oregon, 97403, 32 pp.

Gerlach, D.C., and Grove, T.L., 1982. Petrology of Medicine Lake Highland volcanics: characterization of endmembers of magma mixing. *Contrib. Mineral. Petrol.*, 80, 147-159.

Gill, J.B., 1981. Orogenic andesites and plate tectonics. Springer Verlag, 390 pp.

Gow, A.J., 1968. Petrographic and petrochemical studies of Mt. Egmont andesites. *N.Z. J. Geol. Geophys.*, 11, 166-190.

Green, T.H., 1972. Crystallization of calc-alkaline andesite under controlled high-pressure hydrous conditions. *Contrib. Mineral. Petrol.*, 34, 150-166.

Green, T.H., 1982. Anatexis of mafic crust and high pressure crystallization of andesite, in Thorpe, R.S., ed., Andesites. John Wiley & Sons, pp. 465-487.

Grove, T.L., Gerlach, D.C., and Sando, T.W., 1982. Origin of calc-alkaline series lavas at Medicine Lake volcano by fractionation, assimilation, and mixing. *Contrib. Mineral. Petrol.*, 80, 160-182.

Hackett, W.R., 1985. Geology and petrology of Ruapehu volcano and related vents. *Unpublished Ph.D thesis*, Victoria University of Wellington, New Zealand.

Haggerty, S.E., 1976. Opaque mineral oxides in igneous rocks, in Rumble, D. III, ed., Oxide minerals, *Mineralogical Society of America Short Course Notes*, pp. Hg.101-300.

Hammarstrom, J.M., and Zen, E., 1986. Aluminum in hornblende: an empirical igneous geobarometer. *Amer. Mineral.*, 71, 1297-1313.

Harvey, P.K., Taylor, D.M., Hendry, R.D., and Bancroft, F., 1973. An accurate fusion method for the analysis of rocks and chemically related materials by X-ray fluorescence spectrometry. *X.R.S.*, 2, 33-44.

Hawkins, J.W., Moore, G.F., Villamor, R., Evans, C., and Wright, E., 1985. Geology of the composite terranes of east and central Mindanao, in Howell, D.G., ed., Tectonostratigraphic terranes of the circum-Pacific region. *Circum-Pacific Council Energy and Mineral Res. Earth Sci. Series 1*, 437-463.

Irvine, T.N., and Baragar, W.R.A., 1971. A guide to the classification of the common volcanic rocks. *Can. J. Earth Sci.*, 8, 523-548.

Jakes, P., and Gill, J.B., 1970. Rare earth elements and the island arc tholeiitic series. *Earth Planet. Sci. Lett.*, 9, 17-28.

Jakes, P., and White, A.J.R., 1969. Structure of the Melanesian arcs and correlation with distribution of magma types. *Tectonophysics*, 8, 222-236.

Jakes, P., and White, A.J.R., 1970. K/Rb ratios of rocks from island arcs. *Geochim. Cosmochim. Acta*, 34, 849-856.

Jakes, P., and White, A.J.R., 1971. Composition of island arcs and continental growth. *Earth Planet. Sci. Lett.*, 12, 224-230.

Jakes, P., and White, A.J.R., 1972. Major and trace element abundances in volcanic rocks of orogenic areas. *Geol. Soc. Amer. Bull.*, 83, 29-40.

Johnson, R.W., Mackenzie, D.E., and Smith, I.E.M., 1971. Seismicity and Late Cenozoic volcanism in parts of Papua New Guinea. *Tectonophysics*, 12, 15-22.

Kingston, Reynolds, Thom and Allardice (KRTA), Limited, 1986. Bacon-Manito Geothermal Project Geology Review (Parts 1 and 2). *Unpublished Report submitted to PNOC-EDC, 54 pp.*

Knittel, U., and Defant, M.J., 1988. Sr isotopic and trace element variations in Oligocene to Recent igneous rocks from the Philippine island arc: evidence for Recent enrichment in the sub-Philippine mantle. *Earth Planet. Sci. Lett.*, 87, 87-99.

Kretz, R., 1982. Transfer and exchange equilibria in a portion of the pyroxene quadrilateral as deduced from natural and experimental data. *Geochim. Cosmochim Acta*, 46, 411-421.

Kudo, A.M., and Weill, D.F., 1970. An igneous plagioclase geothermometer. *Contrib. Mineral. Petrol.*, 41, 205-215.

Kuno, H., 1950. Petrology of Hakone volcano and the adjacent areas, Japan. *Geol. Soc. Amer. Bull.*, 61, 957-1020.

Kuno, H., 1959. Origin of Cenozoic petrographic provinces of Japan and surrounding areas. *Bull. Volcanol. Ser. 2*, 20, 37-76.

Kuno, H., 1966. Lateral variation of basalt magma type across continental margins and island arcs. *Bull Volcanol.*, 29, 195-215.

Larsen, E.S., Irving, J., Gonyer, F.A., and Larsen, E.S. III, 1937. Petrologic results of a study of the minerals from the Tertiary volcanic rocks of the San Juan region, Colorado. 5. The amphiboles. *Amer. Mineral.*, 22, 889-898.

Layugan, D.B., 1986. Resistivity measurements over the Bacon-Manito geothermal area. *Unpublished PNOC-EDC Report*, 70 pp.

Leach, T.M., 1983. Pal-6D petrology report. *Unpublished PNOC-EDC Report*, 32 pp.

Leake, B.E., 1978. Nomenclature of amphiboles. *Can. Mineral.*, 16, 501-520.

Le Maitre, R.W., 1976. The chemical variability of some common igneous rocks. *J. Petrol.*, 17, 589-637.

Lewis, S.D., and Hayes, D.E., 1983. The tectonics of northward propagating subduction along the eastern Luzon, Philippine Islands, in Hayes, D.E., ed., The tectonic and geologic evolution of Southeast Asian seas and islands, *Geophys. Monogr. 27*, 57-78, AGU, Washington, D.C., pp. 57-78.

Lofgren, G.E., and Norris, P.N., 1981. Experimental duplication of plagioclase sieve and overgrowth textures. *Geol. Soc. Amer. Abstracts with Programs*, 13, 498.

MacDonald, G.A., and Alcaraz, A.P., 1956. Nuees ardentes of the 1948-1953 eruption of Hibok-hibok. *Bull. Volcanol.*, 18, 169-178.

Macgregor, A.G., 1938. The volcanic history and petrology of Montserrat with observations on Mt. Pelee in Martinique. *Philos. Trans. R. Soc. London, Ser. B, No. 557*, 229, 1-90.

Mackenzie, W.S., Donaldson, C.H. and Guilford, C., 1982. Atlas of igneous rocks and their textures. Longman Group Limited, 148 pp.

Mason, D.R., 1978. Compositional variations in ferromagnesian minerals from porphyry copper-generating and barren intrusions of the western Highlands, Papua New Guinea. *Econ. Geol.*, 73, 878-890.

Mathez, E.A., 1973. Refinement of Kudo-Weill plagioclase thermometer and its application to basaltic rocks. *Contrib. Mineral. Petrol.*, 41, 61-72.

McBirney, A.R., 1980. Mixing and unmixing of magmas. *J. Volcanol. Geotherm. Res.*, 7, 357-371.

McBirney, A.R., Baker, B.H., and Nilson, R.H., 1985. Liquid fractionation. Part I: basic principles and experimental simulations. *J. Volcanol. Geotherm. Res.*, 24, 1-24.

McCabe, R., Almasco, J.N., and Yumul, G., 1985. Terranes of the central Philippines, in Howell, D.G., ed., Tectonostratigraphic terranes of the circum-Pacific region. *Circum-Pacific Council Energy and Mineral Res. Earth Sci. Series 1*, pp. 421-435.

Miyashiro, A., 1974. Volcanic rock series in island arcs and continental margins. *Amer. J. Sci.*, 274, 321-355.

Miyashiro, A., and Shido, F., 1975. Tholeiitic and calc-alkalic series in relation to the behaviors of titanium, vanadium, chromium and nickel. *Amer. J. Sci.*, 275, 265-277.

Miyashiro, A., Shido, F., and Ewing, M., 1969. Diversity and origin of abyssal tholeiite from the Mid-Atlantic Ridge near 24° and 30° north latitude. *Contrib. Mineral. Petrol.*, 23, 38.

Moody, J.D., and Hill, M.J., 1956. Wrench fault tectonics. *Geol. Soc. Amer. Bull.*, 67, 1207-1246.

Morris, J.D., Jezek, P., Hart, S.R., and Gill, J.B., 1983. The Halmahera island arc, Molucca Sea collision zone, Indonesia, in Hayes, D.E., ed., The tectonic and geologic evolution of Southeast Asian seas and islands, *Geophys. Monogr. 23*, AGU, Washington, D.C., pp.373-387.

Mukasa, S.B., McCabe, R., and Gill, J.B., 1986. Geochemistry and Pb-isotopic compositions of lavas from the Philippine island arc. *Terra cognita*, 6, 198.

Nakamura, Y., and Kushiro, I., 1970. Compositional relations of coexisting orthopyroxene, pigeonite and augite in a tholeiitic andesite from Hakone volcano. *Contrib. Mineral. Petrol.*, 26, 265-275.

Neall, V.E., 1976. Lahars--global occurrence and annotated bibliography. *Publication No.5 of the Geology Department, Victoria University*, New Zealand, 18 pp.

Newhall, C.G., 1979. Temporal variation in the lavas of Mayon volcano, Philippines. *J. Volcanol. Geotherm. Res.*, 6, 61-83.

Nicholls, I.A., 1971. Petrology of Santorini volcano, Cyclades, Greece. *J. Petrol.*, 12, 67-119.

Nicholls, I.A., and Whitford, D.J., 1976. Primary magmas associated with Quaternary volcanism in the western Sunda arc, in Johnson, R.W., ed., Volcanism in Australasia. Elsevier, pp. 77-90.

Norrish, K., and Hutton, J.T., 1969. An accurate X-ray spectrograph method for the analysis of a wide range of geological samples. *Geochim. Cosmochim. Acta* 33, 431-453.

Obusan, R.O., 1977. Preliminary report on the reconnaissance geological survey at Manito geothermal prospect, Albay. *Unpublished PNOC-EDC Report*, 48 pp.

Obusan, R.O., 1979. The potential of the Manito geothermal system, southeastern Luzon, Philippines. *Diploma in Energy Technology (Geothermal) Report No.79.19.* University of Auckland, New Zealand, 62 pp.

O'Hara, M.J., 1977. Geochemical evolution during fractional crystallisation of a periodically refilled magma chamber chamber. *Nature*, 266, 503-507.

Oshima, O., 1975. Mineralogical aspects of volcanic eruption. *Bull. Volcanol. Soc. Jpn., 2nd Ser.*, 20, 275-298.

Panem, C.C., and Alincastre, R.S., 1984a. Structural mapping of west Bacon-Manito geothermal area. *Unpublished PNOC-EDC Report*, 55 pp.

Panem, C.C., and Alincastre, R.S., 1984b. Structural mapping of Palayang Bayan-Cawayan area. *Unpublished PNOC-EDC Report*, 58 pp.

Panem, C.C., and Alincastre, R.S., 1985. Surface geology of Bacon-Manito geothermal field. *Unpublished PNOC-EDC Report*, 320 pp.

Parsons, W.H., 1969. Criteria for the recognition of volcanic breccias: a review, in Larsen, L., ed., Igneous and metamorphic geology. *Geol. Soc. Amer. Mem. 115*, 263-304.

Peccerillo, A., and Taylor, S.R., 1976. Geochemistry of Eocene calcalkaline volcanic rocks from the Kastamonu area, northern Turkey. *Contrib. Mineral. Petrol.*, 58, 63-81.

Pelaez, V.R., 1953. The behaviour and characteristics of volcanoes in the solfataric and fumarolic stage of activity. *Proc. 7th Pacific Sci. Congress*, vol. II, 364-368.

Philippine Bureau of Mines (PBM), 1963. Geological map of the Philippines. Scale 1:1,000,000, 9 sheets.

Philippine National Oil Company-Energy Development Corporation (PNOC-EDC), 1985. A review of the 110 MWe BacMan I development strategy. *Unpublished PNOC-EDC Report*, 138 pp.

Putirka, K.D., and Weigand, P.W., 1987. Miocene volcanic rocks of the western Mojave desert, California: evidence for magma mixing. *Geol. Soc. Amer. Abstracts with Programs*, 19, 441.

Ragland, P.C., and Defant, M.J., 1983. Silica standardization: a discriminant technique applied to a volcanic arc system. *Earth Planet. Sci. Lett.*, 64, 387-395.

Reid, F.W., 1983. Petrology report for Well Pal-5d. *Unpublished PNOC-EDC Report*, 25 pp.

Reyes, A.G., 1984. Petrographic analyses of eastern Bacon-Manito surface sample. *Unpublished PNOC-EDC Report*, 60 pp.

Reyes, A.G., 1985. A comparative study of "acid" and "neutral pH" hydro-thermal alteration in the Bacon-Manito geothermal area, Philippines. *Unpublished MSc thesis*, Auckland University, New Zealand.

Ringwood, A.E., 1974. The petrological evolution of island arc systems. *J. Geol. Soc. London*, 130, 183-204.

Ringwood, A.E., 1977. Petrogenesis in island-arc systems, in Talwani, M., and Pitman III, W.C., eds., Island arcs deep sea trenches and back-arc basins, *Maurice Ewing Series 1*, AGU, 311-324.

Risk, G.F., 1986. Reconnaissance and follow-up resistivity surveying of New Zealand geothermal fields. *Proc. 8th NZ Geotherm. Workshop*, 75-80.

Ritchey, J.L., 1980. Divergent magmas at Crater Lake, Oregon: products of fractional crsytallization and vertical zoning in a shallow, water-undersaturated chamber. *J. Volcanol. Geotherm. Res.*, 7, 373-386.

Rittman, J.L., 1953. Magmatic character and tectonic position of the Indonesian volcanoes. *Bull. Volcanol.*, 14, 45.

Sakuyama, M., 1979. Evidence of magma mixing: petrological study of Shirouma-Oike calc-alkaline andesite volcano, Japan. *J. Volcanol. Geotherm. Res.*, 5, 179-208.

Sakuyama, M., 1981. Petrological study of the Myoko and Kurohime volcanoes, Japan: crystallization sequence and evidence for magma mixing. *J. Petrol.*, 22, 553-583.

Sakuyama, M., 1983. Petrology of arc volcanic rocks and their origin by mantle diapirs. *J. Volcanol. Geotherm. Res.*, 18, 297-320.

Sakuyama, M., 1984. Magma mixing and magma plumbing systems in island arcs. *Bull. Volcanol.*, 47, 685-703.

Saunders, A.D., Tarney, J., and Weaver, S.D., 1980. Transverse geochemical variations across the Antarctic Peninsula: implications for the genesis of calcalkaline magmas. *Earth Planet. Sci. Lett.*, 46, 344-360.

Schmid, R., 1981. Descriptive nomenclature and classification of pyroclastic deposits and fragments: recommendations of the IUGS subcommission on the systematics of igneous rocks. *Geology*, 9, 41-43.

Schroeder, B., Thompson, G., Sulanowska, M., and Ludden, J.N., 1980. Analysis of geologic materials using an automated X-ray fluorescence system. *X.R.S.*, 9, 198-205.

Smedes, H.W., and Prostka, H.J., 1972. Stratigraphic framework of the Absaroka volcanic supergroup in the Yellowstone National Park region, in The geology of Yellowstone National Park. *U.S.G.S. Surv. Prof. Pap. 729-C*, 33 pp.

Sparks, R.S.J., Huppert, H.E., and Turner, J.S., 1984. The fluid dynamics of evolving magma chambers. *Philos. Trans. R. Soc. London, Ser. A*, 310, 511-534.

Stewart, D.C., 1975. Crystal clots in calc-alkaline andesites as breakdown products of high-Al amphiboles. *Contrib. Mineral. Petrol.*, 53, 195-204.

Stormer, J.C., 1983. The effects of recalculation on estimates of temperature and oxygen fugacity from analyses of multicomponent iron-titanium oxides. *Amer. Mineral.*, 68, 586-594.

Sugimura, A., 1960. Zonal arrangement of some geophysical and petrological features in Japan and its environs. *J. Fac. Sci. Tokyo Univ. Ser. 2*, 12, 133-153.

Sun, S., 1980. Lead isotopic study of young volcanic rocks from mid-ocean ridges, oceanic islands, and island arcs. *Philos. Trans. R. Soc. London A 297*, 409-445.

Taylor, R.S., 1969. Trace element chemistry of andesites and associated calc-alkaline rocks, in McBirney, A.R., ed., Proc. Andesite Conference, *Oregon Dept. Geol. and Mineral Industries*, pp.43-64.

Thorarinsson, S., 1954. The eruption of Hekla, 1947-1948, Part II. 3. The tephra-fall from Hekla on March 29, 1947. *Visindafelag Islendinga*, 68 pp.

Travaglia, C., and Baes, A.F., 1976. Geology of the Bicol river basin. *Philippine Bureau of Soils-U.N. Development Programme, AGO, Working Paper 1/2*, Manila, 57 pp.

Travaglia, C., and Baes, A.F., 1979. Geology of Sorsogon Province, *Soil and Land Resources Appraisal and Training Project, Philippines, Bureau of Soils, UNDP/FAO Programme*, Manila, 87 pp.

Tsuchiyama, A., 1985. Dissolution kinetics of plagioclase in the melt of the system diopside-albite-anorthite, and the origin of dusty plagioclase in andesites. *Contrib. Mineral. Petrol.*, 89, 1-16.

Turner, J.S., 1980. A fluid-dynamical model of differentiation and layering in magma chambers. *Nature*, 285, 213-215.

Ui, T., 1986. How to descriminate between debris avalanche and other volcaniclastic formations. *1986 International Volcanological Congress Abstracts*, p. 283.

Van Eysinga, F.W.B., 1970. Stratigraphic terminology and nomenclature; a guide for editors and authors. *Earth Sci. Rev.*, 6, 267-288.

Wallace, R.E., 1977. Profiles and ages of young fault scarps, north-central Nevada. *Geol. Soc. Amer. Bull.*, 88, 1267-1281.

Watanabe, T., Grapes, R., and Palmer, K., 1981. Quantitative analyses of rock forming minerals by JXA-733 electron probe X-ray microanalyser. *Jeol News*, 19E, 15-19.

Watson, E.B., 1979. Calcium content of forsterite coexisting with silicate liquid in the system Na_2O-CaO-MgO-Al_2O_3-SiO_2. *Amer. Mineral.*, 64, 824-829.

Weber, C., 1984. Zur geologie und petrologie des kustenstreifens zwischen Tiwi und Matalibong, Albay (Albay, Philippinen) unter besonderer Berucksichtigung de hydrothermalen flder und tonlagerstatten. *Unpublished Diploma thesis*, University of Aachen, 103 pp.

Whittaker, E.J.W., and Muntus, R., 1970. Ionic radii for use in geochemistry. *Geochim Cosmochim Acta*, 34, 945-956.

Wilcox, R.E., 1979. The liquid line of descent and variation diagrams, in Yoder, H.S., ed., The evolution of the igneous rocks; Fifth anniversary perspective, pp. 205-232.

Williams, H., 1942. Geology of Crater Lake National Park, Oregon. *Carnigie Inst. Wash. Publ. No. 540*, 162 pp.

Williams, H., and McBirney, A.R., 1979. Volcanology. Freeman, Cooper & Co., San Francisco. 391 pp.

Wilkinson, J.F.G., Vernon, R.H., and Shaw, S.E., 1964. The petrology of an adamellite-porphyrite from the New England bathylith (New South Wales). *J. Petrol.*, 5, 461-488.

Wood, D.A., Joron, J.L., Treuil, M., Norry, M., and Tarney, J., 1979. Elemental and Sr isotope variations in basic lavas from Iceland and the surrounding ocean floor. *Contrib. Mineral. Petrol.*, 70, 319-339.

Worner, G. and Schmincke, H.U., 1984. Mineralogical and chemical zonation of the Laacher See tephra sequence (East Eiffel, W. Germany). *J. Petrol.*, 25, 805-835.

Wright, A.E., and Bowes, D.R., 1963. Classification of volcanic breccias : a discussion. *Geol. Soc. Amer. Bull.*, 74, 79-86.

Wright, J.V., Smith, A.L., and Self, S., 1980. A working terminology of pyroclastic deposits. *J. Volcanol. Geotherm. Res.*, 8, 315-336.

Wright, J.V., Smith, A.L., and Self, S., 1981. A working terminology of pyroclastic deposits, in Self, S., and Sparks, R.S.J., eds., Tephra Studies, pp. 457-463.

Zaide, M.C., 1983. Fluid inclusion study of Well Pal-5D, Bacon-Manito geothermal field, southern Luzon, Philippines. *Unpublished PNOC-EDC Report*, 25 pp.

Zanoria, A.S., Domingo, E.G., Bacuta, G.C., and Almeda, R.L., 1984. Geology and tectonic setting of copper and chromite deposits of the Philippines. *Geol. Surv. Japan Report No. 263*, 209-233.

Zapanta, R.R., 1985. 1984 BMGP thermal areas work activity and accomplishment report. *Unpublished PNOC-EDC Report*, 16 pp.

APPENDIX

SAMPLE DETAILS AND PETROGRAPHIC DESCRIPTIONS

APPENDIX

PETROGRAPHIC DESCRIPTIONS

Samples are discussed in the order of increasing silica contents in both WPM and EPM series. Petrographic terminology follows Mackenzie *et al.* (1982), and several terms are abbreviated as follows : porphyritic = por; phenocryst(s) = pheno(s); euhedral = euhed; abundant = abund; crystal = xtal; matrix = mx; olivine = ol; plagioclase = plg; horn-blende = hb; pyroxene = px; clinopyroxene = cpx; orthopyroxene = opx; feldspar = fspar; medium = med; fine = fn; rock = rx).

Samples are plotted in the geologic map inside the back pocket of this thesis.

I. WEST POCDOL MOUNTAINS (WPM) SERIES LAVAS

Field No.	14
Canterbury Univ. No.	20438
Locality	1,441,185 mN/594,055 mE
Volcanic Unit	Malobago volcanics (Mgv)
Rock name	Olivine-phyric basalt

PETROGRAPHIC NOTES

Hypoxtalline por rx showing abund subhed to anhed sieve-textured plg laths (<2.5 mm). Several grains are embayed with mx materials. Plg usually occurs in crystal clots, and show complex twins and sector zoning features. Blebs of melt inclusions are present both in the core and marginal zone area. Average anorthite is An_{50-52}. Mafic phenos comprise euhed to subhed iddingsite-rimmed colourless ol microphenos (<0.1 mm). Few equant anhed ol grains occur as chadacrysts, together with px w/in a poikilitic cpx core (~1 mm) Opx grains are mostly untwinned and unzoned, and several are in contact w/ ol and form clots (+ Fe-Ti oxides + plg). Several orthopyroxenes show corroded faces or resorbed rims. The mx comprises plg, ol and px microlites and abund cryptoxtalline dark glass defining both intersertal and intergranular textures.

Field No.	4
Canterbury Univ. No.	20469
Locality	1,448,510 mN/597,060 mE
Volcanic Unit	Kayabon volcanics (Knv)
Rock Name	Two-pyroxene basaltic andesite

PETROGRAPHIC NOTES :

The rock is por w/ subhed-anhed, simply- to complexly-twinned plg (An_{60-62}) phenos (<3 mm); majority of plg have dusty cores w/ rare px chadacrsyts. Px is zoned/twinned and several show xtals show overgrowth textures (i.e., opx core mantled by a zoned cpx. About 1-2% px microphenos are pseudomorphed by minute opaque minerals. The mx is fn-grained composed of abund microspheres of black glassy material, fspar and px microlites.

Field No.	3
Canterbury Univ. No.	20464
Locality	1,448,850 mN/595,050 mE
Volcanic Unit	Kayabon volcanics (Knv)
Rock Name	Two-pyroxene andesite

PETROGRAPHIC NOTES :

Hypoxtalline med-grained glomeropor rx whose phenos phases are dominated by subhed-euhed plg (An_{50-67})laths which are either zoned/twinned. Few plg grains show partially-corroded outlines, concentric melt inclusions in the margins, and several of these grains host anhed laths of zoned cpx microphenos. Plg is also in aggregates, together with px and opaque minerals. Opx and cpx are the second most abundant, and both show subhed-anhed zoned/twinned xtals, and few of these contain highly frittered cores and rounded outlines. Both display intergrowth and overgrowth textures. The groundmass is composed of plg microlites and brown glass which exhibits intersertal and "pseudo" fluidal textures.

Field No.	12
Canterbury Univ.No.	20468
Locality	1,441,485 mN/592,675 mE
Volcanic Unit	Lison volcanics (Lnv)
Rock Name	Two-pyroxene andesite

PETROGRAPHIC NOTES :

Hypoxtalline med- to fn-grained highly por rx composed of abund subhed-anhed plg microphenos/phenos. Both "clean" and "dirty" plg varieties are present. The "clean" plg is simply-twinned/ zoned; few of these exhibit rounded crystal outlines with concentric melt inclusions. The "dirty" plg is rel larger crystals, twinned/zoned and always show "sieve" texture. Average plg is An_{48-52}. Most px occurs as subhed microphenos, often twinned/ zoned. Opx is blanketed by zoned cpx or subhed hb laths. Hb xtals are poorly-cleaved, pale green pleochroic phenos/microphenos rimmed by opaque oxide.

Field No.	39
Canterbury Univ. No.	20466
Locality	1,438,830 mN/595,848 mE
Volcanic Unit	Lison volcanics (Lnv)
Rock Name	Hornblende-bearing two pyroxene andesite

PETROGRAPHIC NOTES :

Hypoxtalline med-grained por rx showing "clean" subhed-euhed twinned/zoned plg laths. Several of the plg are partially corroded, w/ concentric inclusions, frittered cores and embayments. The "dirty" variety is usually observed in clots. Average plg composition is An_{50-52}. Px occurs as subhed-anhed phenos/microphenos or in clot. Several cpx are embayed with mx materials and show skeletal forms. Skeletal hb is seen only in one xenocryst displaying a highly frittered core with overgrowth minerals consisting of plg + px + opaque oxide. The finer-grained groundmass is composed essentially of fspar microlites and glass.

Field No.	38
Canterbury Univ. No.	20467
Locality	1,443,675 mN/597,605 mE
Volcanic Unit	Lison volcanics (Lnv)
Rock Name	Two pyroxene andesite

PETROGRAPHIC NOTES :

Hypocrystalline medium- to fine-grained porphyritic rock showing abundant euhedral to anhedral, twinned and zoned plagioclase laths (<3.5 mm) which are "clean" varieties, but a few exhibit corroded outlines, melt inclusions, and several chadacrysts of stubby subhedral zoned clinopyroxenes and opaques. Few plagioclasess display frittered cores. The average pagioclase bulk composition is An 50-52. Pyroxene occurs as subhedral to anhedral zoned and twinned prisms. One grain shows a frittered orthopyroxene core (~0.5 mm) which is completely blanketed by a euhedral to subhedral zoned clinopyroxene crystal, and is partially embayed with matrix material. A similar but skeletal pyroxene grain (1 mm) is also observed, occurring among an aggregate of zoned, twinned and corroded plagioclase, clinopyroxene and opaque minerals. The groundmass is fine-grained composed of feldspar and pyroxene microlites and glass.

Field No.	13
Canterbury Univ. No.	20465
Locality	1,442,295 mN/593,727 mE
Volcanic Unit	Lison volcanics (Lnv)
Rock Name	Hornblende andesite

PETROGRAPHIC NOTES :

Hypoxtalline med- to fn-grained rx composed of subhed-anhed zoned/twinned plg laths (<4 mm), usually as crystal clots. Simply-twinned plg has An_{46-48}. Mafic minerals are dominated by subhed pale green pleochroic hb rimmed by microgranular opaques. Several hb (<3.5 mm) occur as poikilitic cumulophenos. Px xtals (<1.5 mm) are subhed-anhed zoned/ twinned showing poikilitic cores, and are always dotted w/ anhed opaque inclusions.

II. WEST POCDOL MOUNTAINS (WPM) SERIES LAVAS

Field No.	**42B**
Canterbury Univ. No.	**20452**
Locality	**1,445,148 mN/609,850 mE**
Volcanic Unit	**Pulog volcanics (Pgv)**
Rock Name	**Two pyroxene basaltic andesite**

PETROGRAPHIC NOTES

Med- to fn-grained hypoxtalline por rx showing abund inclusion-bearing "cloudy" zoned/twinned plg glomerophenocrysts. Some highly frit tered skeletal plg xtals are fringed w/ zoned plg overgrowths. Average anorthite An_{50-58}. Cpx shows strained cores with rounded outlines and are often poikilitic or twinned crystals. Sub to anhed inclusion-bearing opx laths show completely corroded out lines. he matrix is vitrophyric consisting of plg microlites, microxtalline px, and dark interstitial glass.

Field No.	**23**
Canterbury Univ. No.	**20440**
Locality	**1,444,400 mN/602,450 mE**
Volcanic Unit	**Pangas volcanics (Psv)**
Rock Name	**Two pyroxene basaltic andesite**

PETROGRAPHIC NOTES :

Hypoxtalline vesicular med- to fn-grained por rx showing abund subhed-anhed, frittered, zoned and complexly twinned plg laths, and the majority of these occur as microphenos. Average plg composition is An_{44-54}, whose sizes crudely approximate a seriate-textured rock and most of their crystal faces show vestiges of corrosion. Px grains are observed as cumulophenos; usually subhed-anhed poikilitic and partially corroded xtals dotted w/ anhed opaque microphenos. Several cpx and opx are coupled to each other, and exhibit a serrated grain boundary. One poikilitic opx cumulocryst shows corrugated faces, and encloses anhed opaques and cpx chadacrysts, as well as stubby twinned subhed plg microlaths. The mx consists of relatively larger fspar microlites (as compared to sample 29 and 28A) and brown glass which vitrophyric, intersertal and intergranular textures.

Field No.	**30**
Canterbury Univ. No.	**20455**
Locality	**1,445,015 mN/606,615 mE**
Volcanic Unit	**Pulog volcanics (Pgv)**
Rock Name	**Two pyroxene basaltic andesite**

PETROGRAPHIC NOTES :

Highly vesicular hypoxtalline por rx which shows similar mineralogy and textures to sample 40. Subtle differences include a slight modal abundance of opx over cpx, and px glomerocrysts are rare. The mx mineralogy is heavily-masked by a murky brown interstitial glass, same as in sample 40.

Field No.	40
Canterbury Univ. No.	20458
Locality	1,443,040 mN/ 607,740 mE
Volcanic Unit	Pulog volcanics (Pgv)
Rock Name	Two pyroxene basaltic andesite

PETROGRAPHIC NOTES :

Highly vesicular med- to fn-grained hypoxtalline por rx whose phenos phases are set in a murky dark brown vitrophyric mx. Plg fspar laths are generally frittered and corroded, and few are dotted with bleb-like inclusions. "Clean" plg xtals are rare. Cpx grains are the dominant mafic phases which are subhed-anhed twinned/zoned xtals, most of which are seen as glomerophenos, together with minor plg, opx and anhed opaque grains. One subhed inclusion-riddled cpx glomerocryst displays a sector zoning pattern. Px overgrowth textures are present, and exemplified by partially-to completely-mantled opx cores. Several px glomerocrysts show intergrowth textures (serrate or irregular crystal boundaries) between unzoned and zoned corroded cpx. (N.B. Sample 40 is one of the most vesicular specimen in the area).

Field No.	19
Canterbury Univ. No.	20461
Locality	1,441,770 mN/606,340 mE
Volcanic Unit	Pangas volcanics (Psv)
Rock Name	Two pyroxene basaltic andesite

PETROGRAPHIC NOTES :

Hypoxtalline vesicular med-grained por rx showing abund platy plg fspars which are characterised by anhed-subhed corroded outlines, complex twinning, strong zoning, skeletal cores and concentric melt inclusions. Average plg composition is An_{48-50}. Px xtals show embayed and corroded crystal outlines, and form skeletal poikilitic grains, and sometimes occur as twinned and zoned xtals. Rare hb clots are present as xenocrysts. The mx consists of microcrystalline plg laths and interstitial glass.

Field No.	33
Canterbury Univ. No.	20448
Locality	1,446,860 mN/605,600 mE
Volcanic Unit	Pangas volcanics (Psv)
Rock Name	Hornblende-bearing two pyroxene andesite

PETROGRAPHIC NOTES :

Hypoxtalline glomeropor rx consisting of abund subhed to anhed zoned/twinned plg (An_{50-54}). Numerous plg grains exhibit rounded outlines and frittered cores. Embayed plagioclases are also common, usually being enhanced by concentric melt inclusions. Px laths occur usually in crystal clots, few having rounded outlines and others show poikilitic to subophitic textures. Px phenos are large (< 3.5 mm) and are usually twinned and zoned. Most opx form subhed poikilitic grains in aggregates. The groundmass consists of cryptoxtalline material and interstitial brown glass.

Field No.	34
Canterbury Univ. No.	20451
Locality	1,446,975 mN/605,200 mE
Volcanic Unit	Pangas volcanics (Psv)
Rock Name	Two pyroxene andesite

PETROGRAPHIC NOTES :

Hypoxtalline med-grained glomeropor rx composed of abund corroded subhed-anhed zoned plg laths; several of the larger grains (~2 mm) show concentric zoning which in many examples, are define by concentric minute inclusions. Average plg composition is An_{38-55}. Subhed-anhed px occurs as partially corroded poikilitic to skeletal grain, dotted with anhedral opaques. Larger twinned and zoned px xtals are essential components of crystal aggregates that exhibit interdigitating stubby subhed twinned plg laths and opaques. The chadacrysts present in twinned cpx comprise anhed zoned opx microphenos, glass inclusions and plg. Opx grains are essentially poikilitic corroded laths containing numerous opaque microphenos. The mx consists of pilotaxitic fspar microlites, microgranular opaques and glass.

Field No.	35
Canterbury Univ. No.	20450
Locality	1,447,675 mN/606,900 mE
Volcanic Unit	Pangas volcanics (Psv)
Rock Name	Two pyroxene andesite

PETROGRAPHIC NOTES :

Hypoxtalline med- to fn-grained glomeropor rx consisting of abund subhed-anhed zoned/twinned plg phenos. Several stubby zoned plg laths occur as chadacrysts in px. Average plg composition is An_{50-63}, and grain sizes do not exceed 4 mm. Opx phenos >> cpx and both occur as large (<3 mm) subhed poikilitic to subophitic twinned and zoned tabular xtals. Several px s are major components of xtal aggregates, usually associated with subhed zoned stubby plg and anhed opaques. The mx consists of feldspathic microlites showing a flow texture.

Field No.	22
Canterbury Univ. No.	20439
Locality	1,442,080 mN/601,425 mE
Volcanic Unit	Cawayan volcanics (Cnv)
Rock Name	Two pyroxene andesite

PETROGRAPHIC NOTES :

Vesicular hypoxtalline med-grained por rx showing abund large (1.5-2 mm) subhed zoned simply- to complexly-twinned "clean" plg fspar laths, having an average anorthite content of 50-54. Several anhed plg grains (mostly as microphenos) display rounded and corroded xtal outlines, some of these are embayed by mx materials. One corroded plg xtal face is terminated with radiating

crystallites. Sieve textured plg grains are rare. Cpx grains occur as subhed-anhed zoned corroded grains. Opx xtals usually occur as glomerocrysts and form skeletal poikilitic subhedral grains. Px overgrowth textures are either partial or complete mantling of zoned cpx around subhed opx cores. Consertal growth textures between cpx and opx are observed. The groundmass consists of cryptoxtalline to microxtalline fspars masked by murky interstitial brown glass.

Field No.	**29**
Canterbury Univ. No.	**20445**
Locality	**1,443,065 mN/603,740 mE**
Volcanic Unit	**Pangas volcanics (Psv)**
Rock Name	**Two pyroxene andesite**

PETROGRAPHIC NOTES :

Hypoxtalline med- to fn-grained por rx showing two types of plg phenos : (1) a "dirty" variety which is highly frittered, complexly twinned and zoned crystals, and the other type (2) a "clean" variety which are usually complexly twinned subhed microphenos. One large "clean" plg grain (~3.5 mm) encloses a stubby euhed (0.3 mm) poorly-cleaved opx xtal, whereas others enclose zoned anhed cpx chadacrysts. Px phases occur as zoned anhed microphenos, and usually forming variably corroded cumulocrysts. The larger px grains occur as glomerocrysts and show overgrowth textures, similar to sample 28A. A number of anhed-subhed px grains are completely pseudomorphed by microgranular opaques. The groundmass is composed of finer-grained pilotaxitic fspar microlites.

Field No.	**25**
Canterbury Univ. No.	**20456**
Locality	**1,443,550 mN/601,425 mE**
Volcanic Unit	**Cawayan volcanics (Cnv)**
Rock Name	**Two pyroxene andesite**

PETROGRAPHIC NOTES :

Hypoxtalline med- to fn-grained por rx showing vitrophyric groundmass composed of interstitial brown glass and fspar microlites. Embedded on this mx are abundant subhed-anhed twinned/zoned plg laths with average anorthite content of 48-56. The largest grains measure up to 3 mm but a significant proportion lies with the microphenо size range (0.05-0.5 mm). Both "clean" and frittered plg fspars are present, majority of these show varying degrees of corroded outlines and embayments. Several have skeletal cores dotted with concentric melt inclusions. The mafic phases are dominated by px wherein cpx >> opx. Cpx show zoning or twinning or both, and in most instances, they exhibit corrode outlines and skeletal cores. In contrast, opx xtals are euhed-subhed partially corroded grains and few are inclusion-bearing unzoned and untwinned crystals. Both are major constituents of glomerocrysts, together with plg fspars and opaques. Px overgrowth texture is present (i.e., opx is completely jacketed by cpx or in some cases, opx encloses minute zoned cpx chadacrysts.

Field No.	**7B**
Canterbury Univ. No.	**20446**
Locality	**1,438,950 mN/603,482 mE**
Volcanic Unit	**Pangas volcanics (Psv)**
Rock Name	**Hornblende-bearing two pyroxene andesite**

PETROGRAPHIC NOTES :
Hypoxtalline med- to fn-grained glomeropor rx, composed of abund large (~2 mm) subhed twinned frittered plg xtals showing rounded, corroded and zoned overgrowth margins. Stubby subhed-anhed px microphenos, concentric melt inclusions and anhed opaques comprise the chadacrysts in plg. Simply-twinned subhed "clean" plg fspars are also present in minor amounts. Average plg composition is An_{54-62}. Px grains occur prominently in xtal aggregates, often as subhed twinned prisms with variably corroded margins. Several px microphenos show distinct rounded outlines and skeletal cores. Rare anhed green pleochroic hb laths show opacite rim. The mx consists of pyroxene and feldspar microlites, brown glass and anhedral opaques.

Field No.	**28A**
Canterbury Univ. No.	**20441**
Locality	**1,443,760 mN/603,905 mE**
Volcanic Unit	**Pangas volcanics (Psv)**
Rock Name	**Hornblende andesite**

PETROGRAPHIC NOTES :
Hypoxtalline med- to fn-grained por rx showing abund twinned and normally zoned plg xtals (~2 mm) containing cores which are defined by hollows and concentric melt inclusions. Plg xtal faces vary from highly corroded/ embayed to rounded forms. The average plg composition is An_{48-56}. Px grains are the dominant mafic phase, showing subhed-anhed zoned/twinned and poikilitic grains. Cpx are greater than opx; both display the following overgrowth/ intergrowth textures. Several subhed highly corroded pale green pleochroic hb laths are present. The groundmass consists of fspar microlites, anhed opaques and interstitial brown glass.

Field No.	**28B**
Canterbury Univ. No.	**20442**
Locality	**1,443,760 mN/603,905 mE**
Volcanic Unit	**Pangas volcanics (Psv)**
Rock Name	**Two pyroxene andesite**

PETROGRAPHIC NOTES :
Hypoxtalline med- to fn-grained por rx showing abund twinned and normally zoned plg xtals (~2 mm) containing cores which are defined by hollows and concentric melt inclusions. Plg xtal faces vary from highly corroded to rounded forms. The average plg composition is An_{48-62}. Px grains are the dominant mafic phase, showing subhed-anhed zoned/twinned and poikilitic grains. Cpx are greater than opx; both display the following overgrowth/ intergrowth textures. The groundmass consists of fspar microlites, anhed opaques and interstitial brown glass.

Field No.	32
Canterbury Univ. No.	20462
Locality	1,446,000 mN/605,600 mE
Volcanic Unit	Pangas volcanics (Psv)
Rock Name	Hornblende andesite

PETROGRAPHIC NOTES :

Hypoxtalline por rx showing subhed-anhed zoned skeletal complexly-twinned plg fspar laths, and several of these have partially- to completely corroded rims of minute inclusions. Rounded plg xtal outlines are also common. Average plg composition is An_{52-58}. Pale green pleochroic subhed-anhed hb laths dominate the mafic phases. Hb is always rimmed by minute opaque minerals; larger hb grains (>3 mm) always show a core of irregularly-shaped hollows which are sometimes filled with matrix material. Px xtals are few, occurring as subhed-anhed corroded and zoned minerals (<1 mm). The groundmass is composed of fspar microlites and murky interstitial glass.

Field No.	1
Canterbury Univ. No.	20457
Locality	1,443,550 mN/601,425 mE
Volcanic Unit	Cawayan volcanics (Cnv)
Rock Name	Two pyroxene andesite

PETROGRAPHIC NOTES :

Hypoxtalline med- to fn-grained por rx showing vitrophyric groundmass composed of interstitial brown glass and fspar microlites. Embedded on this mx are abundant subhed-anhed twinned/zoned plg laths with average anorthite content of 48-56. The largest grains measure up to 2 mm but a significant proportion lies with the microphenо size range (0.05-0.5 mm). Both "clean" and frittered plg fspars are present, majority of these show varying degrees of corroded outlines and embayments. The mafic phases are dominated by px. Cpx show zoning or twinning or both, and in most instances, they exhibit corrode outlines and skeletal cores. In contrast, opx xtals are euhed-subhed partially corroded grains and few are inclusion-bearing unzoned and untwinned crystals. Both are major constituents of glomerocrysts, together with plg fspars and opaques.

Field No.	16
Canterbury Univ. No.	20453
Locality	1,440,745 mN/605,650 mE
Volcanic Unit	Suminandig
Rock Name	Hornblende andesite

PETROGRAPHIC NOTES :

Hypoxtalline vesicular med-grained por rx showing frittered subhed-anhed zoned/twinned plg (<3.5 mm); a plg overgrowth is usually present. Plg cumulocrysts show either subhed corroded xtal clots or anhed serrated individual grains. A strongly zoned (normal) phenos are dominant. The mafic phases are subhed-anhed reddish

brown pleochroic hb; opacite-rim and skeletal forms are character istic featuresof hb. The poikilitic inclusion-bearing hornblendes contain stubby zoned subhed plg and cpx chadacrysts; few of these type are present in clots. Px microphenos and phenos show anhed zoned and twinned xtals. The groundmass consists of pilotaxitic fspar microlites, microxtalline px and interstitial brown glass.

Field No.	43
Canterbury Univ. No.	20449
Locality	1,441,295 mN/609,595 mE
Volcanic Unit	Suminandig volcanics (Sgv)
Rock Name	Hornblende andesite

PETROGRAPHIC NOTES :

Hypoxtalline glomeropor rx consisting of abund subhed to anhed zoned/twinned plg (An_{50-54}). Numerous plg grains exhibit rounded outlines and frittered cores. Embayed plagioclases are also common, usually being enhanced by concentric melt inclusions. Px laths occur usually in crystal clots, few having rounded outlines and others show poikilitic to subophitic textures. Px phenos are large (< 3.5 mm) and are usually twinned and zoned. Hb xtals very abund and display both brown and green pleochric varieties. Most opx form subhed poikilitic grains in aggregates. The groundmass consists of cryptoxtalline material and interstitial brown glass.

Field No.	37
Canterbury Univ. No.	20443
Locality	1,447,400 mN/603,735 mE
Volcanic Unit	Pangas volcanics (Psv)
Rock Name	Hornblende-bearing twopyroxene andesite

PETROGRAPHIC NOTES :

Hypocrystalline medium- to fine-grained porphyritic rock which is texturally and mineralogically similar to sample HJT36 except that in sample HJT36 : "clean" plagioclase variety is more abundant; greater number of large (~4 mm), partially corroded, subhedral, zoned and twinned plagioclase crystals, and the greater number of anhedral twinned hornblendes with opacite rim. An overgrowth structure observed from a cumulophyric skeletal poikilitic plagioclase lath (~1 mm) shows numerous inclusions of anhedral zoned clinopyroxenes and opaques. One of the clinopyroxene chadacrysts (~0.2 mm) is jacketed by a subparallel rim of orthopyroxene. The groundmass is composed of feldspar and pyroxene microlites and interstitial brown glass, which define a pilotaxitic texture.

Field No.	8
Canterbury Univ. No.	20454
Locality	1,438,500 mN/603,853 mE
Volcani Unit	Suminandig volcanics (Sgv)
Rock Name	Hornblende andesite

PETROGRAPHIC NOTES :

Hypocrystalline medium- to fine-grained porphyritic rock which is texturally and mineralogically similar to sample HJT36 except that in sample HJT36 : "clean" plagioclase variety is more abundant; greater number of large (~4 mm), partially corroded, subhedral, zoned and twinned plagioclase crystals, and the greater number of anhedral twinned hornblendes with opacite rim. An overgrowth structure observed from a cumulophyric skeletal poikilitic plagioclase lath (~1 mm) shows numerous inclusions of anhedral zoned clinopyroxenes and opaques. One of the clinopyroxene chadacrysts (~0.2 mm) is jacketed by a subparallel rim of orthopyroxene. The groundmass is composed of feldspar and pyroxene microlites and interstitial brown glass, which define a pilotaxitic texture.

Field No.	36
Canterbury Univ. No.	20444
Locality	1,447,690 mN/603,735 mE
Volcanic Unit	Pangas
Rock Name	Biotite-bearing hornblende-phyric andesite

PETROGRAPHIC NOTES :

Hypoxtalline med-grained por rx consisting of subhedto anhed corroded plg laths (An_{50-58}). Several plg megacrysts (~4 mm) are present. Subhed to anhed corroded zoned and/or twinned px are abund as microphenos and phenos. These are present also in clots. Several anhed skele poikili pale green pleochroic hb are noted, and one grain measures about 3.5 mm occupying the core of a crystal aggre gate consisting of cpx, plg and opaques. Two anhed biotite xtals are enclosed within a skeletal opx cumulocryst; one biotite grain interdigitates with an anhedral opaque lump. The groundmass is composed of a finer-grained material, mostly fspar microlites which define a pilotaxitic texture.

Field No.	17
Canterbury Univ. No.	20460
Locality	1,440,950 mN/607,170 mE
Volcanic Unit	Rangas microdiorite
Rock Name	Two pyroxene hornblende microdiorite

PETROGRAPHIC NOTES :

Holoxtalline coarse- to med-grained por rock consisting of large (<4 mm) subhed zoned plg fspar laths, and several of these are skeletal frittered with concentric melt inclusions. Several plg also occur as subhed-anhed complexly-twinned cumulophenos.

Average plg composition is An_{20-28}. Qtz phenos show characteristic rounded anhed xtal outlines, devoid with cleavage, unzoned and several have skeletal cores. Px occur in minor amounts, usually as anhed highly corroded inclusion-bearing glomerocrysts. Most px are riddled with specks of microgranular opaque minerals. Subhed opaque-rimmed brown pleochroic tabular hornblende xtals dominate the mafic phases.

Field no.	**10C**
Canterbury Univ. No.	**20463**
Locality	**1,439,550 mN/606,200 mE**
Volcanic Unit	**Suminandig volcanics (Sgv)**
Rock Name	**Hornblende dacite**

PETROGRAPHIC NOTES :

Holoxtalline med-grained por rock consisting of large (<4 mm) subhed-anhed zoned plg fspar laths, and several of these are skeletal strongly-frittered with concentric melt inclusions. Several plg also occur as subhed-anhed complexly-twinned cumulophenos. Average plg composition is An_{20-28}. Qtz phenos show characteristic rounded anhed xtal outlines, devoid with cleavage, unzoned and untwinned, and few have skeletal cores. Px occur in minor amounts, usually as anhed-subhed highly corroded inclusion-bearing glomerocrysts. Most px are riddled with specks of microgranular opaque minerals. Subhed-anhed opaque-rimmed brown pleochroic tabular hornblende xtals dominate the mafic phases. These are usually inclusion-bearing skeletal grains with chadacrysts of stubby anhed px xtals, plg, qtz and opaques. The mx is a finer-grained equigranular mosaic of qtz and fspars.